

UNCLASSIFIED

AD 277 525

*Reproduced
by the*

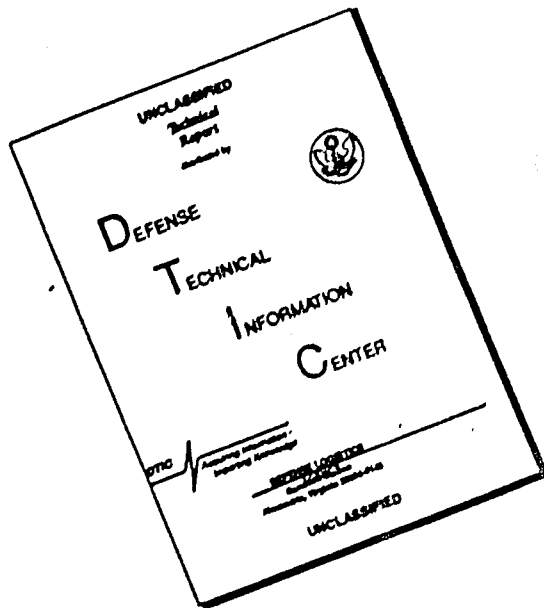
**ARMED SERVICES TECHNICAL INFORMATION AGENCY
ARLINGTON HALL STATION
ARLINGTON 12, VIRGINIA**



UNCLASSIFIED

NOTICE: When government or other drawings, specifications or other data are used for any purpose other than in connection with a definitely related government procurement operation, the U. S. Government thereby incurs no responsibility, nor any obligation whatsoever; and the fact that the Government may have formulated, furnished, or in any way supplied the said drawings, specifications, or other data is not to be regarded by implication or otherwise as in any manner licensing the holder or any other person or corporation, or conveying any rights or permission to manufacture, use or sell any patented invention that may in any way be related thereto.

DISCLAIMER NOTICE



THIS DOCUMENT IS BEST
QUALITY AVAILABLE. THE COPY
FURNISHED TO DTIC CONTAINED
A SIGNIFICANT NUMBER OF
PAGES WHICH DO NOT
REPRODUCE LEGIBLY.

ASD-TR-61-668

OPERATING POINTS, PARTICLE DYNAMICS, AND COORDINATE SYSTEMS FOR AEROSPACE VEHICLE STABILITY AND CONTROL

TECHNICAL REPORT No. ASD-TR-61-668

MARCH 1962

FLIGHT CONTROL LABORATORY
AERONAUTICAL SYSTEMS DIVISION
AIR FORCE SYSTEMS COMMAND
WRIGHT-PATTERSON AIR FORCE BASE, OHIO

PROJECT No. 8219, TASK No. 821904

(Prepared under Contract No. AF 33(616)-5961
by Systems Technology, Inc.
Authors: Duane T. McRuer & Irving Ashkenas)

NOTICES

When Government drawings, specifications, or other data are used for any purpose other than in connection with a definitely related Government procurement operation, the United States Government thereby incurs no responsibility nor any obligation whatsoever; and the fact that the Government may have formulated, furnished, or in any way supplied the said drawings, specifications, or other data, is not to be regarded by implication or otherwise as in any manner licensing the holder or any other person or corporation, or conveying any rights or permission to manufacture, use, or sell any patented invention that may in any way be related thereto.

Qualified requesters may obtain copies of this report from the Armed Services Technical Information Agency, (ASTIA), Arlington Hall Station, Arlington 12, Virginia.

This report has been released to the Office of Technical Services, U. S. Department of Commerce, Washington 25, D. C., for sale to the general public.

Copies of ASD Technical Reports and Technical Notes should not be returned to the Aeronautical Systems Division unless return is required by security considerations, contractual obligations, or notice on a specific document.

UNCLASSIFIED

Aeronautical Systems Division, Wright-Patterson Air Force Base, Ohio. Rpt No. ASD-TR-61-668. OPERATING POINTS, PARTICLE DYNAMICS, & COORDINATE SYSTEMS FOR AEROSPACE VEHICLE STABILITY AND CONTROL. Final Rpt. Mar 62, 109p. incl illus & tables. 36 Refs. Unclassified Report

Conventional aeronautical stability and control usage is extended into the aerospace flight regime with particular reference to the definition of operating points and coordinate systems. Implied and studied in this extension are the basic particle-dynamic equations of motion, the magnitudes of possible external forces, and the flight

1. Dynamics
2. Coordinate systems
3. Orbital flight paths
I. Project 8219, Task 821904
II. Contract AF33(616)-5961

III. Systems Technology, Inc, Inglewood, Calif.

IV. D.T. McRuer & Irving Ashkenas

V. In ASTIA collection
VI. Aval fr OTS

UNCLASSIFIED

(over)

UNCLASSIFIED

(over)

UNCLASSIFIED

Aeronautical Systems Division, Wright-Patterson Air Force Base, Ohio. Rpt No. ASD-TR-61-668. OPERATING POINTS, PARTICLE DYNAMICS, & COORDINATE SYSTEMS FOR AEROSPACE VEHICLE STABILITY AND CONTROL. Final Rpt. Mar 62, 109p. incl illus & tables. 36 Refs. Unclassified Report

Conventional aeronautical stability and control usage is extended into the aerospace flight regime with particular reference to the definition of operating points and coordinate systems. Implied and studied in this extension are the basic particle-dynamic equations of motion, the magnitudes of possible external forces, and the flight

1. Dynamics
2. Coordinate systems
3. Orbital flight paths
I. Project 8219, Task 821904
II. Contract AF33(616)-5961

III. Systems Technology, Inc, Inglewood, Calif.

IV. D.T. McRuer & Irving Ashkenas

V. In ASTIA collection
VI. Aval fr OTS

UNCLASSIFIED

(over)

regimes of fundamental interest. Simplified solutions of the particle-dynamic equations of motion are obtained, and certain low-frequency modes common to both particle and rigid-body motion are explored.

regimes of fundamental interest. Simplified solutions of the particle-dynamic equations of motion are obtained, and certain low-frequency modes common to both particle and rigid-body motion are explored.

UNCLASSIFIED

Aeronautical Systems Division, Wright-Patterson Air Force Base, Ohio. Rpt No. ASD-TR-61-668. OPERATING POINTS, PARTICLE DYNAMICS, & COORDINATE SYSTEMS FOR AEROSPACE VEHICLE STABILITY AND CONTROL. Final Rpt. Mar 62, 109p. incl illus & tables, 36 Refs.

Conventional aeronautical stability and control usage is extended into the aerospace flight regime with particular reference to the definition of operating points and coordinate systems. Implied and studied in this extension are the basic particle-dynamic equations of motion, the magnitudes of possible external forces, and the flight

1. Dynamics
2. Coordinate systems
3. Orbital flight paths
I. Project 8219, Task E21904
II. Contract AF33(616)-5961

III. Systems Technology, Inc, Inglewood, Calif.

IV. D.T. McRuer & Irving Ashkenas

V. In ASTIA collection
VI. Avail fr OTS

UNCLASSIFIED

Aeronautical Systems Division, Wright-Patterson Air Force Base, Ohio. Rpt No. ASD-TR-61-668. OPERATING POINTS, PARTICLE DYNAMICS, & COORDINATE SYSTEMS FOR AEROSPACE VEHICLE STABILITY AND CONTROL. Final Rpt. Mar 62, 109p. incl illus & tables, 36 Refs.

Conventional aeronautical stability and control usage is extended into the aerospace flight regime with particular reference to the definition of operating points and coordinate systems. Implied and studied in this extension are the basic particle-dynamic equations of motion, the magnitudes of possible external forces, and the flight

1. Dynamics
2. Coordinate systems
3. Orbital flight paths
I. Project 8219, Task E21904
II. Contract AF33(616)-5961

III. Systems Technology, Inc, Inglewood, Calif.

IV. D.T. McRuer & Irving Ashkenas

V. In ASTIA collection
VI. Avail fr OTS

UNCLASSIFIED

regimes of fundamental interest. Simplified solutions of the particle-dynamic equations of motion are obtained, and certain low-frequency modes common to both particle and rigid-body motion are explored.

regimes of fundamental interest. Simplified solutions of the particle-dynamic equations of motion are obtained, and certain low-frequency modes common to both particle and rigid-body motion are explored.

FOREWORD

This report represents one phase of an analytical investigation which, overall, is aimed at the development of generalized dynamic requirements for advanced vehicle flight control systems.

The research reported here was sponsored by the Flight Control Laboratory, Aeronautical Systems Division, Air Force Systems Command, as part of Project No. 8219, Task No. 821904. It was conducted at Systems Technology, Inc., under Contract AF 33(616)-5961. The ASD project engineers have been Mr. George Xenakis and Mr. Ronald O. Anderson.

The authors wish to acknowledge helpful discussions with Mr. Malcolm Abzug relating to the axis systems proposed, and Messrs. Junichi Taira and Vincent Kovacevich, who performed several of the developments in Chapters III and IV.

ABSTRACT

Conventional aeronautical stability and control usage is extended into the aerospace flight regime with particular reference to the definition of operating points and coordinate systems. Implied and studied in this extension are the basic particle-dynamic equations of motion, the magnitudes of possible external forces, and the flight regimes of fundamental interest. Simplified solutions of the particle-dynamic equations of motion are obtained, and certain low-frequency modes common to both particle and rigid-body motion are explored.

PUBLICATION REVIEW

This report has been reviewed and is approved.

FOR THE COMMANDER:


C. B. WESTBROOK
Chief, Aerospace Mechanics Branch
Flight Control Laboratory

CONTENTS

<u>Chapter</u>	<u>Page</u>
I INTRODUCTION	1
II GENERAL EQUATIONS OF MOTION	3
A. Elementary High Thrust Solutions.	6
B. Fundamental Coordinate Systems and Total Acceleration.	8
C. Resolution of the Aerodynamic Forces into $X'Y'Z'$ Coordinates	13
D. Gravity Force Expressed in the $X'Y'Z'$ System	14
E. Scalar Form of the Equations of Motion.	17
F. Simplified Equations of Motion with No Oblateness	20
III SIMPLIFIED EQUATIONS FOR EXTRA-ATMOSPHERIC FREE FLIGHT	27
A. The Areal Velocity Law	27
B. Inertial Space Velocities and Trajectories	28
C. Velocities and Time Behavior	32
D. Orbit Specifications.	39
E. General Effects of Oblateness and Aerodynamic Drag on the Idealized Trajectory.	42
IV SIMPLIFIED EQUATIONS FOR POWER-OFF FLIGHT WITHIN THE ATMOSPHERE	49
V LINEARIZED EQUATIONS OF MOTION	67
A. Linearization	67
B. Linearized Equations for Atmospheric Flight	70
REFERENCES.	81
<u>Appendix</u>	
SUMMARY OF AXIS SYSTEMS FOR AEROSPACE VEHICLE STABILITY AND CONTROL	85

ILLUSTRATIONS

1	Variation of the Instantaneous Mass Ratio and its Logarithm.	7
2	Vertical Plane of Simplified Physical Situation.	8
3	Definition of Inertial Axes for Aerospace Vehicles.	9
4	Definition of Vehicle-Centered Northerly- and Geocentrically-Directed Axis System.	10
5	Unit Sphere Development Showing Derivation of Body-Centered Radially Directed Axes System from Geocentric Inertial System . . .	10
6	Relationships Between \mathbf{xyz} and $\mathbf{x'y'z'}$ Axes	11
7	Components of the Vehicle Velocity in the $\mathbf{x'y'z'}$ Coordinate System	12
8	Directions of Lift and Drag Relative to the Velocity Vector. . . .	13
9	Modified Definition of Inertial Space and Radially Directed Rotating Axis System.	22
10	Areal Velocity Relationship	28
11	Geometry of Equations of Motion in Inertial Coordinates	29
12	The Hodograph, or Polar Diagram of Velocity	29
13	Some Elliptical Orbit Parameters.	32
14	Flight Path Angle Relationships	35
15	Approximate Geometric Relationship Between Mean and True Anomaly .	38
16	Orientation of the Trajectory Plane Relative to Inertial Space. .	41
17	Regression of the Ascending Node.	44
18	Departure of Vehicle from Conic and Rotation of Line of Apsides .	45
19	Comparison of Exponential with ARDC 1956 Model Atmosphere . . .	51
20	Comparison of Mean Value with ARDC Model Atmosphere	51
21	Regions of Validity for $\frac{dr}{dU}/U \ll 1$ and $\frac{L}{D} \tan \gamma \ll 1$	52
22	Normalized Variables Versus Altitude, Ballistic Flight	57
23	Time Variation of U , h , and q , Gliding Flight	60

24	Variation of U , h , q , and ρ for Typical Skipping Flight	63
25	Variation of Characteristic Equation Approximate Factors.	74
26	Time Vector Diagrams. .	77
27	Time Span, Δt , for "Valid" Constant Coefficient Solutions	78

Appendix

A-1	Vertical Reference Possibilities.	86
A-2	Basic Axis System Development (Homogeneous Spherical Earth). . . .	90-91
A-3	Simplified Situation for Homogeneous Spherical Central Body. . . .	89
A-4	Supplementary Relationships Between Vehicle-Centered Geocentrically Directed and Aries-Directed Geocentric Systems . .	92-93
A-5	Vehicle-Fixed Axis System and Notation.	94
A-6	Relationship Between Vehicle-Centered Geocentrically-Directed and Vehicle-Fixed Axis Systems	95

TABLES

I	Varieties of Keplerian Motion.	31
II	Conversions Between Geometric Parameters of Elliptic Orbit	33
III	Summary of Readily Solvable Particle Dynamics Cases with Aerodynamic Forces	54
IV	Summary of Dynamic Flight Parameters for Readily Solvable Cases of Aerospace Vehicle Particle Dynamics.	64

Appendix

A-I	Relationships Between Axes Oriented to Each Other Via Ψ , Θ , and Φ	96
A-II	Summary of Major Axis or Reference Systems	97

NOMENCLATURE

A	Apofocus, apogee (also used as subscript); constant of integration
a_e	Equatorial radius of the earth
b_e	Polar radius of the earth
C	Areal velocity constant, $2(dS/dt)$
C_D	Drag coefficient, $D/(1/2)\rho U_0^2 S$
C_L	Lift coefficient, $nW/(1/2)\rho U_0^2 S$
c.g.	Center of gravity
D, \underline{D}	Drag vector; drag
E	Complete elliptic integral of the second kind
E	Eccentric anomaly
f	Non-dimensional altitude - equation 76
\underline{F}	Force
g_e	Acceleration due to gravity at surface of earth (32.1740 ft/sec^2)
\underline{g}, g	Gravity vector; local acceleration due to gravity
G	Gravitational constant ($3.45 \times 10^{-8} \text{ ft}^4/\text{lb-sec}^4$)
h	Perturbed height of vehicle, perturbed altitude
\underline{h}	Height of vehicle measured from the surface of the earth, altitude
\underline{H}	Angular momentum
I_{xx} I_{yy} I_{zz}	Moments of inertia of the earth
I_1 I_2 I_3	Principal moments of inertia of the vehicle
\underline{L}, L	Lift vector, lift

m	Mass of body
M	Mass of principal gravitating body; molecular weight
p	Semilatus rectum, parameter; ambient pressure
\mathbf{p}	Linear momentum
q	Dynamic pressure
r, \mathbf{r}	Distance between centers of mass
r_c	Circular orbit radius
R	Universal gas constant; resultant aerodynamic force, $R = \sqrt{L^2 + D^2}$
R_a, R_b	Semi-major and semi-minor axes of ellipse
R_A, R_P	Apogee and perigee radii
s	Path distance, length of chord, displacement
s	Laplace transform variable, $s = \sigma + j\omega$
s_p	Perimeter of an ellipse
S	Total area swept out by the radius vector from the gravitating body to the orbital vehicle; reference area for aerodynamic coefficients
t	Time
T	Time of perigee passage; absolute temperature
\underline{T}, T	Thrust vector, thrust, non-dimensional time
T	Orbital period
U	Linear velocity along the X (or X') axis
u	Perturbed velocity along the X axis
\bar{u}	U/\sqrt{gr}
v_e	Effective exhaust velocity
v	Linear velocity along the Y (or Y') axis
$\underline{v} ()$	Instantaneous velocity of the vehicle observed in a particular axis system, e.g., $\underline{v} (XYZ)$
\underline{v}	Total velocity relative to inertial space
v_c	Local circular velocity, $a_e \sqrt{g_e/r_c}$

v_{av}	Mean orbital velocity
w	Linear velocity along the z (or z') axis
w	Perturbed velocity along the z axis; argument of perigee
β	Atmospheric density decay rate with height
γ	Longitudinal flight path angle; also perturbed flight path angle
γ_1	Lateral flight path angle
Γ	Ideal power-off constant speed glide angle = $\tan^{-1}(-D/L)$
Δ	Increment change
$\Delta(s)$	Denominator of vehicle transfer functions; characteristic equation when set equal to zero
Δh	Radial semivariation, $\Delta h = a\epsilon = (1/2)(r_A - r_P)$
ϵ	Eccentricity of conic section
ι	Inclination angle of trajectory plane to equatorial plane
ψ, θ, ϕ	Perturbed quantities of Euler angles Ψ , Θ , and Φ , respectively
Ψ, Θ, Φ	Euler angles (yaw, pitch, and bank angles) relating XYZ and XYZ -axes
Φ	Earth's gravitational potential
λ	Latitude of the vehicle
Λ	Longitude of the vehicle, measured from the inertial- z axis
Λ_Ω	Longitude of the ascending node
μ	Earth's oblateness parameter
ν	True anomaly
ρ	Mass density of air
τ	Rocket burning time
ω_0	Mean motion
Ω	Angular velocity of vehicle center of mass about the geocenter; angular velocity of the XYZ -axis system relative to inertial space
$\underline{\Omega}()$	Angular velocity observed in a particular axis system, e.g., $\underline{\Omega}(XYZ)$

T First point of Aries (the ascending node of the sun as seen from the earth)

Special Subscripts:

a Aerodynamic

A Apogee, apofocus

b Burned, corresponding to rocket fuel burn time

c Circular orbit

d Disturbances

f Final

i Initial value

n n^{th} moving part

o Initial value or operating point

P Perifocus, perigee, etc.

NOTE: For summary of major axis and reference systems see Table A-II

CHAPTER I
INTRODUCTION

Over the last 60 years an enormous amount of engineering and scientific effort has been devoted to the study of aircraft dynamics. With the current expansion of flight regimes to include extra-atmospheric phases, it becomes desirable to extend familiar aeronautical stability and control usage (Ref. 1 to 5) to include the more general aerospace situation. The present report treats some of the initial topics which are essential preliminaries to this desirable direct extension.

Stability and control is but one of the three broad categories—performance, stability and control, and aeroelasticity—which together make up the field of aircraft dynamics. Analytically, these classifications correspond to consideration of the aircraft as a particle, rigid body, and flexible body. Overlap and fringe areas naturally exist between the categories; one of the most important is that between performance and stability and control. Because the general rigid-body equations are complex and nonlinear, they are ordinarily linearized about "operating points" which define flight situations representative of "mean" conditions. This procedural step results in linear differential equations valid for small perturbations about the operating points. Before this can be done, however, physically reasonable operating points must be in hand. These are supplied by the performance, or particle dynamic equations. Consequently, any stability and control problem implicitly involves performance considerations even when attention is confined only to small departures from operating point conditions. One purpose of this report is to define such possible operating points. Another, and perhaps more important purpose, is to provide background information on the gross motions of the vehicle. With such data available, the analyst is better equipped to assess the regions of validity for rigid- and/or flexible-body equations based upon operating points which have been selected primarily for analytical convenience.

Manuscript released by the authors November 1961 for publication as an ASD Technical Report

In the course of developing the particle dynamic equations of aerospace vehicles in terms compatible with aircraft stability and control, certain forces and physical effects which are assumed negligible in aircraft must be taken into account. Consequently, a relatively large number of new axis systems are required. To allow as much carryover between aircraft and aerospace vehicle dynamics as possible, these axis systems must reduce to the conventional aerodynamic case when the physical effects which caused their introduction are reduced to zero. Another purpose of the report has been to define the necessary axes so that such a reduction is possible.

Another fringe area between performance and stability and control involves the motions and dynamics of the vehicle center-of-mass. Although aerospace vehicles can have significant coupling forces between translational and rotational degrees of freedom, this coupling is often quite weak for the very lowest frequency modes. These modes are implicit in the particle dynamics formulation. Consequently, the final purpose of this report is to elucidate some of the characteristic modes of perturbed motion occurring in the more complex rigid-body situation, which are more simply revealed by a study of particle dynamics.

CHAPTER II

GENERAL EQUATIONS OF MOTION

As the first step toward the goals mentioned in the introduction, the general equations of motion for an aerospace vehicle, considered as a particle, shall be developed in this chapter. Initially the equations are stated in general vector form. The various forces are then resolved into an axis system which can be transformed readily into axes suitable for study of the rigid body motions. The general particle-dynamic scalar equations resulting from this resolution are then specialized into various simplified sets which are considered in more detail in subsequent chapters.

By Newton's second law the time rate of change of linear momentum equals the sum of all externally applied forces,

$$\frac{dp}{dt} = F \quad (1)$$

In rocket-powered flight the thrust forces, usually considered external, are produced by the expenditure of vehicle mass; and the mass variation must be considered in determining the rate of change of linear momentum (Ref. 6 and 7). At time t let the linear momentum be

$$p_1 = m\underline{V}$$

where m is the mass and \underline{V} the velocity of the vehicle. Then, if at time $t + dt$, $-dm$ is the mass which has left the vehicle with an effective exhaust velocity \underline{v}_e , relative to the vehicle, the linear momentum will be

$$p_2 = (m + dm)(\underline{V} + d\underline{V}) + (-dm)(\underline{V} + \underline{v}_e)$$

Here $\underline{V} + d\underline{V}$ and $m + dm$ are the velocity and mass of the vehicle at time $t + dt$, and $\underline{V} + \underline{v}_e$ is the effective exhaust velocity relative to inertial space. It should be noted in passing that the effective exhaust velocity depends upon the exit area, the differential between exit and ambient pressures, and the exit velocity of the mass leaving the vehicle.

The incremental change in momentum from time t to time $t + dt$ is then

$$\begin{aligned} d\underline{p} &= \underline{p}_2 - \underline{p}_1 = (m + dm)(\underline{V} + d\underline{V}) - dm(\underline{V} + \underline{v}_e) - m\underline{V} \\ &= md\underline{V} - \underline{v}_e dm + dm d\underline{V} \end{aligned}$$

Dividing by dt , and taking limits, the time rate of change of momentum becomes,

$$\frac{d\underline{p}}{dt} = m \frac{d\underline{V}}{dt} - \underline{v}_e \frac{dm}{dt} = \underline{F}$$

or $m \frac{d\underline{V}}{dt} = \underline{F} + \underline{v}_e \frac{dm}{dt} = \underline{F} + \underline{T}$ (2)

where the thrust, \underline{T} , is defined by $\underline{v}_e(dm/dt)$.

Thus, for a particle where mass is expelled to produce thrust, the rate of change of momentum can be computed as if the mass were constant, and the product of the change in mass per unit time and the relative velocity between the exhausted mass and the particle were an external force. [Although $\underline{p} = m\underline{V}$, the rate of change $d\underline{p}/dt \neq m(d\underline{V}/dt) + \underline{V}(dm/dt)$]. Eq. (2) directly follows from Eq. (1) when the thrust is developed by a momentum exchange other than one directly involving the particle mass, as in a propeller (in the present context such a thrust would constitute an external force). Thus, if the thrust force includes exhaust products, Eq. (2) is correct in general for nonrelativistic (i.e., total mass is constant) particle vehicles.

The remaining external forces on the vehicle-particle are due to gravity, to the motion of the vehicle through the atmosphere, and to extraneous disturbances. The gravitational force is represented by the vector quantity mg , where g is the local acceleration due to gravity. The aerodynamic force is resolved into two components, the lift, \underline{L} , normal to the velocity vector and the drag, \underline{D} , along the velocity vector. An additional force, \underline{F}_d , is used to represent the summation of all other forces applied to the vehicle. These include (Ref. 8):

1. Radiation expulsion from the vehicle

Electromagnetic radiation (7.5×10^{-7} lb/kw)
Thermal radiation (2.0×10^{-9} lb/cal/sec)

2. Ambient field forces *

Gravitation (from bodies other than the principal source)
Electromagnetic fields

3. Incident momentum

Solar radiation (1.8×10^{-7} lb/ft²)
Meteorite bombardment
Cosmic ray bombardment

All of these forces are either very small, or have low probabilities of occurrence (e.g., meteorites), for aerospace vehicles.

Summing all the forces, the vector equation of motion becomes

$$m(t) \frac{d\mathbf{V}}{dt} = m(t)\mathbf{g} + \underline{\mathbf{L}} + \underline{\mathbf{D}} + \underline{\mathbf{T}} + \underline{\mathbf{F}_d} \quad (3)$$

where the velocity vector, $\underline{\mathbf{V}}$, is implicitly referred to an axis system which is fixed relative to inertial space. Since the scalar equations to follow will be referred to an axis system, \mathbf{XYZ} , having an angular velocity, $\underline{\Omega}$, with respect to inertial space, the acceleration will be given by

$$\frac{d\mathbf{V}}{dt} = \dot{\underline{\mathbf{V}}}(\mathbf{XYZ}) + \underline{\Omega}(\mathbf{XYZ}) \times \underline{\mathbf{V}}(\mathbf{XYZ})$$

The time derivative, $\dot{\underline{\mathbf{V}}}(\mathbf{XYZ})$, is the derivative of $\underline{\mathbf{V}}(\mathbf{XYZ})$ obtained by treating the \mathbf{XYZ} reference system as if it were inertial space. The centripetal acceleration caused by the curved path (relative to inertial space) of the \mathbf{XYZ} axis system is taken into account by the vector cross-product $\underline{\Omega} \times \underline{\mathbf{V}}$. With these modifications, the vector equation of motion becomes

$$\dot{\underline{\mathbf{V}}} + \underline{\Omega} \times \underline{\mathbf{V}} = \mathbf{g} + \frac{1}{m(t)} [\underline{\mathbf{L}} + \underline{\mathbf{D}} + \underline{\mathbf{T}} + \underline{\mathbf{F}_d}] \quad (4)$$

where all of the quantities are those seen by an "observer" having a frame of reference which is rotating at an angular velocity, $\underline{\Omega}$, with respect to inertial space.

Neither Eq. (3) nor Eq. (4) can be solved in general. There are, however, two extremely simple solutions to Eq. (3) which are applicable to high thrust situations; these will be examined before approaching the difficulties of Eq. (4).

A. ELEMENTARY HIGH THRUST SOLUTIONS

The two cases of interest involve situations where

- (1) All external forces are negligible relative to the thrust.
- (2) All external forces except those arising from a uniform gravitational field are negligible relative to the thrust.

Implicit in the statement of the above assumptions is the further assumption that the thrust is not an external force but is generated by mass expulsion (i.e., a rocket engine).

Because case (1) is a specialization of case (2) only the latter need be considered in detail. Then from Eq. (3) for $g = \text{constant}$, $\underline{T} = \underline{v}_e (\frac{dm}{dt})$, and all other forces taken as zero,

$$\frac{d\underline{V}}{dt} = g + \underline{v}_e \frac{1}{m(t)} \frac{dm}{dt}$$

If the effective exhaust velocity is constant this can be integrated to give

$$\underline{V}(t) = \underline{V}_0 + gt + \underline{v}_e \ln \frac{m(t)}{m_0} \quad (5)$$

where \underline{V}_0 , m_0 , are the initial ($t = 0$) and $\underline{V}(t)$, $m(t)$ the present ($t = t$) velocities and mass, respectively; and \underline{v}_e and \underline{V} are oppositely directed (\underline{v}_e negative).

The displacement, \underline{s} , can be found if the mass flow is constant, $dm/dt = -c$; then, denoting the rocket burning time by τ , and the final mass, $m_0 - c\tau$, by m_f ,

$$\begin{aligned} \int_{s_0}^{\underline{s}} \frac{ds}{dt} &= \int_0^\tau \underline{V}(t)dt + \int_\tau^t \underline{V}(t)dt \\ &= \underline{V}_0 t + \frac{1}{2} gt^2 + \int_0^\tau \underline{v}_e \ln \left(\frac{m_0 - ct}{m_0} \right) dt + \int_\tau^t \underline{v}_e \ln \frac{m_f}{m_0} dt \end{aligned}$$

and

$$\underline{s} = \underline{s}_0 + \underline{V}_0 t + \frac{1}{2} gt^2 - \underline{v}_e \left[t \ln \frac{m_0}{m_f} + \tau \left(1 - \frac{m_0}{m_0 - c\tau} \ln \frac{m_0}{m_f} \right) \right] \quad (6)$$

The term on the right multiplied by τ will always be negative, and therefore will reduce the distance the vehicle travels. Maximum distance will occur when the burning time, τ , approaches zero. Then, although the velocity equation remains unchanged, the displacement approaches

$$s = s_0 + v_0 t + \frac{1}{2} g t^2 - v_e t \ln \frac{m_0}{m_f}$$

Thus the most efficient propulsion method (to maximize the vehicle displacement) is one in which the entire fuel mass is consumed instantly so that the impulse is applied only to the payload, and is not expended in imparting velocity to the mass of unburned fuel.

Eqs. (5) and (6) may be expressed in terms of an impulse $\underline{I} = \underline{T}\tau$, or by a "specific impulse" based upon the expelled weight, $(m_0 - m_f)g$, and defined as

$$\underline{I}_{sp} \equiv \frac{\underline{T}\tau}{(m_0 - m_f)g}$$

by noting that

$$v_e = \frac{\underline{T}}{dm/dt} = - \frac{\underline{T}\tau}{m_0 - m_f} = - \frac{\underline{I}}{m_0 - m_f} = -g\underline{I}_{sp} \quad (7)$$

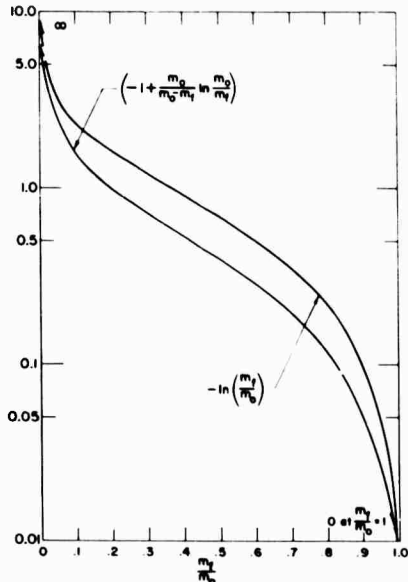


Figure 1. Variation of the Instantaneous Mass Ratio and its Logarithm

Another common term in propulsion, the "Characteristic velocity," v_c , is defined as

$$v_c \equiv -v_e \ln \frac{m_0}{m_f} \equiv g\underline{I}_{sp} \ln \frac{m_0}{m_f} \quad (8)$$

Physically, if there were no gravitational field, the maximum velocity of the vehicle starting from rest would be the characteristic velocity. The functions of m_f/m_0 pertinent to the velocity and displacement equations, Eqs. (5) and (6), are plotted in Figure 1.

B. FUNDAMENTAL COORDINATE SYSTEMS AND TOTAL ACCELERATION

The elementary case considered above is indicative of typical simplified solutions to Eq. (3) in its present vector form. Eq. (4) is not even this tractable. Therefore, the next major step is to replace Eq. (4) by equivalent scalar equations. Before this can be done, a set of reference axis systems must be defined into which the vector quantities may be resolved.

The selection of primary reference axes for the study of vehicle particle dynamics generally reflects the types of answers desired from the subsequent analytical treatment and the types of forces to be described mathematically. In the present study, the main axis system is chosen to have its origin at the particle itself, both for analytical convenience and so it can serve as one of the axis systems required in a study of rigid body dynamics. In general, there are several requirements and desires entering into the coordinate systems selected for use:

- a. The systems are only intended to be adequate for dynamic situations arising in aerospace vehicle stability and control. Thus only one principal gravitating body (the earth) has important gravitational effects and the problem time spans are relatively short.
- b. Both the systems chosen and the notation used should reduce to that conventional in aeronautical stability and control as one limit.
- c. The rotational sequences in going from one axis system to another should be similar. In this way only a very few basic transformation matrices are required.

The implications of these requirements and desires are treated below and in the appendix.

The physical situation which will ultimately be treated most extensively in this report is illustrated in Figure 2. This restricted problem is coplanar, i.e., the velocity vector, \mathbf{V} , is in the \mathbf{XZ} plane, the \mathbf{Z} axis is directed to the geocenter, the origin is fixed at the particle, and the \mathbf{Y} axis is directed into the plane of the paper. The earth is taken as inertial space. In normal aerodynamic stability

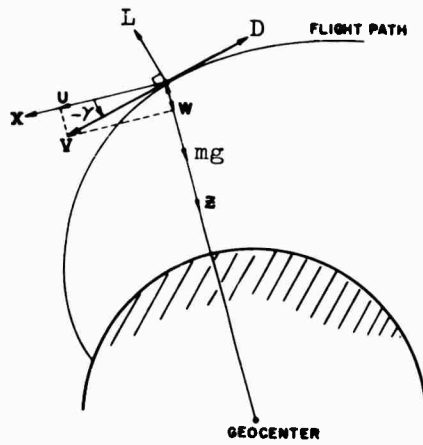


Figure 2. Vertical Plane of Simplified Physical Situation

and control problems the \mathbf{XYZ} system shown becomes a reasonable approximation to inertial space since at normal aircraft speeds the rotation of \mathbf{XYZ} relative to the earth (a "better" version of inertial space) is negligible. Instead of starting with the relatively simple situation of Figure 2, the complete series of steps required to derive quite general equations which can then be restricted to the simplified case will be taken. The purpose of the procedure is not to induce coordinate psychosis, but rather to illustrate some of the assumptions implicitly involved in getting to the simplified situation which will ultimately be studied.

The first problem is to define inertial space. For aerospace vehicles an axis system with its origin at the center of the earth, and nonrotating with respect to the fixed stars, is suitable. This system, denoted as $\mathbf{x'yz'}$, is shown in Figure 3. The \mathbf{x} axis is directed along the north polar axis of the earth, and the $-\mathbf{z}$ axis is directed to \mathbf{T} , the First Point of Aries (the sun's ascending node as seen from the earth).* The vehicle is oriented relative to inertial space via a longitude angle, Λ (measured from $-\mathbf{z}$), a latitude angle, λ , and a radius r .

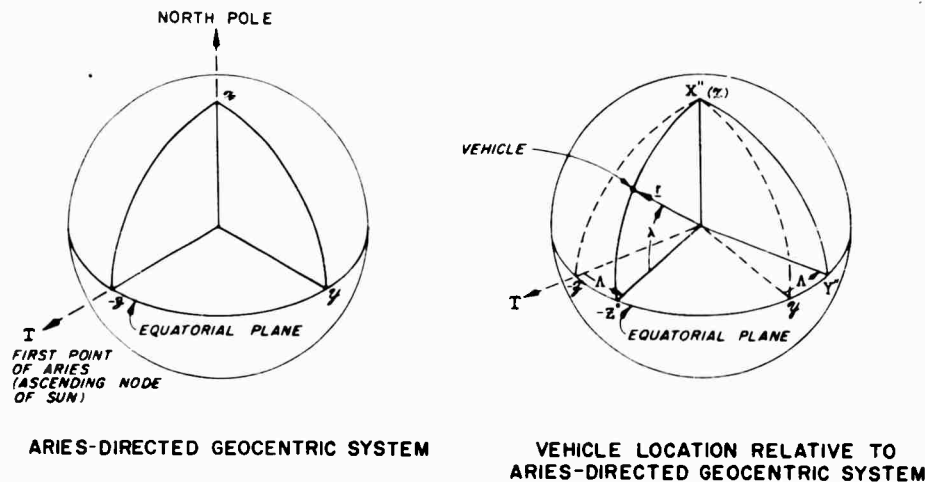


Figure 3. Definition of Inertial Axes for Aerospace Vehicles

An axis system with its origin in the body can now be defined as shown in Figure 4. This set of coordinates, denoted as $\mathbf{X'Y'Z'}$, is the basic system for the formulation of the particle dynamics equations in their most general form. (The specification that $\mathbf{X'}$ be in the direction of increasing latitude

*On the celestial sphere \mathbf{T} is the intersection of the earth's equator and the sun's path as the sun passes across the equator from south to north, i.e., the vernal equinox.

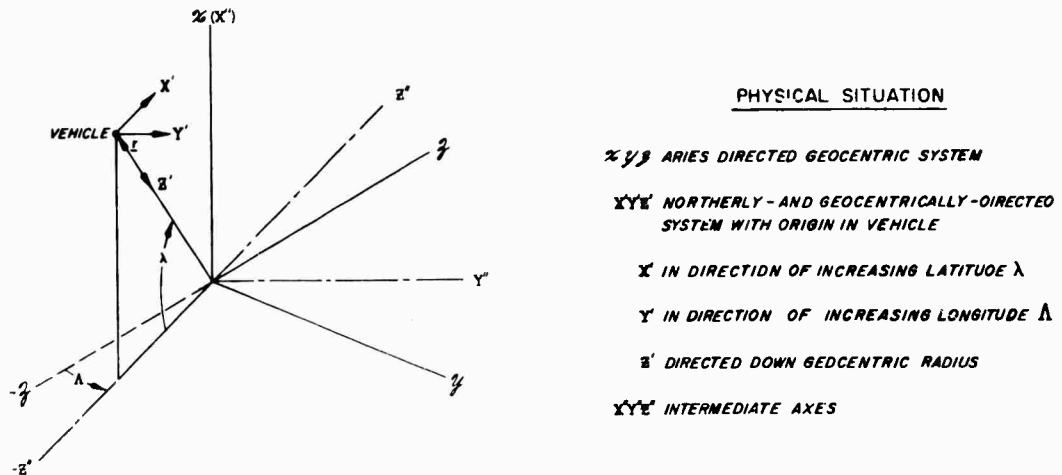


Figure 4. Definition of Vehicle-Centered Northerly- and Geocentrically-Directed Axis System

will be relieved later by establishing an \mathbf{xyz} system with $\mathbf{z} = \mathbf{z}'$, but with \mathbf{x} oriented in the plane of equilibrium flight.) The unit sphere development of Figure 5 shows the derivation of the $\mathbf{x}'\mathbf{y}'\mathbf{z}'$ system from the inertial reference $\mathbf{x}\mathbf{y}\mathbf{z}$. This figure should make the rather awkward choice of measuring longitude from the $-\mathbf{z}$ axis more understandable, since some such artifice is necessary if the \mathbf{z}' axis is to be directed toward the geocenter (in common with conventional stability and control definitions) and $\mathbf{x}'\mathbf{y}'\mathbf{z}'$ is to be readily derived from $\mathbf{x}\mathbf{y}\mathbf{z}$. The directional cosine relationships between these two systems are summarized in Figure 6.

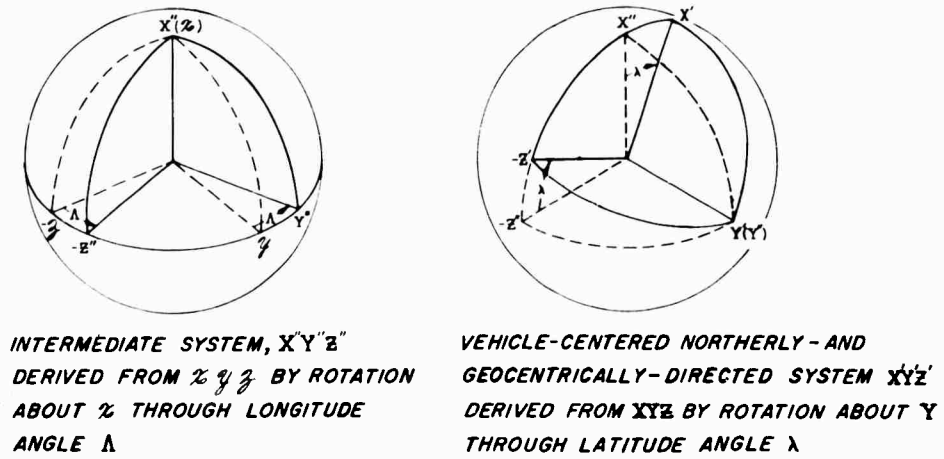


Figure 5. Unit Sphere Development Showing Derivation of Body-Centered Radially Directed Axes System from Geocentric Inertial System

COMPLETE ARRAY:	
\mathcal{L}	\mathcal{R}
$\cos \lambda$	$-\sin \lambda \sin \lambda$
0	$\cos \lambda$
π	$-\sin \lambda \cos \lambda$
$\pi/2$	0
$-\pi/2$	$-\sin \lambda$
π	$\cos \lambda$
2π	$\sin \lambda$

COMPLETE ARRAY:

As an array, this may be read either left to right or down. As matrices, these correspond to:

EXTRACTED FROM:

$$[L] = \begin{bmatrix} \cos \lambda & -\sin \lambda & 0 & 0 \\ \sin \lambda & \cos \lambda & 0 & 0 \\ 0 & 0 & \cos \Delta & \sin \Delta \\ 0 & 0 & -\sin \Delta & \cos \Delta \end{bmatrix} = \begin{bmatrix} \lambda & [A] & [L'] & [\lambda'] \\ [A] & \lambda & [L'] & [\lambda'] \end{bmatrix}$$

LINEARIZED FORM:

Similarly, $[L^{-1}] = [L_0^{-1}] + [1']$, where $[1'] \neq [1]$, but is obtained by subtracting $[L_0]$ term by term from $[L^{-1}]$.

$$[L] =$$

where: $[L]$ is the matrix made up of the operating point quantities alone (underlined, square bracketed terms); and $[H]$ is the matrix made up of the perturbation quantities alone.

For the special case where $\Lambda_0 = \lambda_0 = 0$,

Figure 6. Relationships Between x , y , z and X , Y , Z Axes

The components of the velocity vector, \underline{V} , along $X'Y'Z'$ are U , V , and W . These are shown in Figure 7 together with the definition of lateral and longitudinal flight path angles.

The longitudinal flight path angle is measured between the velocity vector, \underline{V} , and its projection on the $X'Y'$ plane, and the lateral flight path angle is measured from the X' axis to this same projection of \underline{V} . If \underline{l}' , \underline{m}' , and \underline{n}' are defined as unit vectors along X' , Y' , and Z' , respectively, then the velocity vector becomes

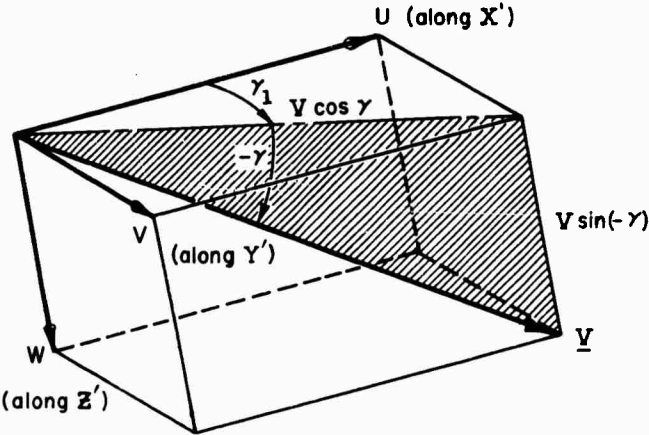


Figure 7. Components of the Vehicle Velocity in the $X'Y'Z'$ Coordinate System

$$\underline{V} = \underline{V}(X'Y'Z') = U\underline{l}' + V\underline{m}' + W\underline{n}' \quad (9)$$

where

$$U = V \cos \gamma \cos \gamma_1$$

$$V = V \cos \gamma \sin \gamma_1$$

$$W = -V \sin \gamma$$

The flight path angles are defined as

$$\begin{aligned} \gamma &= \sin^{-1} \frac{-W}{V} \equiv \frac{dr/dt}{V} \\ \gamma_1 &= \tan^{-1} \frac{V}{U} \end{aligned} \quad \left. \right\} \quad (10)$$

In terms of components in the $X'Y'Z'$ coordinates, the angular velocity of the $X'Y'Z'$ system relative to inertial space is

$$\underline{\Omega}(X'Y'Z') = \frac{1}{r} \left[V\underline{l}' - U\underline{m}' \right]$$

and the total acceleration [the left side of Eq. (4)] then becomes

$$\begin{aligned}
 \dot{\underline{V}} + \underline{\Omega} \times \underline{V} &= \dot{U} \underline{l}' + \dot{V} \underline{m}' + \dot{W} \underline{n}' + \frac{1}{r} \begin{vmatrix} \underline{l}' & \underline{m}' & \underline{n}' \\ V & -U & 0 \\ U & V & W \end{vmatrix} \\
 &= (\dot{U} - \frac{UW}{r}) \underline{l}' + (\dot{V} - \frac{VW}{r}) \underline{m}' + (\dot{W} + \frac{U^2 + V^2}{r}) \underline{n}' \quad (11)
 \end{aligned}$$

The applied accelerations [the right side of Eq. (4)] are developed in the following sections.

C. RESOLUTION OF THE AERODYNAMIC FORCES INTO X' Y' Z' COORDINATES

The aerodynamic force acting on a body is normally resolved into two components: the lift, L , normal to the velocity vector and the drag, D , along the velocity vector (see Figure 8). As normally computed, lift and drag depend upon the relative velocity between the air mass and the vehicle, and not the total velocity, V . This does not prevent resolving the total aerodynamic force relative to the total linear velocity, as above, but such a procedure can lead to difficulties if care is not taken when L and D are actually computed.*

Since the drag force acts along the velocity vector it can be resolved into the X' Y' Z' system using the flight path angles already defined, i.e.,

$$D = -D[\cos \gamma_l \cos \gamma_l' + \sin \gamma_l \cos \gamma_m' - \sin \gamma_n'] \quad (12)$$

The lift, on the other hand, is thus far defined only as normal to the velocity vector, so it can conceivably be anywhere in the normal plane. Consequently an aerodynamic axis system, with V and L as two of the axes, must be related to the X' Y' Z' system. This resolution can proceed as follows:



Figure 8. Directions of Lift and Drag Relative to the Velocity Vector

*The entire problem can be skirted by assuming that the air mass is stationary relative to inertial space — an assumption that throws away certain interesting second order effects due to atmospheric rotation caused by the earth's rotation.

- a. Initially, let \underline{V} be aligned with \underline{X}' , with \underline{L} directed along $-\underline{Z}'$.
- b. Rotate \underline{V} about \underline{Z}' through the lateral flight path angle, γ_1 (\underline{L} is still directed along $-\underline{Z}'$).
- c. Rotate \underline{V} about an axis normal to both \underline{V} and \underline{Z}' through the longitudinal flight path angle, γ . At this point \underline{V} is as shown in Figure 7.
- d. Finally, rotate \underline{L} about \underline{V} , through an aerodynamic roll angle, Φ_a , to its final position.

These rotations are identical to those shown in the Appendix. (There a set of unit vectors, \underline{l} , \underline{m} , and \underline{n} , are related to another set, \underline{i} , \underline{j} , and \underline{k} , via rotations through Ψ , Θ , and Φ . If these angles are replaced by those above, i.e., $\Psi = \gamma_1$, $\Theta = \gamma$, and $\Phi = \Phi_a$, the same form of directional cosine array may be used.) For the present case this is:

	\underline{l}'	\underline{m}'	\underline{n}'
$-\underline{D}$	$\cos \gamma_1 \cos \gamma$	$\sin \gamma_1 \cos \gamma$	$-\sin \gamma$
	$\cos \gamma_1 \sin \gamma \sin \Phi_a - \sin \gamma_1 \cos \Phi_a$	$\sin \gamma_1 \sin \gamma \sin \Phi_a + \cos \gamma_1 \cos \Phi_a$	$\cos \gamma \sin \Phi_a$
$-\underline{L}$	$\cos \gamma_1 \sin \gamma \cos \Phi_a + \sin \gamma_1 \sin \Phi_a$	$\sin \gamma_1 \sin \gamma \cos \Phi_a - \cos \gamma_1 \sin \Phi_a$	$\cos \gamma \cos \Phi_a$

The lift force when resolved into the $\underline{X}' \underline{Y}' \underline{Z}'$ system is, accordingly,

$$\begin{aligned}
 \underline{L} = & -L[(\cos \gamma_1 \sin \gamma \cos \Phi_a + \sin \gamma_1 \sin \Phi_a)\underline{l}' \\
 & + (\sin \gamma_1 \sin \gamma \cos \Phi_a - \cos \gamma_1 \sin \Phi_a)\underline{m}' + (\cos \gamma \cos \Phi_a)\underline{n}'] \quad (13)
 \end{aligned}$$

D. GRAVITY FORCE EXPRESSED IN THE $\underline{X}' \underline{Y}' \underline{Z}'$ SYSTEM

The gravitational acceleration applied to the vehicle at a distance, r , from the geocenter would be

$$\underline{g} = -\frac{GM}{r^2} \underline{l} = \frac{GM}{r^2} \underline{n} \quad (14)$$

if the earth were a homogeneous sphere. When based upon the arithmetic mean of the polar and equatorial radii, the value of g at the earth's surface, the earth's radius, a_e , and GM are about (Ref. 9)

$$g_e = 983.05 \text{ cm/sec}^2$$

$$= 32.252 \text{ ft/sec}^2$$

$$a_e = 6.367650 \times 10^6 \text{ m}$$

$$= 2.089120 \times 10^7 \text{ ft}$$

$$GM = 3.9858 \times 10^{14} \text{ m}^3/\text{sec}^2$$

$$= 1.40753 \times 10^{16} \text{ ft}^3/\text{sec}^2$$

These numbers are most correct at latitudes of about 45° . Some idea of the differences due to the actual earth shape and structure may be obtained from the table below, which lists standard values for gravitational acceleration of a non-rotating earth (Ref. 9).

Latitude	g_e	
	cm/sec ²	ft/sec ²
0°	981.43	32.199
45°	983.01	32.251
90°	983.22	32.258

To obtain a more precise form of the gravitational force due to the earth, a better representation of the earth's field is required. This may be derived from the gravitational potential function for a homogeneous ellipsoidal earth, with moments of inertia I_{zz} about the polar axis and I_{yy} and I_{zz} about the principal axes in the equatorial plane. The gravitational potential can be shown to be

$$\Phi = -\frac{GM}{r} \left\{ 1 + \frac{1}{2Mr^2} \left[I_{zz} - \frac{I_{yy} + I_{zz}}{2} \right] (1 - 3 \sin^2 \lambda) + \frac{3(I_{yy} - I_{zz})}{4Mr^2} \cos^2 \lambda \cos 2\lambda + \dots \right\}$$

to the first terms in latitude and longitude (Ref. 10). The \mathbf{y} and \mathbf{z} axes used here are similar to those defined in Figure 3 but not quite the same; i.e., \mathbf{x} and \mathbf{z} are selected to be principal axes of a nonrotating earth, and are not necessarily directed toward \mathbf{T} . The definition of longitude is also modified accordingly. Experiments with pendula indicate that the gravity vector varies only very slightly with longitude so $I_{yy} = I_{zz}$; and the earth is thus usually supposed to be approximately an oblate spheroid. Under these circumstances, the second term in the above equation will have the coefficient

$$\frac{1}{2Mr^2} \left[I_{zz} - \frac{I_{yy} + I_{zz}}{2} \right] = \frac{a_e^2}{10r^2} \left(1 - \frac{b_e^2}{a_e^2} \right) = \mu \frac{a_e^2}{r^2}$$

where b_e and a_e are the minor (polar) and major (equatorial) radii of the earth, respectively. A close approximation to the gravitational potential of the earth, including the first order oblateness effects, is then

$$\Phi = -\frac{GM}{r} \left\{ 1 + \mu \left(\frac{a_e}{r} \right)^2 (1 - 3 \sin^2 \lambda) + \dots \right\} \quad (15)$$

The fact that the vehicle mass distribution is not actually that of a point introduces a small increment in potential, $\Delta\Phi$, given by

$$\Delta\Phi = -\frac{GM}{2r^3} \left[1 + 3\mu \left(\frac{a_e}{r} \right)^2 (1 - 5 \sin^2 \lambda) \right] (I_1 + I_2 + I_3)$$

where I_1 , I_2 , and I_3 are the principal moments of inertia of the vehicle (Ref. 11). This increment is entirely negligible when compared with Eq. (15), so the vehicle essentially acts as a point mass in this instance. On the other hand, the potential function itself is not precise, since the earth is probably pear-shaped, nonhomogeneous, etc.

To the extent that Eq. (15) represents the gravitational potential function of the vehicle, the gravitational force can be found by taking the gradient of this potential.

$$\begin{aligned}\mathbf{g} &= -\mathbf{grad} \Phi \\ &= \frac{\partial \Phi}{\partial r} \mathbf{n}' + \frac{1}{r} \frac{\partial \Phi}{\partial \lambda} \mathbf{l}'\end{aligned}$$

Since

$$\frac{\partial \Phi}{\partial r} = \frac{GM}{r^2} \left\{ 1 + 3\mu \left(\frac{a_e}{r}\right)^2 (1 - 3 \sin^2 \lambda) + \dots \right\}$$

and

$$\frac{\partial \Phi}{\partial \lambda} = \frac{3GM}{r} \mu \left(\frac{a_e}{r}\right)^2 \sin 2\lambda$$

the acceleration due to gravity in the $\mathbf{X}' \mathbf{Y}' \mathbf{Z}'$ system becomes

$$\mathbf{g} = \frac{GM}{r^2} \left\{ \left[1 + 3\mu \left(\frac{a_e}{r}\right)^2 (1 - 3 \sin^2 \lambda) \right] \mathbf{n}' + 3\mu \left(\frac{a_e}{r}\right)^2 \sin 2\lambda \mathbf{l}' \right\} \quad (16)$$

Treating the coefficients of this expansion as empirical constants of the earth, the following sets of values have been suggested (Ref. 12):

$$\begin{aligned}GM &= 3.986277 \times 10^{14} \text{ m}^3/\text{sec}^2 \\ &= 1.407732 \times 10^{16} \text{ ft}^3/\text{sec}^2 \\ a_e &= 6.378388 \times 10^6 \text{ m} \\ &= 2.092643 \times 10^7 \text{ ft} = 3.963339 \times 10^3 \text{ miles} \\ \mu &\approx 5.461 \times 10^{-4}\end{aligned}$$

Note that the values of GM and a_e given here are different from those previously given for a spherical earth.

E. SCALAR FORM OF THE EQUATIONS OF MOTION

With the various forces resolved into $\mathbf{X}' \mathbf{Y}' \mathbf{Z}'$ coordinates, Eq. (4) can be written as the scalar set:

Along \mathbf{X}' :

$$\dot{U} - \frac{UW}{r} = \frac{1}{m(t)} \left\{ -D \cos \gamma_1 \cos \gamma \left[1 + \frac{L}{D} \left(\tan \gamma \cos \Phi_a + \tan \gamma_1 \frac{\sin \Phi_a}{\cos \gamma} \right) \right] + T_{X'} + F_{dX'} \right\} + \frac{GM}{r^2} 3\mu \left(\frac{a_e}{r} \right)^2 \sin 2\lambda$$

Along \mathbf{Y}' :

$$\dot{V} - \frac{VW}{r} = \frac{1}{m(t)} \left\{ -D \sin \gamma_1 \cos \gamma \left[1 + \frac{L}{D} \left(\tan \gamma \cos \Phi_a - \frac{\sin \Phi_a}{\tan \gamma_1 \cos \gamma} \right) \right] + T_{Y'} + F_{dY'} \right\} \quad (17)$$

Along \mathbf{Z}' :

$$\dot{W} + \frac{U^2 + V^2}{r} = \frac{1}{m(t)} \left\{ D \sin \gamma \left[1 - \frac{L}{D} \operatorname{ctn} \gamma \cos \Phi_a \right] + T_{Z'} + F_{dZ'} \right\} + \frac{GM}{r^2} \left[1 + 3\mu \left(\frac{a_e}{r} \right)^2 (1 - 3 \sin^2 \lambda) \right]$$

The dependent variables are U , V , and W . Other quantities in the equations are connected to these by

$$\begin{aligned} \gamma_1 &= \tan^{-1} \frac{V}{U} \quad ; \quad \gamma = \sin^{-1} \frac{-W}{\sqrt{U^2 + V^2 + W^2}} \\ -W &= \frac{dr}{dt} \quad ; \quad \dot{\lambda} = \frac{U}{r} \end{aligned} \quad (18)$$

$$L \equiv qSC_L \quad ; \quad D \equiv qSC_D$$

$$q \equiv \frac{1}{2} \rho (V_{\text{rel}})^2; V_{\text{rel}} \equiv \mathbf{V} - \mathbf{V}_{\text{air mass/inertial space}}$$

The atmospheric density, ρ , is, among other things, a function of altitude and hence of r ; and the thrust components may also (but not necessarily) be functions of altitude, speed, or dynamic pressure. Thus all the quantities in Eqs. (17) are connected with the three dependent variables in a fairly direct fashion except the aerodynamic roll angle, Φ_a , and the disturbances, F_d . From the particle-dynamics point of view Φ_a can be an arbitrary function of time. Most of the disturbances can also be approximated by functions of time alone for the periods

of interest here. Some of these disturbances have already been mentioned, but a more complete list is now appropriate. This list reflects assumptions made in deriving the above equations, since F_d is used here as a catch-all to take otherwise ignored phenomena at least into partial account. Thus, to the extent their effects can be approximated for fairly short intervals by functions of time only, the components of F_d might include the following:

a. Ambient Field Forces

- (1) Gravitational effects of the sun, moon, and planets. These have been completely ignored in the equations thus far. For close-in orbits and trajectories, these gravitational attractions can be approximated by periodic functions of time (with the basic period that of the vehicle about the earth). When the vehicle is farther out, or for long time periods, this crude approach will not suffice. In these circumstances, the whole formulation of the equations of motion will change. As a first step, the "inertial space" axes would become a heliocentric ecliptic system, the angular velocity of X' Y' Z' relative to inertial space would be modified accordingly, etc. Some idea of when such a transfer should be made is given by the "activity sphere," which describes the space in which the planet, rather than the sun, should be regarded as the center body. Reference 9 cites an activity sphere of 0.00618 astronomical units. This region extends far beyond the "aerospace" considered here. References 13 and 14 summarize the effects of the sun and moon upon close-in extra-atmospheric orbits about the earth, and conclude that such effects are quite small. Over a year, for example, maximum changes in the longitude of the ascending node are about 10 minutes, and fluctuation in the orbital inclination is less than about 40 seconds. Consequently, the gravitational effects of the sun, moon, and planets may be ignored for almost any conceivable aerospace vehicle situation.
- (2) Gravitational effects of the earth over and above those represented in the assumed gravitational potential of Eq. (15). The basic assumptions leading to Eq. (15) were that the polar axis was a principal axis of inertia, that the moments of inertia about the other two principal axes were equal, and that the higher order oblateness effects were negligible. There is some evidence that a difference exists in the moments of inertia, but none of the assumptions noted are of consequence for the time periods (several orbits as a maximum) and accuracies of interest here.
- (3) Forces on the vehicle due to electromagnetic fields. The vehicle will normally have a magnetic moment and may have a net charge. The first of these is due to magnetic fields originating in internal equipment or, by induction, from the earth's magnetic field. The net electrical charge could arise from frictional effects within the atmosphere (normal build-up of static charge), collection of ions, etc. Reference 12, while noting that a detailed analysis is very

difficult, also conjectures that the force from these sources would be entirely negligible relative to the perturbation force from the oblateness of the earth.

b. Incident Momentum

- (1) Solar radiation forces. To be precise these should be based upon a heliocentric system, and the total effect will be dependent upon the actual configuration.
- (2) Meteorite and cosmic ray bombardment.

c. Aerodynamic Disturbances

Motions of the air mass relative to inertial space enter into the equations presently through the lift and drag. Depending upon the way in which such air mass movements are treated, it may be possible to put them into the form of forcing functions, and hence into the F_d terms.

The above list covers most of the phenomena which could be taken into account, if desired, as part of the disturbance force, F_d . The only additional terms that might be included are due to radiation expulsion from the vehicle, and these might better be considered part of the thrust force.

Besides the assumptions implicit in the above itemizations, Eqs. (17) are valid only when relativistic and tidal friction effects are negligible, and when the attitude motions of the vehicle are completely uncoupled from the translational motions. Reference 12 notes that both tidal and relativistic effects are indeed negligible compared with other quantities included in the equations, and that the rotational and translational motions are essentially decoupled for extra-atmospheric vehicles. However, within the atmosphere the air forces can create significant translational-rotational couplings.

F. SIMPLIFIED EQUATIONS OF MOTION WITH NO OBLATENESS

The major physical forces of interest for aerospace vehicles are included explicitly in Eqs. (17), and the equations themselves are extremely complex and non-linear. The inclusion of the oblateness terms, in particular, is responsible for a large amount of the complexity. The effects due to oblateness are important for long term or extremely precise definition of close-in orbits, but, as might be expected from the size of μ , these effects can be safely ignored when only a few orbital periods and approximate answers are of interest. Accordingly the first

step in simplifying the equations for present purposes is to discard oblateness. (Oblateness effects on orbital behavior will be discussed later in this report.)

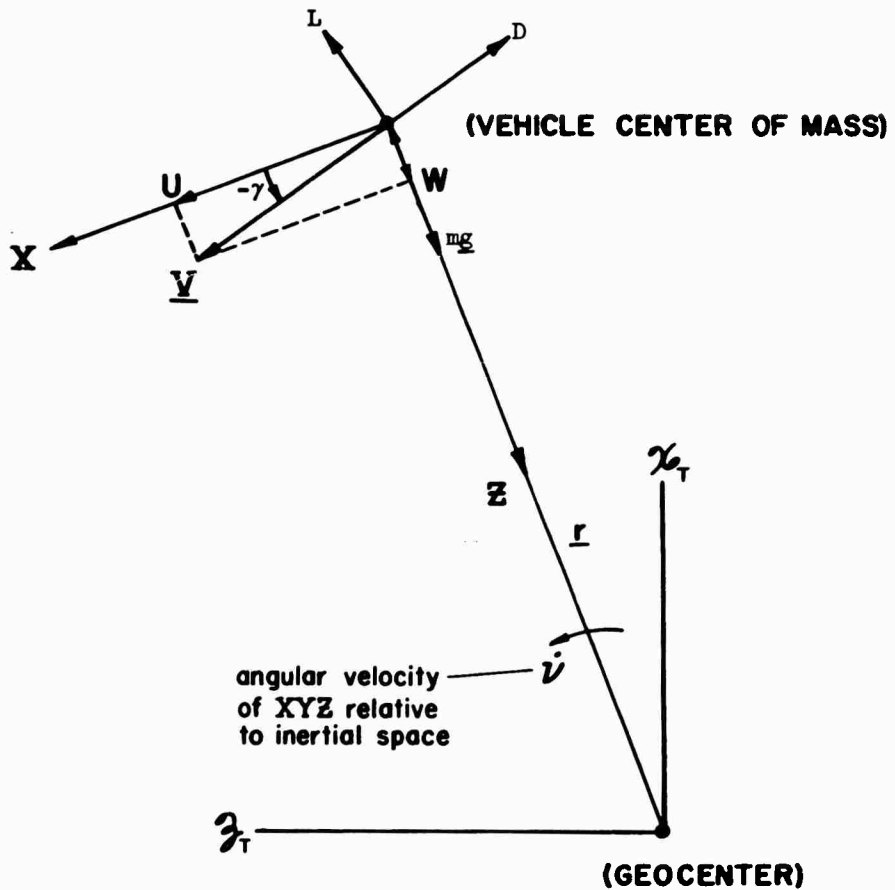
With the oblateness factor removed, it is no longer desirable to keep the $X' Y' Z'$ coordinate system oriented as in Figure 4. Instead, it is now possible, as foretold, to direct the X' axis such that the $X' Z'$ plane contains the velocity vector when the vehicle is in equilibrium flight. The vehicle-centered, geocentrically-directed axis system resulting from this step will be denoted as XYZ , and will henceforth be the reference system of primary interest. The U, V, W and γ, γ_1, Φ_a notation for velocities and flight path angles will be retained, although these components are now understood to lie along, or be referred to, X, Y , and Z instead of X', Y' , and Z' . Inertial space may also be redefined by an X_T, Y_T, Z_T axis system. This new version of inertial space has its origin at the geocenter and is oriented so that the $X_T Z_T$ plane contains the equilibrium flight velocity vector. Also X_T, Y_T, Z_T is nonrotating relative to the XYZ system; and it is not necessary at this time to specify the precise angular relationships between them. Figure 9 illustrates the new axis system structure, and introduces $\dot{\nu}$ as the angular velocity of XYZ relative to inertial space. This is done in anticipation of the true anomaly ν used in the next chapter.

With the equilibrium value of V now contained in the XZ plane, the ratio V/U will always be small relative to unity; then

$$\frac{V^2}{U^2} \ll 1 ; \sin \gamma_1 \doteq \tan \gamma_1 = \frac{V}{U} ; \cos \gamma_1 \doteq 1$$

and Eqs. (17) simplify to

$$\begin{aligned} \dot{U} - \frac{UW}{r} &= \frac{1}{m(t)} \left\{ -D \cos \gamma \left[1 + \frac{L}{D} (\tan \gamma \cos \Phi_a) \right] - L \sin \Phi_a \frac{V}{U} + T_X + F_{d_X} \right\} \\ \dot{V} - \frac{VW}{r} &= \frac{1}{m(t)} \left\{ -D \cos \gamma \frac{V}{U} + L(\sin \Phi_a - \sin \gamma \cos \Phi_a \frac{V}{U}) + T_Y + F_{d_Y} \right\} \\ \dot{W} + \frac{U^2}{r} &= g + \frac{1}{m(t)} \left\{ D \sin \gamma - L \cos \gamma \cos \Phi_a + T_Z + F_{d_Z} \right\} \end{aligned} \quad (19)$$



AXES	UNIT VECTORS	DESCRIPTION
$x_i y_i z_i$	$l_i m_i n_i$	Inertial system with origin at geocenter. x_i plane coincident with equilibrium flight velocity vector.
XYZ	$l m n$	Rotating system with origin at vehicle center of mass. z directed toward geocenter. xz plane coincident with equilibrium flight velocity vector.

Figure 9. Modified Definition of Inertial Space and Radially Directed Rotating Axis System

These equations may be separated into longitudinal and lateral particle dynamics sets if the aerodynamic roll angle is small enough, i.e., $\cos \Phi_a \approx 1$, $\sin \Phi_a \approx \Phi_a$, and $\Phi_a V/U \ll \sin \gamma$. The longitudinal equations of motion are then

$$\begin{aligned}\dot{U} - \frac{UW}{r} &= \frac{1}{m(t)} \left[-D \cos \gamma (1 + \frac{L}{D} \tan \gamma) + T_x + F_{d_x} \right] \\ \dot{W} + \frac{U^2}{r} &= g + \frac{1}{m(t)} \left[D \sin \gamma - L \cos \gamma + T_z + F_{d_z} \right]\end{aligned}\quad (20)$$

and the lateral equation, which is still partially coupled to the longitudinal set through U , is

$$\dot{V} - \frac{VW}{r} = \frac{1}{m(t)} \left[L \Phi_a - D \cos \gamma \frac{V}{U} (1 + \frac{L}{D} \tan \gamma) + T_y + F_{d_y} \right] \quad (21)$$

As noted earlier, Eqs. (20) could have been simply derived by inspection from Figure 2, but all of the implicit assumptions involved would not then have been so clearly delineated.

Although Eqs. (20) and (21) will be considered basic for most of the particle dynamics situations of this report, a set that is even simpler in some respects is also commonly used. These are equations in so-called relative wind axes which are set up by directing the **X** axis along the total velocity vector **V**. (The **XYZ** system would then be true relative wind axes if the atmosphere were fixed relative to inertial space.) The equations of motion for this set of axes can be derived from Eqs. (19) by suitable resolution, remembering that the wind axis system rotates with respect to the radially directed system of Eqs. (19). A much simpler process is to write the equations by inspection of Figure 9, using Eqs. (19) as a guide and noting that, by definition of the axes, there is never any component of velocity normal to **V**. Then,

Longitudinal:

$$\begin{aligned}\dot{V} &= -g \sin \gamma - \frac{D}{m(t)} + T'_x + F'_{d_x} \\ -V\dot{\gamma} + \frac{V^2}{r} \cos \gamma &= g \cos \gamma - \frac{L}{m(t)} \cos \Phi_a + T'_z + F'_{d_z}\end{aligned}\quad (22)$$

Lateral:

$$V\dot{\gamma}_1 = \frac{L}{m(t)} \sin \Phi_a + T'_Y + F'_{dY} \quad (23)$$

where the primed notation on the T and F_d components indicates resolution into the coordinates based upon the total velocity, V. Subsidiary equations, largely definitions, for both Eqs. (20) and (21) or (22) and (23) are

$$\left. \begin{aligned} \gamma_1 &= \frac{V}{U}, \quad \gamma = \sin^{-1} \frac{-W}{V} = \sin^{-1} \frac{dr/dt}{V} = \tan^{-1} \frac{-W}{U} \\ V^2 &= U^2 + W^2; \quad g = \frac{GM}{r^2} \\ \frac{dr}{dt} &= -W = V \sin \gamma = U \tan \gamma = \frac{dh}{dt} \\ q &= \frac{1}{2} \rho V^2 = \frac{1}{2} \rho \frac{U^2}{\cos^2 \gamma} \quad \left(\begin{array}{l} \text{Assumes air mass velocity} \\ \text{relative to inertial space = 0} \end{array} \right) \end{aligned} \right\} \quad (24)$$

Either set of simplified equations is still so complex and nonlinear that no general solution is possible. Therefore, only specific numerical solutions can be obtained if every term in the equations is of consequence to the physical situation being described. Such specific solutions are routine using automatic computation, but physical interpretation generally then requires calculations for a large number of cases involving suitable variations in flight conditions, configuration, etc. Accordingly, it is highly desirable to develop general solutions for further-simplified equations as an adjunct to specific numerical solutions of more exact formulations.

Further simplification can be obtained either by neglecting enough terms to allow the remaining equations to be solved readily, or by restricting the range of the variables to "small perturbations" about steady-state "operating point" conditions. When terms are neglected the resulting equations, which may still be nonlinear, will have meaningful solutions as long as the neglected quantities are physically negligible. On the other hand, keeping all the terms but restricting their perturbations to "small" values always results in a set of linear differential equations. If these are of the constant coefficient type then solution is simple, and the restrictions on the range of the variables is minor considering

the resulting general and easily used information. When the "perturbed" equations are linear with time-varying coefficients, no particular advantage may accrue since such equations are often as difficult to solve as the nonlinear variety. Both techniques are useful devices for the study of aerospace vehicle particle dynamics. In the two chapters immediately following, attention is confined to the longitudinal equations of motion, Eqs. (20), for the two major limiting situations of interest in aerospace vehicles. The first corresponds to extra-atmospheric conditions where both lift and drag are zero, and the second to flight within the atmosphere. In both instances power-off (or free flight) conditions are assumed.

CHAPTER III

SIMPLIFIED EQUATIONS FOR EXTRA-ATMOSPHERIC FREE FLIGHT

Extra atmospheric free flight implies the absence of lift, drag, and thrust forces. Under such conditions Eqs. (20) become

$$\dot{U} - \frac{UW}{r} = 0 \quad (25)$$

$$\dot{W} + \frac{U^2}{r} = g \quad (26)$$

From Figure 9 the angular velocity of **XYZ** relative to inertial space, $\dot{\nu}$, is

$$\dot{\nu} = \frac{U}{r}$$

and $\ddot{\nu} = \frac{\dot{U}}{r} - \frac{U}{r^2} \dot{r}$ or $\dot{U} = r \ddot{\nu} + \frac{U}{r} \dot{r}$

Using these relationships, and noting that $W = -\dot{r}$, $\dot{W} = -\ddot{r}$, and $g = GM/r^2$, Eq. (25) reduces to

$$r \ddot{\nu} + 2 \dot{r} \dot{\nu} = 0 \quad (27)$$

$$\ddot{r} - r \dot{\nu}^2 = -\frac{GM}{r^2} \quad (28)$$

Eqs. (27) and (28) are the familiar classical equations for particle motion in an inverse square field. The properties of this motion have been well known since Newton (e.g., Ref. 6, 9, and 15), so only a few salient features are summarized below.

A. THE AREAL VELOCITY LAW

The constant areal velocity, or angular momentum, property follows directly from Eq. (27), which is equivalent to

$$r^2 \ddot{\nu} + 2r \dot{r} \dot{\nu} = \frac{d}{dt} (r^2 \dot{\nu}) = 0$$

Integrating,

$$r^2 \dot{\nu} = \text{constant} = C \quad (29)$$

Consider now an infinitesimal element of area, $d\underline{S}$, swept out by the radius vector, \underline{r} , over a path length ds , then

$$d\underline{S} = \frac{1}{2} (\underline{r} \times d\underline{s})$$

Since $d\underline{s}/dt$ is the velocity vector \underline{V} , and the linear momentum of the particle is $\underline{p} = m\underline{V}$, the areal velocity becomes

$$\frac{d\underline{S}}{dt} = \frac{1}{2} (\underline{r} \times \frac{d\underline{s}}{dt}) = \frac{1}{2} (\underline{r} \times \underline{V}) = \frac{1}{2m} (\underline{r} \times \underline{p})$$

$\underline{r} \times \underline{p}$ is the angular momentum, \underline{H} , in magnitude also equal to $r(r\dot{\nu})m$ so the areal velocity in terms of the angular momentum per unit mass becomes

$$2 \frac{d\underline{S}}{dt} = \frac{\underline{H}}{m} = r^2 \dot{\nu} = C \quad (30)$$

For this reason the constant C , which physically is the angular momentum per unit mass, is often called the "areal velocity constant." Eq. (30) is a mathematical expression of Kepler's second law: "The radius vector between two gravitating masses sweeps over equal areas in equal times." This is illustrated in Figure 10.

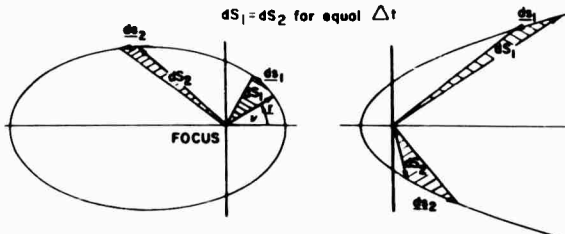


Figure 10. Areal Velocity Relationship

B. INERTIAL SPACE VELOCITIES AND TRAJECTORIES

Eqs. (25) and (26) are the components along X and Z of the vector equation $d\underline{V}/dt = -(GM/r^3)\underline{r}$. In terms of inertial space quantities defined by $X_T Z_T$ coordinates, the scalar equivalent of this vector equation (see Figure 11) is the set:

$$\frac{d\dot{x}_T}{dt} = -\frac{GM}{r^2} \sin v$$

$$\frac{d\dot{y}_T}{dt} = \frac{GM}{r^2} \cos v$$

Using the areal velocity law, $r^2 = C/\dot{v}$, and dividing by $\dot{v} = dv/dt$,

$$\frac{d\dot{x}_T}{dv} = -\frac{GM}{C} \sin v$$

$$\frac{d\dot{y}_T}{dv} = \frac{GM}{C} \cos v$$

Separating the variables and integrating,

$$\dot{x}_T = \frac{GM}{C} \cos v + A \quad (31)$$

$$\dot{y}_T = \frac{GM}{C} \sin v$$

In Eqs. (31) the inertial $\dot{x}_T \dot{y}_T$ system has been oriented to make one of the constants of integration zero, e.g., by directing the axes such that $\dot{y}_T = 0$ when $v = 0$. When this is done the angle v becomes the "true anomaly" of celestial mechanics. Eqs. (31) can be combined to obtain an expression containing both velocity components:

$$(\dot{x}_T - A)^2 + \dot{y}_T^2 = \left(\frac{GM}{C}\right)^2 \quad (32)$$

In $\dot{x}_T \dot{y}_T$ coordinates Eq. (32) is a circle, centered at $\dot{x}_T = A$, $\dot{y}_T = 0$, with radius GM/C as shown in Figure 12. This is the hodograph, or polar diagram of velocity, for the motion. The total velocity is the vector from the origin (pole) to the circle. The "velocity" of this vector in the hodograph plane is equivalent to the acceleration of the particle along its trajectory. V_{\max} and V_{\min} are just

$$V_{\max} = \frac{GM}{C} + A$$

$$V_{\min} = \frac{GM}{C} - A$$

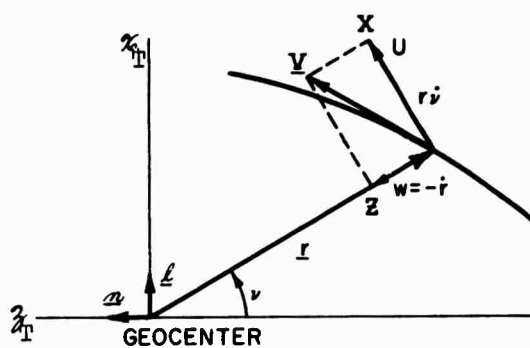


Figure 11. Geometry of Equations of Motion in Inertial Coordinates

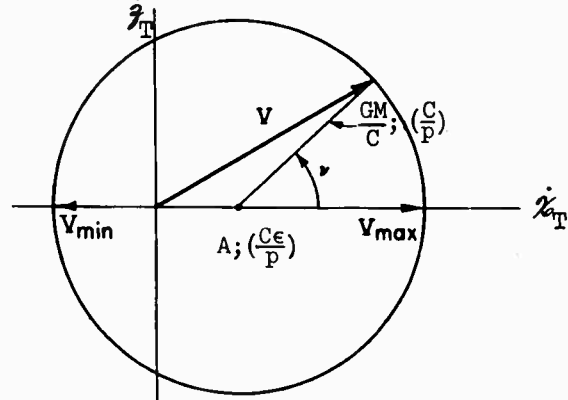


Figure 12. The Hodograph, or Polar Diagram of Velocity

The trajectory may be found from Eqs. (31) without a further integration by resolving into polar coordinates,

$$\begin{aligned}\dot{x}_T &= r \sin \nu & \dot{x}_T &= \dot{r} \sin \nu + r \dot{\nu} \cos \nu \\ \dot{y}_T &= -r \cos \nu & \dot{y}_T &= -\dot{r} \cos \nu + r \dot{\nu} \sin \nu\end{aligned}$$

substituting the result into Eq. (31), and eliminating \dot{r} to obtain

$$r \dot{\nu} = \frac{GM}{C} + A \cos \nu$$

The areal velocity relationship is then used to obtain

$$\frac{1}{r} = \frac{GM}{C^2} + \frac{A}{C} \cos \nu \quad (33)$$

which is the expression for a conic section in polar coordinates with the origin at one of the foci. This may be more readily seen by changing to the form

$$\frac{1}{r} = \frac{1 + \frac{AC}{GM} \cos \nu}{(C^2/GM)} = \frac{1 + \epsilon \cos \nu}{p} \quad (34)$$

where $\epsilon = AC/GM$ and $p = C^2/GM$ are the eccentricity and the parameter (or semilatus rectum), respectively. The radius of the hodograph, GM/C , is then the ratio of the areal velocity constant to the parameter, C/p , and the center of the hodograph is at $\dot{x}_T = A = C\epsilon/p$. The maximum and minimum distances occur when ν is π and zero, respectively.

$$R_A = \frac{p}{1 - \epsilon}, \quad R_p = \frac{p}{1 + \epsilon} \quad (35)$$

The corresponding velocities are

$$\left. \begin{aligned}V_A &= \frac{GM}{C} - A = \frac{GM}{C} (1 - \epsilon) \\ V_p &= \frac{GM}{C} + A = \frac{GM}{C} (1 + \epsilon)\end{aligned}\right\} \quad (36)$$

which are the minimum and maximum velocities on the hodograph. The true anomaly is thus seen to be referenced (i.e., $\nu = 0$) to conditions at perigee; a similar development with the constant, A , changed in sign leads to defining ν with respect to apogee conditions. Both definitions have been used in the literature, but the former seems to be preferred and will be used in this report.

Eq. (34) defines all varieties of Keplerian motion. Some of the features of the several possible conic forms are summarized in Table I.

TABLE I
VARIETIES OF KEPLERIAN MOTION

Trajectory	Eccentricity ϵ	Location of Hodograph Origin	$ V_p $	$ V_A $
Circle	0	Center of hodograph	$\frac{GM}{C}$	$\frac{GM}{C}$
Ellipse	< 1	Hodograph includes origin	$\frac{GM}{C} < V_p < \frac{2GM}{C}$	$0 < V_A < \frac{GM}{C}$
Parabola	1	Hodograph passes through origin	$\frac{2GM}{C}$	0
Hyperbola	> 1	Hodograph excludes origin	$> 2 \frac{GM}{C}$	

For aerospace vehicles the trajectory of primary interest is the ellipse; henceforth, attention shall be devoted only to this form. For an ellipse the semimajor axis, R_a , is just $(R_A + R_p)/2$, and the semiminor axis is $\sqrt{1 - \epsilon^2} R_a$, or

$$\begin{aligned}
 R_a &= \frac{p}{1 - \epsilon^2} \\
 R_b &= \frac{p}{\sqrt{1 - \epsilon^2}} \\
 \epsilon &= \sqrt{1 - \left(\frac{R_b}{R_a}\right)^2}
 \end{aligned}
 \quad \left. \right\} \quad (37)$$

where

Several of these relationships are illustrated in Figure 13, which also shows the "eccentric anomaly," E , and other astronomical terms that are used later, including the radial semivariation, Δh , which is defined as

$$\Delta h = \frac{1}{2} (R_A - R_p) = \epsilon R_a \quad (38)$$

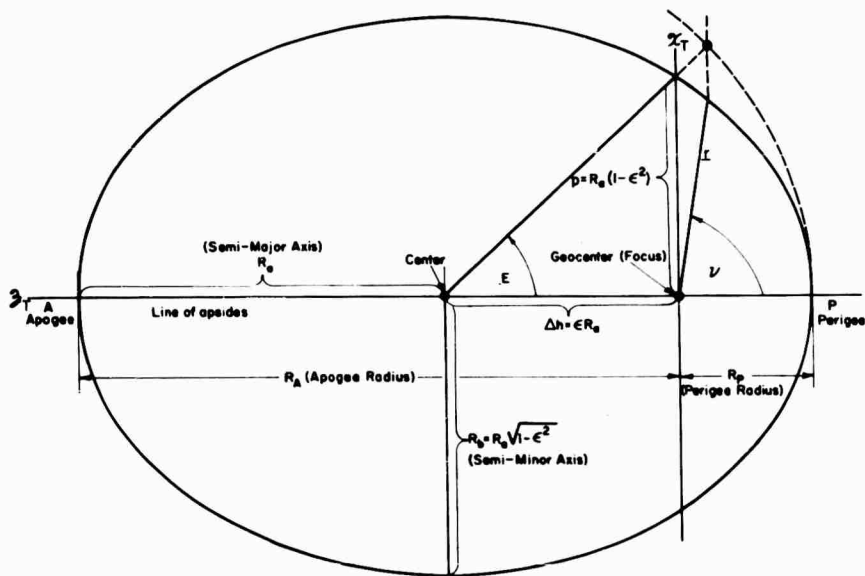


Figure 13. Some Elliptical Orbit Parameters

By re-examining the several equations immediately above, it can be seen that any two of the quantities ϵ , R_A , R_p , R_a , R_b and Δh may be used to describe the orbit. Reference 12 provides a very useful conversion table relating these various quantities which, with slight adaptations, is reproduced here as Table II.

C. VELOCITIES AND TIME BEHAVIOR

Much of the discussion to this point has been concerned with the geometrical properties of extra-atmospheric phases of aerospace vehicle dynamics. The velocities, both linear and angular, of the vehicle-particle are more important to the present report.

The total velocity, V , is given by

$$V^2 = \dot{x}_T^2 + \dot{y}_T^2$$

TABLE II
CONVERSIONS BETWEEN GEOMETRIC PARAMETERS OF ELLIPTIC ORBIT

ASSIGNED PARAMETER PAIRS	DESIRED PARAMETERS					
	MAJOR SEMAxis R_a	MINOR SEMAxis R_b	APOGEE RADIUS R_a	PERIGEE RADIUS R_p	ECCENTRICITY ϵ	RADIAL SEMIvariation Δh
R_a, R_b			$R_a + \sqrt{R_a^2 - R_b^2}$	$R_a - \sqrt{R_a^2 - R_b^2}$	$\sqrt{1 - \frac{R_b^2}{R_a^2}}$	$\sqrt{R_a^2 - R_b^2}$
R_a, R_A		$\sqrt{2R_A R_a - R_A^2}$		$2R_a - R_A$	$\frac{R_A - R_a}{R_a}$	$R_A - R_a$
R_a, R_p		$\sqrt{2R_p R_a - R_p^2}$	$2R_a - R_p$		$\frac{R_a - R_p}{R_a}$	$R_a - R_p$
R_a, ϵ		$R_a \sqrt{1 - \epsilon^2}$	$R_a(1 + \epsilon)$	$R_a(1 - \epsilon)$		ϵR_a
$R_a, \Delta h$		$\sqrt{R_a^2 - \Delta h^2}$	$R_a + \Delta h$	$R_a - \Delta h$	$\frac{\Delta h}{R_a}$	
R_b, R_A	$\frac{1}{2} \left(\frac{R_A^2 + R_b^2}{R_A} \right)$			$\frac{R_b^2}{R_A}$	$\frac{R_A^2 - R_b^2}{R_A^2 + R_b^2}$	$\frac{R_A^2 - R_b^2}{2R_A}$
R_b, R_p	$\frac{1}{2} \left(\frac{R_p^2 + R_b^2}{R_p} \right)$		$\frac{R_b^2}{R_p}$		$\frac{R_b^2 - R_p^2}{R_b^2 + R_p^2}$	$\frac{R_b^2 - R_p^2}{2R_p}$
R_b, ϵ	$\frac{R_b}{\sqrt{1 - \epsilon^2}}$		$R_b \sqrt{\frac{1 + \epsilon}{1 - \epsilon}}$	$R_b \sqrt{\frac{1 - \epsilon}{1 + \epsilon}}$		$\frac{R_b \epsilon}{\sqrt{1 - \epsilon^2}}$
$R_b, \Delta h$	$\sqrt{R_b^2 + \Delta h^2}$		$\sqrt{R_b^2 + \Delta h^2 + \Delta h}$	$\sqrt{R_b^2 + \Delta h^2 - \Delta h}$	$\sqrt{1 - \frac{R_b^2}{R_b^2 + \Delta h^2}}$	
R_A, R_p	$\frac{1}{2} (R_A + R_p)$	$\sqrt{R_A R_p}$			$\frac{R_A - R_p}{R_A + R_p}$	$\frac{R_A - R_p}{2}$
R_A, ϵ	$\frac{R_A}{1 + \epsilon}$	$R_A \sqrt{\frac{1 - \epsilon}{1 + \epsilon}}$		$\frac{R_A(1 - \epsilon)}{1 + \epsilon}$		$\frac{R_A \epsilon}{1 + \epsilon}$
$R_A, \Delta h$	$R_A - \Delta h$	$\sqrt{R_A^2 - 2R_A \Delta h}$		$R_A - 2\Delta h$	$\frac{\Delta h}{R_A - \Delta h}$	
R_p, ϵ	$\frac{R_p}{1 - \epsilon}$	$R_p \sqrt{\frac{1 + \epsilon}{1 - \epsilon}}$	$\frac{R_p(1 + \epsilon)}{1 - \epsilon}$			$\frac{R_p \epsilon}{1 - \epsilon}$
$R_p, \Delta h$	$R_p + \Delta h$	$\sqrt{R_p^2 + 2R_p \Delta h}$	$R_p + 2\Delta h$		$\frac{\Delta h}{R_p + \Delta h}$	
$\epsilon, \Delta h$	$\frac{\Delta h}{\epsilon}$	$\frac{\Delta h}{\epsilon} \sqrt{1 - \epsilon^2}$	$\frac{\Delta h}{\epsilon} + \Delta h$	$\frac{\Delta h}{\epsilon} - \Delta h$		

which, from the hodograph relationships, Eq. (31), can be written

$$V^2 = 2GM \left(\frac{GM}{C^2} + \frac{A}{C} \cos v \right) - GM \left(\frac{GM}{C^2} - \frac{A^2}{GM} \right)$$

From Eq. (33) the first bracketed term is equal to $1/r$; and from the definitions of ϵ and p given in Eq. (34), the second bracketed term becomes

$$\begin{aligned} \frac{GM}{C^2} - \frac{A^2}{GM} &= \frac{GM}{C^2} (1 - \epsilon^2) \\ &= \frac{(1 - \epsilon^2)}{p} = \frac{1}{R_a} \end{aligned}$$

whereby

$$V^2 = GM \left(\frac{2}{r} - \frac{1}{R_a} \right) \quad (39)$$

This is one form of the conservation of energy principle, since V^2 is proportional to the kinetic energy and $GM(2/r - 1/R_a)$ to the potential energy measured from a constant reference, GM/R_a . At an intermediate point in the above development the velocity can be obtained as a function of the true anomaly, i.e.,

$$\begin{aligned} V^2 &= GM \left[\frac{2(1 + \epsilon \cos v)}{p} - \frac{1 - \epsilon^2}{p} \right] \\ V &= \sqrt{\frac{GM}{p}} [1 + 2\epsilon \cos v + \epsilon^2]^{1/2} \\ &= \frac{GM}{C} [1 + 2\epsilon \cos v + \epsilon^2]^{1/2} \end{aligned} \quad (40)$$

The quantity GM/C which appears here and in other places throughout this chapter is, as noted earlier, the radius of the hodograph plot. It can be delineated in physical terms directly from the definitions of GM and C , but C may itself have little direct physical significance for most readers. Accordingly, a few alternative expressions for this quantity which may lead to easier interpretation are listed below.

$$\begin{aligned}
 \frac{GM}{C} &= \frac{\mathbf{V}_A + \mathbf{V}_P}{2} \\
 &= \frac{\mathbf{V}_P}{1 + \epsilon} = \frac{\mathbf{V}_P}{2} \left(1 + \frac{R_P}{R_A}\right) \\
 &\doteq \frac{\mathbf{V}_{avg}}{\sqrt{\left(1 - \frac{\epsilon^2}{2}\right)\left(1 - \epsilon^2\right)}} \doteq \mathbf{V}_{avg} \left(1 + \frac{3}{4} \epsilon^2\right) \\
 &= \omega_b \frac{R_a^2}{R_b}
 \end{aligned} \tag{41}$$

The last two expressions involve ω_b , the mean motion, and \mathbf{V}_{avg} , the mean orbital velocity, both of which are treated in the following paragraphs [see Eqs. (45) and (47)]. The first expression follows directly from Eq. (36), and the second is a variant of the first. The first is perhaps the most physically satisfying, and shows that the quantity is the average of the maximum and minimum orbital speeds. For a circular orbit with $\mathbf{V}_A = \mathbf{V}_P = \mathbf{V}_C$, $GM/C = \mathbf{V}_C$ which follows directly from either the first three expressions above, or from Eq. (40). The "circular velocity," \mathbf{V}_C , is discussed further later.

The flight path angle,

$$\gamma = \tan^{-1} \frac{-W}{U} = \tan^{-1} \frac{r}{r\nu} \tan^{-1} \frac{1}{r} \frac{dr}{d\nu}$$

may be obtained by operating on Eq. (34) to give

$$\tan \gamma = \frac{\epsilon \sin \nu}{1 + \epsilon \cos \nu} \tag{42}$$

This relationship, converted into the triangle of Figure 14, allows the direct determination of the horizontal and vertical velocity components U and W as

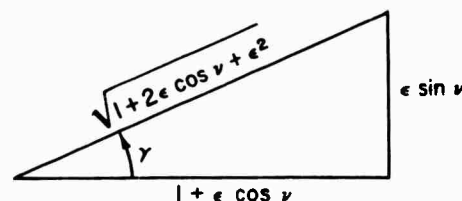


Figure 14. Flight Path Angle Relationships

$$U = V \cos \gamma = \frac{GM}{C} (1 + \epsilon \cos \nu) \quad (43)$$

$$W = -V \sin \gamma = -\frac{GM}{C} \epsilon \sin \nu$$

The fundamental time parameter is the orbital period, T . Since the areal velocity is a constant, and equal to $C/2$, the period will be simply

$$T = \frac{2S}{C}$$

where S is the total area swept out by the radius vector in a complete period. Since the trajectory is an ellipse, which has an area equal to $\pi R_a R_b$, the orbital period will be

$$T = \frac{2\pi R_a R_b}{C} = \frac{2\pi p^2}{(\sqrt{1 - \epsilon^2})^3 C} = \frac{2\pi R_a^2 \sqrt{1 - \epsilon^2}}{C} \quad (44)$$

or

$$T^2 = \frac{4\pi^2 R_a^4 (1 - \epsilon^2)}{C^2} = \frac{4\pi^2}{GM} R_a^3$$

The last is an expression of Kepler's third law, i.e., "The squares of the periodic times are proportional to the cubes of the major axes." From Eq. (44) the mean orbital angular velocity, ω_0 , called the "mean motion," is

$$\omega_0 = \frac{2\pi}{T} = \frac{C}{R_a R_b} = \frac{C(1 - \epsilon^2)^{3/2}}{p^2} = \sqrt{\frac{GM}{R_a^3}} \quad (45)$$

The mean orbital velocity, V_{avg} , can now be computed by simply dividing the distance traveled in one revolution by the period. The perimeter of an ellipse is

$$\begin{aligned} s_p &= 4R_a \int_0^{\pi/2} \sqrt{1 - \epsilon^2 \sin^2 x} dx \\ &= 4R_a E \\ &= 2\pi R_a \left(1 - \frac{\epsilon^2}{2^2} - \frac{3\epsilon^4}{2^2 4^2} - \dots\right) \\ &\doteq 2\pi R_a \sqrt{\frac{2 - \epsilon^2}{2}} = \sqrt{2} \pi \sqrt{R_a^2 + R_b^2}, \quad \epsilon^2 \ll 1 \end{aligned}$$

where E is the complete elliptic integral of the second kind. The mean orbital velocity is then

$$V_{\text{avg}} = \frac{s_p}{T} = \frac{4R_a E}{2\pi R_a} \sqrt{\frac{GM}{R_a}} = \frac{2}{\pi} \sqrt{\frac{GM}{R_a}} E \quad (46)$$

Using the approximate expression valid for $\epsilon^2 \ll 1$,

$$V_{\text{avg}} \doteq \sqrt{\frac{GM(2 - \epsilon^2)}{2R_a}} \doteq \frac{GM}{C} \sqrt{(1 - \frac{\epsilon^2}{2})(1 - \epsilon^2)} \quad (47)$$

When the eccentricity becomes zero the linear velocities all become equal to V_c (with the exception of W , which becomes zero), i.e.,

$$V = U = V_{\text{avg}} = V_c = \frac{GM}{C} = \sqrt{\frac{GM}{p}} = \sqrt{\frac{GM}{r_c}} = \sqrt{gr_c} = a_e \sqrt{\frac{g_e}{r_c}} \quad (48)$$

where V_c is the radius of the circular orbit, and g_e is the acceleration due to gravity at the earth's surface. The mean motion for this same condition is

$$\omega_0 = \sqrt{\frac{GM}{r_c^3}} = \sqrt{\frac{g}{r_c}} = \frac{a_e}{r_c} \sqrt{\frac{g_e}{r_c}} = \frac{V}{r_c} \quad (49)$$

The angular velocity of the vehicle on the orbit, and hence the angular velocity of the XZ axes relative to inertial space, may be obtained from the areal velocity law, i.e.,

$$\begin{aligned} \dot{v} &= \frac{C}{r^2} = \frac{C}{p^2} (1 + \epsilon \cos \nu)^2 \\ &= \frac{\omega_0}{\sqrt{1 - \epsilon^2}} \left(\frac{1 + \epsilon \cos \nu}{\sqrt{1 - \epsilon^2}} \right)^2 \end{aligned}$$

Separating the variables and integrating,

$$\int \omega_0 dt = (1 - \epsilon^2)^{3/2} \int \frac{d\nu}{(1 + \epsilon \cos \nu)^2} \quad (50)$$

which becomes, if $v = 0$ when $t = 0$,

$$\begin{aligned}\omega_0 t &= 2 \tan^{-1} \left[\sqrt{\frac{1-\epsilon}{1+\epsilon}} \tan \frac{v}{2} \right] + \frac{\epsilon \sqrt{1-\epsilon^2} \sin v}{1+\epsilon \cos v} \\ &= 2 \tan^{-1} \left[\sqrt{\frac{1-\epsilon}{1+\epsilon}} \tan \frac{v}{2} \right] - \sqrt{1-\epsilon^2} \tan \gamma \quad (51)\end{aligned}$$

$$\begin{aligned}\doteq v - \tan \gamma, \text{ when } \epsilon^2 \ll 1 \\ \doteq v - \gamma \quad (52)\end{aligned}$$

The last step, Eq. (52), follows from Eq. (51) because $\tan \gamma \doteq \gamma$ when ϵ is small. The simple form of Eq. (52) allows the physically satisfying picture of Figure 15 to be drawn. Here the "mean anomaly," $\omega_0 t$, is approximately given by the angle

between the line through perigee and a radial line drawn normal to the tangential velocity vector at the true anomaly, v . The relationship between the mean and the eccentric anomaly (see Figure 13) is given by "Kepler's equation" (Ref. 15).

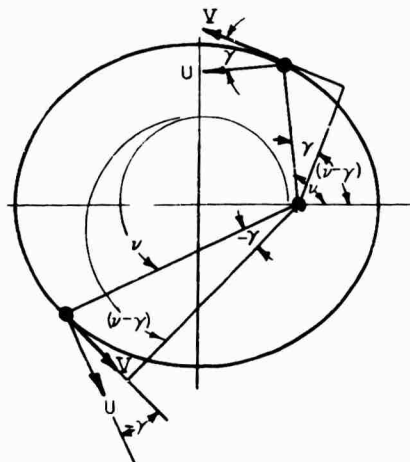


Figure 15. Approximate Geometric Relationship Between Mean and True Anomaly

before integrating. The result (Ref. 15) is

$$\omega_0 t = v - 2\epsilon \sin v + \frac{3\epsilon^2}{4} \left(1 + \frac{\epsilon^2}{6} \right) \sin 2v - \frac{\epsilon^3}{3} \sin 3v + \dots \quad (54)$$

Another series, essentially the reverse of Eq. (54), which gives the true anomaly as a periodic function of the mean anomaly, can also be derived (Reference 15).

$$v = \omega_0 t + 2\epsilon \left(1 - \frac{\epsilon^2}{8} \right) \sin \omega_0 t + \frac{5\epsilon^2}{4} \left(1 - \frac{11\epsilon^2}{30} \right) \sin 2\omega_0 t + \dots \quad (55)$$

Finally, the radius as a function of time (again with $t = 0$ when $v = 0$) can be developed by noting that

$$\frac{dv}{dt} = \sqrt{1 - \epsilon^2} \omega_0 \left(\frac{1 + \epsilon \cos v}{1 - \epsilon^2} \right)^2 = \sqrt{1 - \epsilon^2} \omega_0 \left(\frac{R_a}{r} \right)^2$$

so $\frac{dv}{d(\omega_0 t)} = \sqrt{1 - \epsilon^2} \left(\frac{R_a}{r} \right)^2$

and from Eq. (55)

$$\left(\frac{R_a}{r} \right)^2 = \frac{1}{\sqrt{1 - \epsilon^2}} \left\{ 1 + 2\epsilon \left(1 - \frac{\epsilon^2}{8} \right) \cos \omega_0 t + \frac{5\epsilon^2}{2} \left(1 - \frac{11\epsilon^2}{30} \right) \cos 2\omega_0 t + \dots \right\} \quad (56)$$

D. ORBIT SPECIFICATIONS

As noted previously, the size and shape of a particle's orbit about a sphere of much larger mass is specified completely by a knowledge of any two of the trajectory parameters:

R_a	Semimajor axis
$R_b = R_a \sqrt{1 - \epsilon^2}$	Semiminor axis
$\epsilon = \sqrt{1 - \left(\frac{R_b}{R_a} \right)^2}$	Eccentricity
$R_A = R_a(1 + \epsilon)$	Radius at apogee
$R_p = R_a(1 - \epsilon)$	Radius at perigee
$\Delta h = \epsilon R_a = \frac{R_A - R_p}{2}$	Radial semivariation
$p = R_a(1 - \epsilon^2)$	The parameter, or semilatus rectum

However, such knowledge is not sufficient to define the spatial orientation, as a function of time, of the particle relative to coordinates imbedded in the sphere. The first additional requirement is to establish a reference time, thereby completing the definition of the trajectory within the orbital plane. A convenient reference time is that corresponding to apogee or perigee passage. Of these two, perigee passage is the more commonly used. This time, plus any two of the above parameters, completely specifies the orbit.

Besides the location of the particle on its orbit, the orientation of the orbital plane relative to an axis system in the principal gravitating body is of consequence. In an idealized situation, a natural choice for the reference axes is a rectangular system fixed in inertial space with the origin at the center of the gravitating body. For the case of a spherical homogeneous earth with no oblateness, the orientation of the axes is a matter of convenience. The $x_T y_T z_T$ axes, considered inertial in the last articles (and illustrated in Figure 11), were chosen on this basis. When the earth's oblateness is to be taken into account, this arbitrary definition of inertial space is no longer permissible. Instead, a basic reference frame like the $x y z$ system shown in Figure 3 is appropriate. In general, the orbital plane and line of apsides will rotate relative to this reference frame. The angular velocities of these rotations will ordinarily make only small contributions to the total angular velocity of the vehicle, but it is still desirable to have some idea of their magnitude.

To present such magnitude information, and also to develop the fact that additional quantities over and above those already developed are required to describe the total trajectory situation, it is first necessary to define angles and axes which orient the trajectory plane relative to the $x y z$ version of inertial space. The ultimate axis set defining the trajectory plane is to have the same origin as the $x y z$ inertial axes system — at the focus of the trajectory. Two axes of this set will be chosen to lie in, and the third to be normal to, the orbital plane.

The trajectory plane axes should also be compatible with the requirements and desires set forth on page 8. These requirements imply that the axis normal to the orbital plane be designated z_T . Also, if the coordinate system origin were translated to the trajectory, the z_T axis should point toward the geocenter, and the x_T axis along the trajectory. The two axes in the orbital plane should also reflect the requirement that a specific point of reference on the trajectory is needed to define a time origin. All of these requirements are met if the $-z_T$ axis is directed toward perigee. With the directions of y_T and z_T specified in this way, the x_T axis naturally falls along an appropriate line which is coincident with the semilatus rectum of the trajectory. The directional sense of the x_T axis is not yet uniquely determined, so this sense is arbitrarily made compatible with a west to east vehicle trajectory.

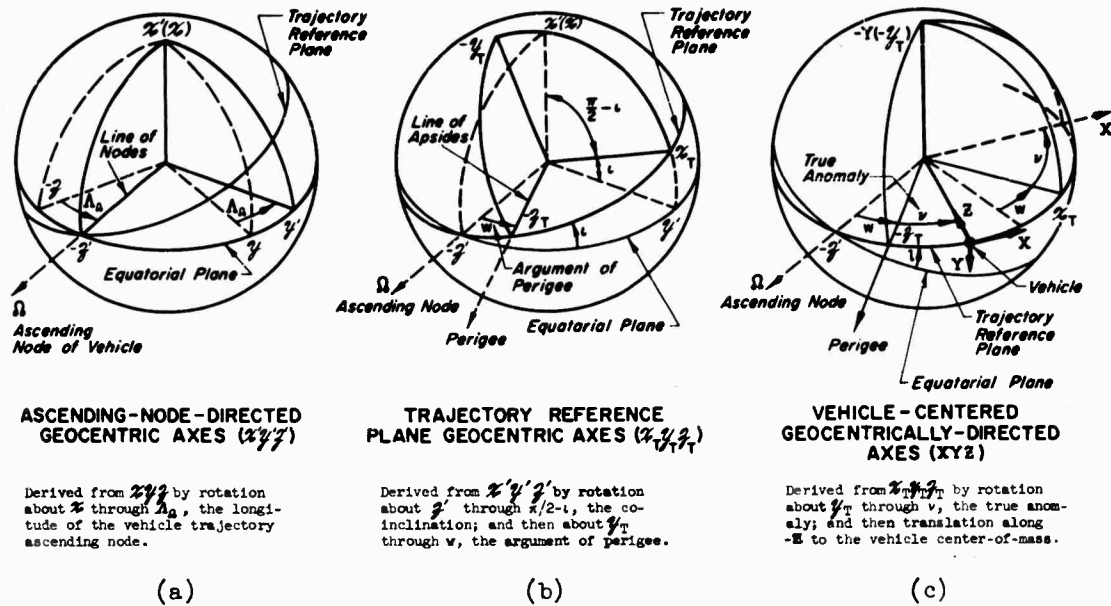


Figure 16. Orientation of the Trajectory Plane Relative to Inertial Space

This trajectory plane axis system can now be referred by orientation angles to the inertial axis system $X'Y'Z'$. The evolution is illustrated in Figure 16. As the vehicle crosses the equatorial plane, two orientation elements between the equatorial and orbital planes are immediately apparent. The first is the point at which the vehicle trajectory ascends the equator, called the ascending node. This is located by an angle Λ_0 , the arc measured eastward along the celestial equator from the vernal equinox to the ascending node. Λ_0 is referred to as the longitude of the ascending node. Thus the first intermediate axis system between "inertial space," $X'Y'Z'$, and the trajectory plane axes is the $X'Y'Z'$ ascending node-directed system of Figure 16(a).

The second orientation element between the two planes is the orbital inclination angle, i . To take this orientation element into account an intermediate axis system (between $X'Y'Z'$ and $X_T Y_T Z_T$) is formed by rotating $X'Y'Z'$ about Z' through an angle $\pi/2 - i$, the coinclination. This intermediate system (not shown in Figure 16) defines the orbital plane, i.e., Y_T , but does not provide a reference point or line (major axis) for the orbit itself. To do this, an angle, w , the "argument of perigee," is chosen in the orbital plane to measure the arc from the ascending node to the perigee point. The trajectory plane reference system is

then established by rotating the intermediate axes about \mathcal{Y}_T through ω [see Figure 16(b)].

With the trajectory reference plane geocentric axes as now developed, the entire trajectory is defined from the viewpoint of an observer fixed relative to the \mathcal{XYZ} "inertial" system. It should now be apparent that six quantities are required to specify the total trajectory situation, three to define the orbital plane and an orbit plane reference line, and three to define the actual vehicle time history in the orbital plane.

One final axis system is required to tie in the present rather involved set of references with the simplified situation of Figures 9, 11, and 13. This is the vehicle-centered, geocentrically-directed system \mathbf{XYZ} . These axes are derived from \mathcal{XYZ}_T by rotation about \mathcal{Y}_T through the true anomaly, ν , to form axes with an origin which is then translated to the vehicle center-of-mass [Figure 16(c)]. For normal aircraft stability and control purposes, the angular velocity of \mathbf{XYZ} (which is just $\dot{\nu}$ if the principal gravitating body is a homogeneous sphere) is ordinarily small enough to be neglected. For these circumstances, the earth can be considered flat, and \mathbf{XYZ} takes on the character of inertial space.

When the rigid body motions of the vehicle are considered, further axis systems are required. Some of these are illustrated in the appendix, together with a summary of all the systems discussed here. The appendix also contains figures relating the Northerly- and Geocentrically-Directed System (Figure 4) with the \mathbf{XYZ} axes via a northerly heading angle ψ_N .

For the case of a single central gravitating body which can be considered as either a particle or a homogeneous sphere, all of the script axes, \mathcal{XYZ} , \mathcal{XYZ}' , and \mathcal{XYZ}_T , possess the qualities of inertial space in that none of them rotates relative to the \mathcal{XYZ} inertial reference frame. When spherical asymmetry or aerodynamic drag is present, however, the orbit is no longer fixed relative to inertial space. For example, oblateness effects will cause angular velocities $\dot{\alpha}$, $d\epsilon/dt$, \dot{w} , and have other influences on the orbital situation. A cursory summary of variations due to oblateness and drag is given below.

E. GENERAL EFFECTS OF OBLATENESS AND AERODYNAMIC DRAG ON THE IDEALIZED TRAJECTORY

As mentioned several times above, there are a number of forces which tend to perturb the classical Keplerian orbit of a vehicle. Of these, the disturbances

caused by the attraction of the sun, moon, and planets, solar pressure, the earth's electromagnetic field, meteorite impact, etc., are all small relative to those due to earth's oblateness and atmospheric drag. A great deal of attention has recently been given to the first-order effects of both these perturbing influences, and the qualitative consequences are well understood. Quantitatively, the effects of oblateness on orbital behavior are more accurately predictable than those due to air drag. This follows because the magnitude of the oblateness is fairly well known, while the detailed characteristics of the upper atmosphere and the aerodynamic characteristics of vehicles traveling therein are not. Also, to a first order, the oblateness effects are independent of vehicle configuration, while aerodynamic effects are heavily dependent upon configuration details.

In terms of the five geometrical orbital elements (ϵ , R_a , w , ι , and Λ_Ω), and the period (T), oblateness and air drag have the following major first order effects:

Oblateness Effects

- (a) Secular, or aperiodic, rotation of the line of nodes (causing a $\dot{\Lambda}_\Omega$) and of the semimajor axis relative to the line of nodes (causing a component of \dot{w}).
- (b) Periodic variations of the semimajor axis (R_a), eccentricity (ϵ), period (T), and inclination (ι).

Aerodynamic Drag Effects

- (a) Secular decreases in R_a , ϵ , and T , at ever increasing rates.
- (b) Periodic variation in the argument of perigee (w).

A large number of investigators have studied these effects for close satellites (e.g., Ref. 12 and 16-22). In particular, Ref. 21 presents a detailed treatment which includes working equations for the changes in orbital elements due to oblateness and air drag. These changes are expressed there as functions of the true anomaly, v , or the eccentric anomaly, E , (both measured from perigee) and of the elements (R_{a0} , ϵ_0 , ι_0 , w_0) of an "initial" elliptical orbit. This initial elliptical orbit may be thought of as one established about a spherical earth with no atmosphere. The changes in orbital elements are then brought about by "turning on" the oblateness and atmospheric drag as if they were thrust terms. A summary of some of the simpler results given in Ref. 21 is presented below to give some idea of the magnitudes and forms of the various effects on the orbital elements.

Longitude of the Ascending Node (Ω) — Air drag has no effect on the position of the line of nodes. Oblateness, however, rotates the plane of the orbit about the earth's polar axis an amount, $\Delta\Omega$, which, for a vehicle in circular orbit, is given by

$$\Delta\Omega = -3\mu \left(\frac{a_e}{R_a}\right)^2 [v - \sin v \cos (2w_0 + v)] \cos i_0 \quad (57)$$

A similar result is obtained in Ref. 12 which shows that a rotating reference frame can be found in which the orbital variations are periodic. This reference orbital plane will have an angular rate

$$\frac{d\Omega}{dv} = -3\mu \frac{(GM)^2 a_e^2}{C^4} \cos i_{avg} = -3\mu \left[\frac{a_e}{R_a(1 - \epsilon^2)} \right]^2 \cos i_{avg} \quad (58)$$

where i_{avg} is the mean inclination of the orbital plane. The general effect described by Eqs. (57) and (58) can be visualized as a slow rotation of the line of nodes in the earth's equatorial plane as the vehicle proceeds on its orbital path. The line of nodes will "regress," i.e., rotate clockwise as seen from the north pole, when $i_0 < 90^\circ$, and will "progress" when $i_0 > 90^\circ$. The existence of this rotating orbital plane, within which the orbit is periodic, is one good way of considering the major secular, or aperiodic, effects of oblateness. From Ref. 21 again, in one revolution this rotation amounts, in general, to

$$\Delta\Omega = -0.589 \left[\frac{a_e}{R_{a_0}(1 - \epsilon_0^2)} \right]^2 \cos i_0 \quad (\text{deg/revolution}) \quad (59)$$

and the mean rate of rotation of the plane of the orbit about the polar axis is

$$\dot{\Omega} = -10.05 \left[\frac{a_e}{R_{a_0}(1 - \epsilon_0^2)} \right]^{3.5} \cos i_0 \quad (\text{deg/day}) \quad (60)$$

This effect is illustrated in Figure 17.

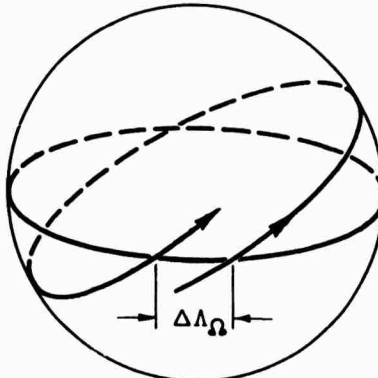


Figure 17. Regression of the Ascending Node

Inclination of the Orbital Plane (ι) — Drag does not influence the orbital plane inclination, although oblateness does cause an oscillation of this plane about the line of nodes. The amplitude of this oscillation for a circular orbit is

$$\Delta\iota = -\frac{3}{2}\mu \left(\frac{a_e}{R_a}\right)^2 \sin 2\iota_0 \sin v \sin (2w_0 + v) \quad (61)$$

Argument of Perigee (w) — Both oblateness and air drag rotate the line of apsides (major axis). The air drag, if acting alone, would result in an "effective" perigee which, as the vehicle goes around the earth, would oscillate about the actual perigee with a period equal to the orbital period. Oblateness results in a secular rotation of the line of apsides. This rotation will be in the same direction as satellite motion for inclination angles less than about $63\frac{1}{2}^\circ$, and in the opposite direction for higher values. The secular effect alone may be considered by examining the Δw which exists at times when the air drag effect is zero. This occurs when the vehicle is at perigee. After one revolution the perigee has moved, due to oblateness, through an angle

$$\Delta w = -3\pi\mu \left[\frac{a_e}{R_a(1 - \epsilon_0^2)} \right]^2 (1 - 5 \cos^2 \iota_0) \quad (62)$$

The mean rate for one revolution is then obtained by dividing by the orbital period, Eq. (44), whereby

$$\dot{w}_{avg} = -5.0 \left(\frac{a_e}{R_a} \right)^{3.5} \frac{(1 - 5 \cos^2 \iota_0)}{(1 - \epsilon_0^2)^2} \text{ (deg/day)} \quad (63)$$

A general illustration of this secular effect is presented in Figure 18.

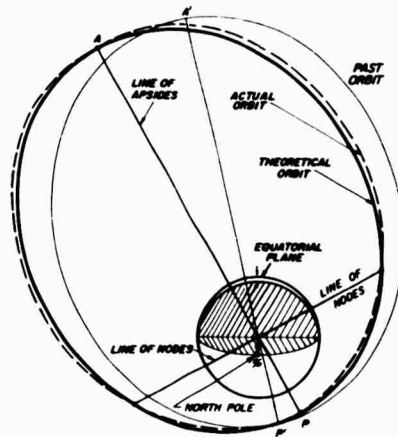


Figure 18. Departure of Vehicle from Conic and Rotation of Line of Apsides

Semimajor Axis (R_a) — Since the energy level of an extra-atmospheric vehicle is proportional to $1/R_a$, (Eq. 39), any dissipation forces, such as air drag, will be directly reflected in the length of the semimajor axis. R_a is also influenced by oblateness in a periodic fashion. This latter effect, illustrated in Figure 18, tends to alter the conic form of the trajectory with the vehicle traveling slightly outside its ideal elliptical orbit when near the equator, and slightly inside when near the apex of the trajectory. For a circular orbit, the change in R_a is

$$\frac{\Delta R_a}{R_{a_0}} = -6\mu \left(\frac{a_e}{R_{a_0}}\right)^2 \sin v \sin (2w_0 + v) \sin^2 \iota_0 + \frac{C_D S \rho R_{a_0}}{m} v \quad (64)$$

The change due to oblateness is periodic, and vanishes at apogee ($v = \pi$) and perigee ($v = 0$). The secular variation per revolution is given by the drag term. For an assumed orbital altitude of 200 nautical miles and $C_D S/m = 6.44$, $\Delta R_a/R_{a_0}$ per revolution is of the order of 2×10^{-6} .

Eccentricity (ϵ) — The eccentricity of the orbit is continually decreased by combined air drag and oblateness, although the latter influence is oscillatory and vanishes at perigee. A primary effect of drag is to "circularize" the orbit, since the apogee changes much more rapidly than the perigee. The oblateness effect alone is maximum at apogee, with a change in "local" eccentricity equal to

$$\Delta \epsilon = -6\mu \left[\frac{a_e}{R_{a_0}(1 - \epsilon_0^2)} \right]^2 \left[(1 + \frac{\epsilon_0^2}{3})(1 - 3 \sin^2 \iota_0 \sin^2 w_0) - \frac{2}{3}(1 - \epsilon_0^2) \sin^2 \iota_0 \cos 2w_0 \right] \quad (65)$$

Period (T) — A decrease in period occurs due to combined oblateness and air drag. For a circular orbit the average change in period per revolution is

$$\frac{\Delta T_{avg}}{T_0} = -\frac{3}{2}\mu \left(\frac{a_e}{R_{a_0}}\right)^2 \sin^2 \iota_0 \cos 2w_0 - \frac{3}{2} \frac{\rho S C_D}{m} R_{a_0} (R_{a_0} - a_e) \quad (66)$$

Eq. (66) indicates that there is a difference in period between a satellite on an inclined orbit and one on an equatorial orbit. This difference, in seconds, considering oblateness alone, is

$$-12.65 \left(\frac{a_e}{R_{a_0}}\right)^{1/2} \sin^2 \iota_0 \cos 2w_0 \quad (67)$$

For more general formulas the reader should see Ref. 21.

It can be appreciated from the foregoing summary that, for time spans of the order of a few orbital periods, all oblateness and drag effects are ordinarily of

negligible consequence from the standpoint of vehicle stability and control if any reasonable level of automatic or manual control is present. This statement is not valid for precision orbit determination, many guidance situations, and very long time, trimming only, flight control operations. In any event, the above discussion and simplified formulas are helpful in determining whether or not these effects should be taken into account in a given problem.

CHAPTER IV

SIMPLIFIED EQUATIONS FOR POWER-OFF FLIGHT WITHIN THE ATMOSPHERE

When attention is confined to power-off flight well within the atmosphere where the air forces are much larger than those due to oblateness and external disturbances, a good representation of the true motions of the vehicle-particle is obtained by modifying Eqs. (20) and (24) to

$$\left. \begin{aligned} \dot{U} - \frac{UW}{r} &= -\frac{D}{m} (\cos \gamma + \frac{L}{D} \sin \gamma) = -q \frac{C_D S}{m} (\cos \gamma + \frac{C_L}{C_D} \sin \gamma) \\ \dot{W} + \frac{U^2}{r} &= g - \frac{L}{m} \cos \gamma + \frac{D}{m} \sin \gamma = g + q \frac{C_D S}{m} (\sin \gamma - \frac{C_L}{C_D} \cos \gamma) \\ \dot{h} &= -W = U \tan \gamma \end{aligned} \right\} \quad (68)$$

$$\text{where } q = \frac{1}{2} \rho \frac{U^2}{\cos^2 \gamma}, \quad g = \frac{GM}{r^2}, \quad h = r - a_e$$

To complete this set requires that the atmospheric density, ρ , be connected with the motion variables (Ref. 23).

For a perfect gas the ambient pressure in terms of the density is given by

$$p = \rho \frac{RT}{M}$$

where R is the universal gas constant, T the ambient absolute temperature, and M the molecular weight of the gas. The ratio of total differential to ambient pressure is, then,

$$\frac{dp}{p} = \frac{dp}{\rho} + \frac{dT}{T} - \frac{dM}{M}$$

Over a large part of the atmosphere, especially those regions where the aerodynamic forces are of major consequence in the particle dynamics problem,

$$\left| \frac{dp}{\rho} \right| \gg \left| \frac{dT}{T} \right|, \left| \frac{dM}{M} \right|$$

and

$$\frac{dp}{p} \doteq \frac{dp}{\rho}$$

When the atmosphere is in, or approximates, hydrostatic equilibrium, the ambient pressure variation with altitude is

$$dp = -\rho g dh$$

then

$$\frac{dp}{p} = -\frac{Mg}{RT} dh = -\beta dh \doteq \frac{dp}{\rho}$$

and, to the extent that β is independent of h ,

$$\rho \doteq \rho_0 e^{-\beta h} \text{ where } \beta \equiv \frac{Mg}{RT} \quad (69)$$

Reference 23 compares this exponential atmosphere with the ARDC 1956 model atmosphere when the following values are used for the parameters listed:

$$\rho_0 = 0.0027 \text{ slug/ft}^3$$

$$\frac{1}{\beta} = 23,500 \text{ ft}$$

$$\sqrt{\beta a_e} = 30$$

Two figures appearing there are reproduced here as Figures 19 and 20, and justify, for present purposes, the exponential model as a first approximation (although βa_e will vary with temperature, etc., to add an additional 10% or so variation in $\sqrt{\beta a_e}$ over and above that shown in Figure 20).

Eq. (69) completes the set of Eqs. (68), but to obtain solutions in terms of literal (rather than numerical) values of the parameters requires further simplification of the equations. This can be accomplished either by neglecting terms or by linearizing the equations. The first possibility is explored below, while linearization is the subject of the next chapter.

In the general region of interest, the fractional change in the radius, r , is small relative to the fractional change in forward velocity, i.e.,

$$\left. \begin{aligned} \frac{dr}{r} &\ll \frac{dU}{U} \\ \left| \frac{\frac{dr}{r}}{\frac{dU}{U}} \right| &= \left| \frac{\frac{1}{r} \frac{dr}{dt}}{\frac{1}{U} \frac{dU}{dt}} \right| = \left| \frac{UW}{r} \right| \ll 1 \end{aligned} \right\} \quad (70)$$

or

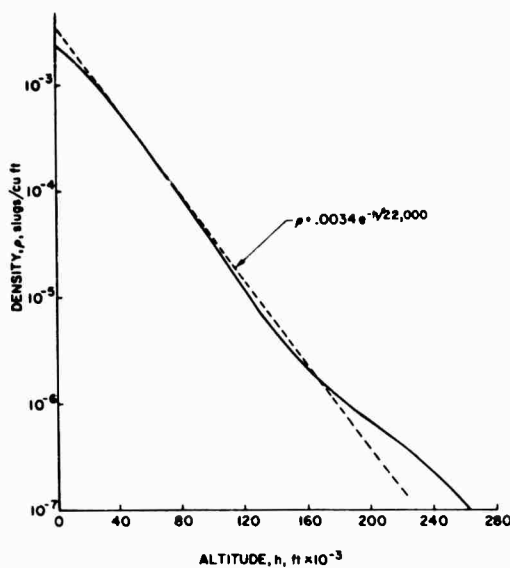


Figure 19. Comparison of Exponential with ARDC 1956 Model Atmosphere

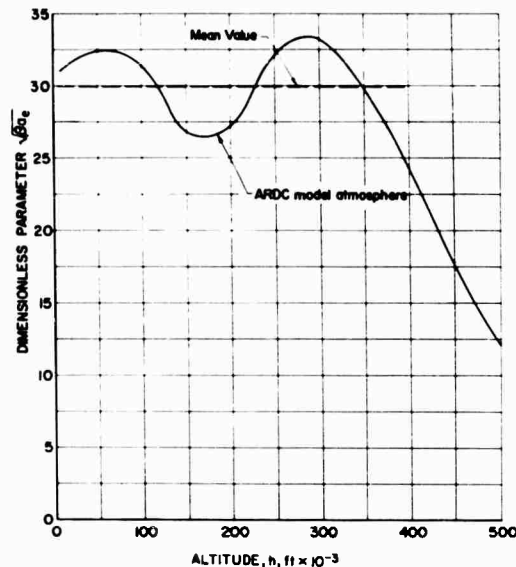


Figure 20. Comparison of Mean Value with ARDC Model Atmosphere

Above some altitude this inequality obviously will not hold, since in extra-atmospheric free flight Eq. (25) gives

$$\dot{U} = \frac{UW}{r}$$

However, Reference 23 shows that only a small decrease in velocity below orbital conditions is required to make the inequality of Eq. (70) a reasonably good one. For example, in a typical re-entry, $dr/r = 0.1(dU/U)$ at a point where drag has slowed the vehicle by only a percent or so of its orbital velocity. Situations for which the assumption is reasonably valid are illustrated in Figure 21.

Another simplification to the equations stems from the fact that kinetic energy changes are much larger than potential energy changes for the general flight regime of interest here. The product $(L/D) \tan \gamma$ is, accordingly, usually small relative to unity. This is always true in pure ballistic (zero lift) flight, but, with lift present, the magnitude of the acceleration, \dot{U} ,

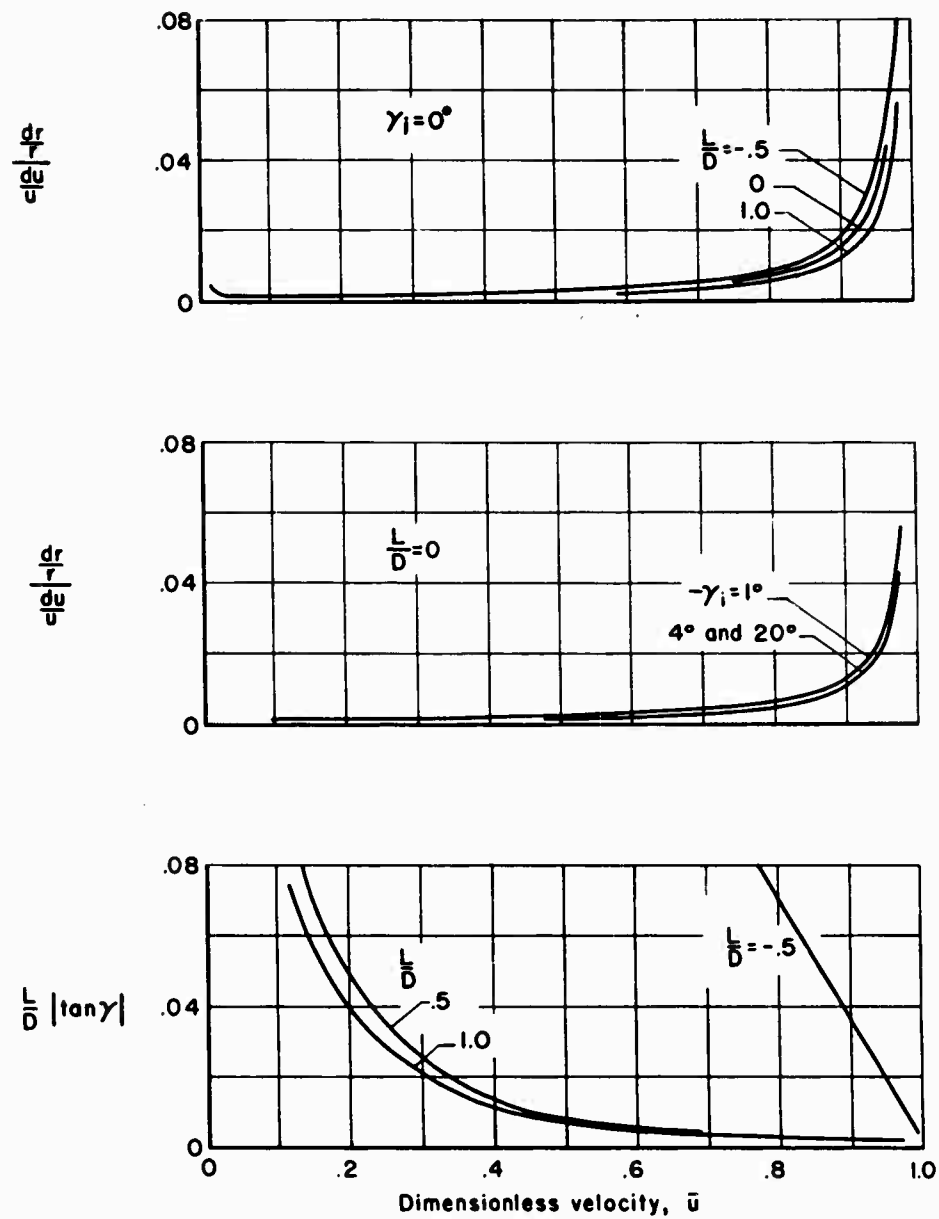


Figure 21. Regions of Validity for $\frac{dr}{r} \frac{du}{u} \ll 1$ and $\frac{L}{D} \tan \gamma \ll 1$

must be fairly large. In normal subsonic glides, for instance, \dot{U} is small and $(L/D) \tan \gamma \approx 1$. Use of the assumption

$$\left(\frac{L}{D}\right) \tan \gamma \ll 1 \quad (71)$$

thus implies a general flight regime in which either $L = 0$, or, if $L \neq 0$, flight path angles are small and \dot{U} is large.

With the two assumptions discussed above, and combining Eqs. (68) and (69),

$$\begin{aligned} \dot{U} &= -\frac{D}{m} \cos \gamma = -\frac{\rho_0 e^{-\beta h} U^2}{2 \left(\frac{m}{C_{DS}}\right) \cos \gamma} \\ \dot{W} + \frac{U^2}{r} &= g - \frac{L}{m} \cos \gamma + \frac{D}{m} \sin \gamma \end{aligned} \quad (72)$$

Reference 23 treats these equations in considerable detail, and presents many numerical solutions in terms of a dimensionless dependent variable, $Z \equiv \rho_0 C_{DS} U / 2m \sqrt{gr}$. To obtain analytical solutions in literal terms, however, still further simplifications must be made; and three relatively simple limiting cases are of special interest. These are shown in Table III with the assumptions required (over and above the two already given) to reduce the equations to solvable circumstances.

As indicated, the simplified equations can be justified using various assumptions, some of which are not necessarily as restrictive as others. The basic assumption, which is also least restrictive, is given first. It indicates the minimum condition under which Eqs. (72) may be truncated to those shown in the table. Note in particular that when the third set of assumptions applies, the "effective" ballistic and the glide cases become identical. The equations for the simplified cases are considered in more detail below. (See also Ref. 23-27)

1. Ballistic Flight

For "effective" ballistic flight the equations of motion are

$$\begin{aligned} \dot{U} &= -\frac{D}{m} \cos \gamma = -\frac{\rho_0 e^{-\beta h} U^2}{2 \left(\frac{m}{C_{DS}}\right) \cos \gamma} \\ \dot{W} &= \frac{D}{m} \sin \gamma \end{aligned} \quad \left. \right\} \quad (73)$$

TABLE III
SUMMARY OF READILY SOLVABLE PARTICLE DYNAMICS CASES WITH AERODYNAMIC FORCES

SITUATION	ASSUMPTIONS	EQUATIONS OF MOTION
Effective ballistic	<p>Gravity, centripetal, and lift forces negligible</p> <p>So: $\left \frac{U^2}{r} - g + \frac{L}{m} \cos \gamma \right \ll \dot{w} , \frac{D}{m} \sin \gamma$</p> <p>or $\frac{U^2}{r}, g, \frac{L}{m} \cos \gamma \ll \dot{w} , \frac{D}{m} \sin \gamma$</p> <p>or $\frac{U^2}{r} \doteq g - \frac{L}{m} \cos \gamma$</p>	$\dot{U} = - \frac{D}{m} \cos \gamma$ $\dot{W} = \frac{D}{m} \sin \gamma$
Glide	<p>Vertical acceleration and vertical component of drag negligible</p> <p>So: $\left \dot{w} - \frac{D}{m} \sin \gamma \right \ll \frac{U^2}{r}, g, \frac{L}{m} \cos \gamma$</p> <p>or $\dot{w} , \frac{D}{m} \sin \gamma \ll \frac{U^2}{r}, g, \frac{L}{m} \cos \gamma$</p> <p>or $\dot{w} \doteq \frac{D}{m} \sin \gamma$</p>	$\dot{U} = - \frac{D}{m} \cos \gamma$ $\frac{U^2}{r} = g - \frac{L}{m} \cos \gamma$
Skip	<p>Gravity and centripetal forces negligible</p> <p>So: $\left g - \frac{U^2}{r} \right \ll \dot{w} , \frac{L}{m} \cos \gamma, \frac{D}{m} \sin \gamma$</p> <p>or $g, \frac{U^2}{r} \ll \dot{w} , \frac{L}{m} \cos \gamma, \frac{D}{m} \sin \gamma$</p> <p>or $\frac{U^2}{r} \doteq g$</p>	$\dot{U} = - \frac{D}{m} \cos \gamma$ $\dot{W} = - \frac{L}{m} \cos \gamma + \frac{D}{m} \sin \gamma$

Eliminating D/m ,

$$\tan \gamma = - \frac{\dot{w}}{\dot{U}} = - \frac{dw}{dU}$$

But, by definition,

$$\tan \gamma = \frac{\dot{h}}{\dot{U}} = - \frac{w}{U} \quad (74)$$

and for both expressions to be valid, w/U must be constant. The simplified equations imply, therefore, that the flight path angle is constant, recognized hereafter by adding a subscript zero to γ .

Eliminating time by dividing the first of Eqs. (73) by Eq. (74) and separating the variables,

$$\frac{dU}{U} = - \frac{\rho_0}{2 \left(\frac{m}{C_D S} \right) \sin \gamma_0} e^{-\beta h} dh \quad (75)$$

Defining a nondimensional altitude, f , (Ref. 27)

$$f \equiv \beta h - \ln \frac{\rho_0}{2 \left(\frac{m}{C_D S} \right) \beta \sin \gamma_0}, \quad df = \beta dh \quad (76)$$

Eq. (75) becomes

$$\frac{dU}{U} = e^{-f} df$$

and, after integration, with the initial velocity taken as U_0 ,

$$\frac{U}{U_0} = e^{-(e^{-f})} \quad (77)$$

Since $dU/dt = (dU/df)(df/dt)$, the acceleration, \dot{U} , will be

$$\begin{aligned} \dot{U} &= (U e^{-f})(\beta \dot{h}) = U^2 \beta \tan \gamma_0 e^{-f} \\ &= \beta U_0^2 \tan \gamma_0 \left[e^{-(f + 2e^{-f})} \right] \end{aligned} \quad (78)$$

\dot{U} will be a maximum when $e^{-(f + 2e^{-f})}$ is maximum. This occurs at $e^{-f} = 1/2$, or $f = 0.69315$. \dot{U}_{\max} will thus be

$$\begin{aligned}\dot{U}_{\max} &= \beta U_0^2 \tan \gamma_0 \left[e^{-f} e^{-2e^{-f}} \right]_{f = \ln 2} \\ &= \frac{\beta U_0^2 \tan \gamma_0}{2e}\end{aligned}\quad (79)$$

The dynamic pressure, q , will be

$$\begin{aligned}q &= \frac{D}{C_D S} = -\frac{\dot{U}}{\cos \gamma_0} \left(\frac{m}{C_D S} \right) \\ &= -\beta U_0^2 \left(\frac{m}{C_D S} \right) \frac{\tan \gamma_0}{\cos \gamma_0} \left[e^{-(f + 2e^{-f})} \right]\end{aligned}\quad (80)$$

The density variation over the trajectory can be found from the relationship

$$\rho = \frac{2q}{U^2} = -2\beta \left(\frac{m}{C_D S} \right) \frac{\tan \gamma_0}{\cos \gamma_0} e^{-f} \quad (81)$$

Note, from Eqs. (80) and (81), that γ_0 must be negative if q and ρ are to be positive, as they are in a real physical case. Plots of normalized acceleration, \dot{U}/\dot{U}_{\max} , and normalized velocity, U/U_{\max} , are presented in Figure 22 (adapted from Ref. 27).

2. Gliding Flight

Under the restrictions leading to gliding flight, the simplified equations of motion are

$$\begin{aligned}\dot{U} &= -\frac{D}{m} \cos \gamma \\ \frac{U^2}{r} &= g - \frac{L}{m} \cos \gamma\end{aligned}\quad (82)$$

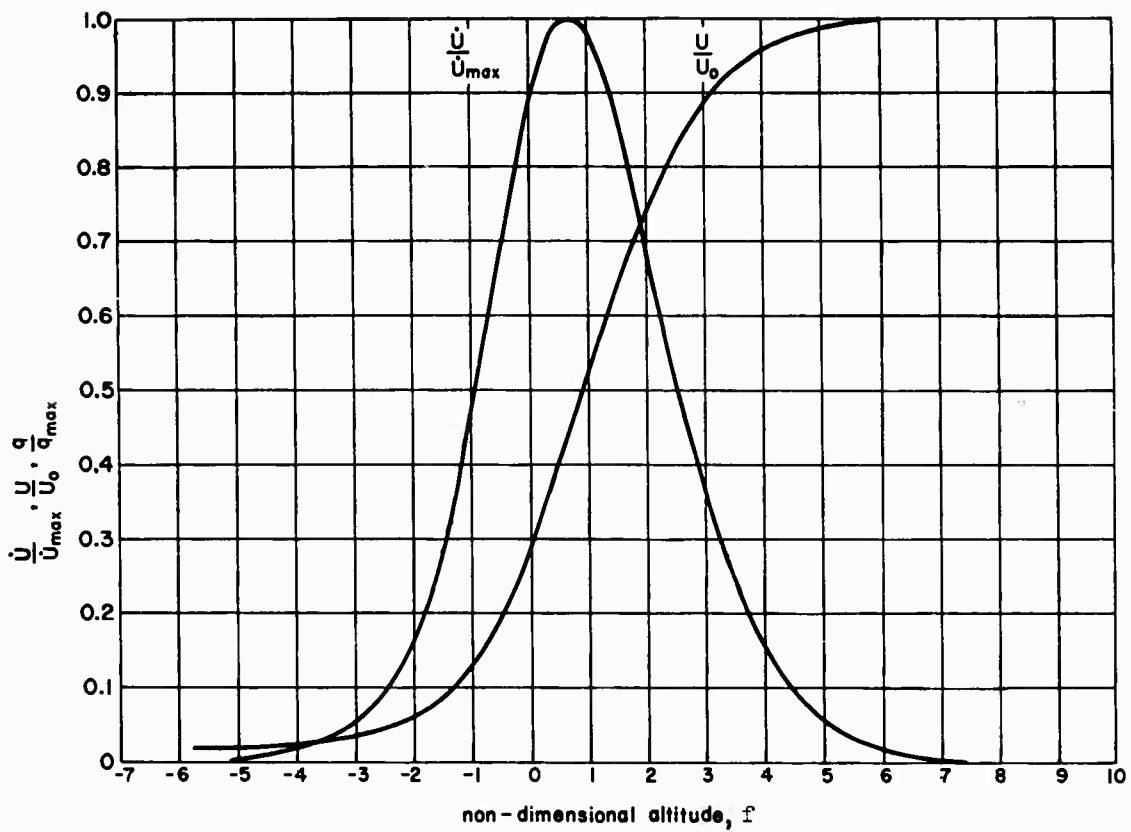


Figure 22. Normalized Variables Versus Altitude, Ballistic Flight

Eliminating $\cos \gamma$,

$$\frac{dU}{dt} = -\frac{g}{(L/D)} (1 - \frac{U^2}{gr}) \quad (83)$$

Let $U/\sqrt{gr} = \bar{U}$. Then,

$$dU = \sqrt{gr} d\bar{U} + \frac{1}{2} \sqrt{\frac{r}{g}} \bar{U} dg + \frac{1}{2} \sqrt{\frac{g}{r}} \bar{U} dr$$

and

$$\frac{dU}{U} = \frac{d\bar{u}}{\bar{u}} + \frac{1}{2} \frac{dg}{g} + \frac{1}{2} \frac{dr}{r}$$

From Newton's law of gravitation,

$$g = \frac{GM}{r^2}, \quad \frac{dg}{g} = -2 \frac{dr}{r}$$

so

$$\frac{dU}{U} = \frac{d\bar{u}}{\bar{u}} - \frac{1}{2} \frac{\dot{r}}{r}$$

Since an assumption underlying all these special cases is $\left|\frac{dr}{r}\right|/\left|\frac{dU}{U}\right| \ll 1$,

$$\frac{dU}{U} \doteq \frac{d\bar{u}}{\bar{u}} \quad \text{or} \quad dU \doteq \frac{U}{\bar{u}} d\bar{u} \doteq \sqrt{gr} d\bar{u}$$

Recognizing that \sqrt{gr} in the above result is, by the nature of the differentiation process, the initial rather than the local value

$$\begin{aligned} dU &\doteq \sqrt{gr_c} d\bar{u} \doteq V_c d\bar{u} \\ U &\doteq V_c \bar{u} \end{aligned} \tag{84}$$

Eq. (83) then becomes

$$\frac{V_c d\bar{u}}{1 - \bar{u}^2} = - \frac{g}{(L/D)} dt \tag{85}$$

Assuming constant L/D , integrating, and using a reference time, t_0 , to provide the constant of integration,

$$\tanh^{-1} \bar{u} = - \frac{g}{V_c (L/D)} (t - t_0) \tag{86}$$

Defining a nondimensional time variable (Ref. 28),

$$T = \frac{g}{V_c (L/D)} (t_0 - t) = \sqrt{\frac{g}{r_c}} \frac{(t_0 - t)}{(L/D)} \tag{87}$$

Eq. (86) can be written

$$\bar{u} = \frac{U}{V_c} = \tanh T \quad \text{or} \quad U = V_c \tanh T \quad (88)$$

The constant t_0 is selected to fit the initial conditions pertinent to the problem at hand.

The dynamic pressure may be found by noting that only small flight path angles are permissible if $L/D \tan \gamma \ll 1$, so that

$$\cos \gamma = \frac{mg}{L} (1 - \bar{u}^2) = \frac{mg}{q C_L S} (1 - \bar{u}^2) \doteq 1$$

$$\begin{aligned} \text{and} \quad q &= \frac{mg}{C_L S} (1 - \bar{u}^2) = \frac{mg}{C_L S} (1 - \tanh^2 T) \\ &= \frac{mg}{C_L S} \operatorname{sech}^2 T \end{aligned} \quad (89)$$

The density ratio ρ/ρ_0 is

$$\frac{\rho}{\rho_0} = \frac{2q}{\rho_0 U^2} = \frac{2m}{C_L S \rho_0 r_c} \operatorname{csch}^2 T \quad (90)$$

and, since $\rho = \rho_0 e^{-\beta h}$, the altitude is

$$h = \frac{1}{\beta} \ln \left[\left(\frac{C_L S \rho_0 r_c}{2m} \right) \sinh^2 T \right] \quad (91)$$

The flight path angle has, to this point, been specified only to the extent that $\cos \gamma$ must approximate unity and that the assumptions of Table III hold. The actual angle may be found by using Eqs. (87) and (91) to obtain dh/dt and then noting that $\tan \gamma = \dot{h}/U$. The result is

$$\frac{1}{\tan \gamma} = - \frac{\beta r_c}{2} \frac{L}{D} \tanh^2 T = - \frac{\beta r_c}{2} \frac{L}{D} \bar{u}^2 \quad (92)$$

Again γ is always negative and further

$$\frac{L}{D} \tan \gamma = - \frac{2}{\beta r_c \bar{u}^2}$$

The condition $|L/D \tan \gamma| \ll 1$ thus is equivalent to

$$\bar{u}^2 \gg \frac{2}{\beta r_c}$$

Assigning a maximum value of $L/D \tan \gamma = 0.05$, for example, corresponds approximately (using a nominal value of $\beta r_c = 900$) to requiring \bar{u} to be greater than 0.21 — not a very stringent limitation.

Plots which illustrate the variation of U , h , and q with the non-dimensional time parameter, T , are given in Figure 23.

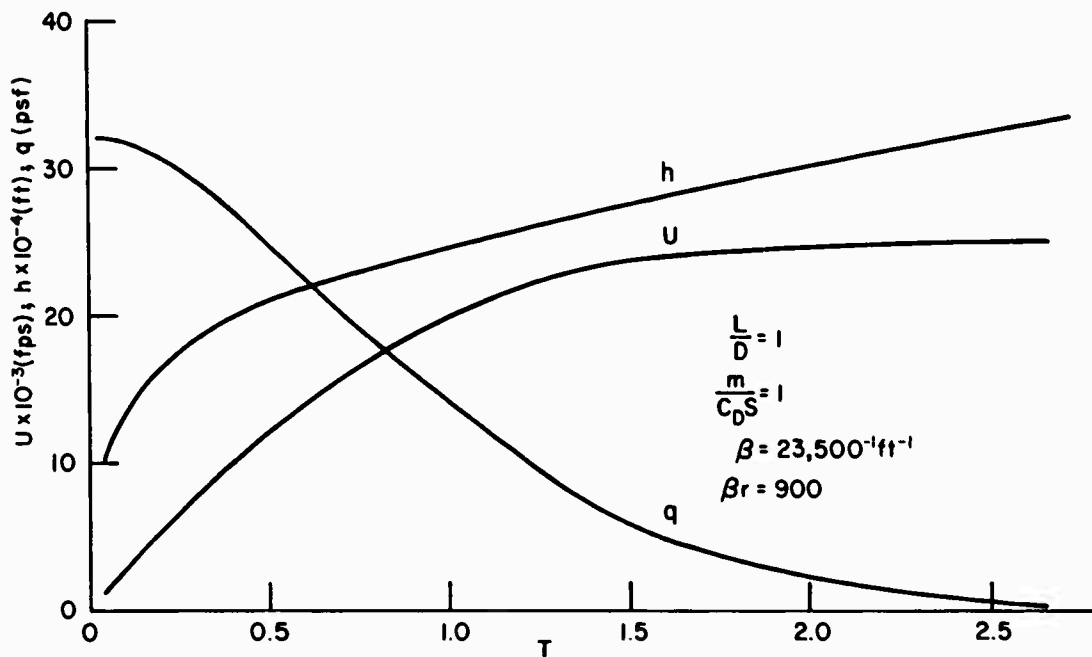


Figure 23. Time Variation of U , h , and q , Gliding Flight

3. Skipping Flight

For the assumptions pertinent to the skip situation, the simplified equations of motion are

$$\left. \begin{aligned} \dot{U} &= -\frac{\rho_0 e^{-\beta h} U^2}{2 \left(\frac{m}{C_D S} \right) \cos \gamma} \\ \dot{W} &= \frac{\rho_0 e^{-\beta h} U^2}{2 \left(\frac{m}{C_D S} \right) \cos^2 \gamma} \left(\sin \gamma - \frac{L}{D} \cos \gamma \right) \end{aligned} \right\} \quad (93)$$

Also, by differentiating the familiar $W = -U \tan \gamma$,

$$\dot{W} = -U \dot{\gamma} \sec^2 \gamma - \dot{U} \tan \gamma$$

Substituting U and W from Eqs. (93),

$$U \dot{\gamma} \sec^2 \gamma = \frac{\rho_0 e^{-\beta h} U^2}{2 \left(\frac{m}{C_D S} \right) \cos^2 \gamma} \left(\frac{L}{D} \cos \gamma - \sin \gamma \right) + \frac{\rho_0 e^{-\beta h} U^2 \sin \gamma}{2 \left(\frac{m}{C_D S} \right) \cos^2 \gamma}$$

or

$$\begin{aligned} \dot{\gamma} \sec^2 \gamma &= \frac{\rho_0 e^{-\beta h} U}{2 \left(\frac{m}{C_D S} \right) \cos \gamma} \\ &= -\frac{L}{D} \frac{\dot{U}}{U} \end{aligned}$$

Assuming constant L/D , integrating, and setting the initial conditions U_0, γ_0

$$\begin{aligned} \ln \frac{U}{U_0} &= \frac{D}{L} (\tan \gamma_0 - \tan \gamma) \\ \text{or} \\ \frac{U}{U_0} &= e^{(D/L)(\tan \gamma_0 - \tan \gamma)} \end{aligned} \quad (94)$$

The flight path angle variation with altitude may be found by recognizing that $\dot{h} = U \tan \gamma$. Then

$$\dot{\gamma} \sec^2 \gamma = \frac{\rho_0}{2 \left(\frac{m}{C_L S} \right) \sin \gamma} e^{-\beta h}$$

or

$$\int \tan \gamma \sec \gamma d\gamma = \frac{\rho_0}{2 \left(\frac{m}{C_L S} \right)} \int e^{-\beta h} dh$$

$$\sec \gamma = - \frac{\rho_0 e^{-\beta h}}{2\beta \left(\frac{m}{C_L S} \right)} + C \quad (95)$$

The constant of integration must be made compatible with that used in Eqs. (94) by associating the initial conditions U_0 and γ_0 used there with a given altitude. For instance, if U_0 and γ_0 are defined at entry into the atmosphere (i.e., at altitudes where $e^{-\beta h}$ approaches zero), then the constant of integration for Eq. (95) should be taken as $\sec \gamma_0$. Thus, for these conditions,

$$\sec \gamma = \sec \gamma_0 - \frac{\rho_0 e^{-\beta h}}{2\beta \left(\frac{m}{C_L S} \right)} \quad (96)$$

Eq. (96) exhibits a single-valued variation of $\sec \gamma$ with altitude. Thus, if the vehicle "skips" in and out of the atmosphere, the exit flight path angle will be the negative of that at entry. After one skip, the velocity will then be [from Eq. (94)],

$$\frac{U_1}{U_0} = e^{2(D/L)} \tan \gamma_0 \quad (97)$$

Since the flight path angles at entry are negative, each skip will result in a velocity decrease. For small flight path angles and L/D of the order of unity, the exit-entry velocity ratio will be

$$\frac{U_1}{U_0} \doteq 1 - \frac{2\gamma_0}{(L/D)} \quad (98)$$

The density ratio ρ/ρ_0 , determined by solving Eq. (96) for $e^{-\beta h}$, will be

$$\frac{\rho}{\rho_0} = \frac{2\beta}{\rho_0} \left(\frac{m}{C_{LS}} \right) (\sec \gamma_0 - \sec \gamma) \quad (99)$$

and the dynamic pressure, q , becomes

$$q = \frac{\rho U^2}{2 \cos^2 \gamma} = \beta \left(\frac{m}{C_{LS}} \right) \frac{(\sec \gamma_0 - \sec \gamma)}{\cos^2 \gamma} U_0^2 e^{2(D/L)} (\tan \gamma_0 - \tan \gamma) \quad (100)$$

The variation of altitude, density, dynamic pressure, and velocity as a function of γ , for $\gamma_0 = -3^\circ$, $L/D = 2$, is shown in Figure 24.

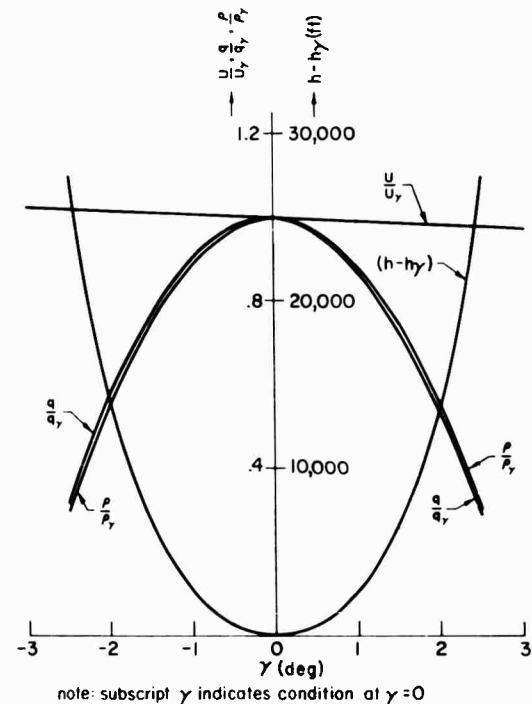


Figure 24. Variation of U , h , q , and ρ for Typical Skipping Flight

The three limiting types of flight considered above are of interest in the present context primarily because they represent simple particle dynamics situations for which the equations may be solved. Table IV summarizes the important results.

TABLE IV
SUMMARY OF DYNAMIC FLIGHT PARAMETERS FOR
READILY SOLVABLE CASES OF AEROSPACE VEHICLE PARTICLE DYNAMICS

FLIGHT QUANTITIES	SITUATION			CHARACTERISTIC PARAMETER
	Ballistic	Glide	Skip	
Horizontal velocity, u	$u_0 e^{-(f-r)}$	$v_c \tanh T$		$u_0 e^{(D/L)(\tan \gamma_0 - \tan \gamma)}$
Flight path angle, γ	γ_0	$\tan^{-1} \frac{u^2}{\beta r_c \left(\frac{u}{D}\right) \tanh^2 T}$ $\tan^{-1} \frac{u^2}{\beta r_c \left(\frac{u}{D}\right) \bar{u}^2}$		$\sec^{-1} \left[\sec \gamma_0 - \frac{p_0 e^{-\beta h}}{2\beta \left(\frac{u}{C_L S}\right)} \right]$
Dynamic pressure, q	$-\rho u_0^2 \left(\frac{u}{C_D S} \right) \frac{\tan \gamma_0}{\cos \gamma_0} \left[e^{-(f+2e^{-f})} \right]$	$\frac{\bar{u}^2}{C_L S} \operatorname{sech}^2 T$ $\frac{\bar{u}^2}{C_L S} (1 - \bar{u}^2)$		$\beta \left(\frac{u}{C_L S} \right) u_0^2 \left(\frac{\sec \gamma_0 - \sec \gamma}{\cos^2 \gamma} \right) e^{2(D/L)(\tan \gamma_0 - \tan \gamma)}$
Density, ρ	$-\rho \left(\frac{u}{C_D S} \right) \frac{\tan \gamma_0}{\cos \gamma_0} e^{-f}$	$\frac{2}{r_c} \left(\frac{u}{C_L S} \right) \operatorname{csch}^2 T$		$2\beta \left(\frac{u}{C_L S} \right) (\sec \gamma_0 - \sec \gamma)$

In a more practical vein, the three limiting cases are of great interest from the standpoint of vehicle performance. The power-off flight performance

problem may be considered to involve fundamentally the conversion of initial velocity into range while maintaining the vehicle structural integrity in the presence of critical aerodynamic heating and loading effects. This problem, which has been extensively studied and documented in recent years, is beyond the scope of this report (see Ref. 23-27).

CHAPTER V

LINEARIZED EQUATIONS OF MOTION

A. LINEARIZATION

The alternative approach to simplification of Eqs. (68) is the method of small perturbations, or linearization. Thus the complete equations

$$\begin{aligned}
 \dot{U} - \frac{UW}{r} &= -q \frac{C_D S}{m} (\cos \gamma + \frac{L}{D} \sin \gamma) \\
 \dot{W} + \frac{U^2}{r} &= g + q \frac{C_D S}{m} (\sin \gamma - \frac{L}{D} \cos \gamma) \\
 \dot{h} &= -W = \dot{r} - Utan \gamma \\
 q &= \frac{1}{2} \rho_0 e^{-\beta h} \frac{U^2}{\cos^2 \gamma}
 \end{aligned} \tag{101}$$

are linearized by taking the total differential of both sides. Terms which enter into the linearization process are:

$$\begin{aligned}
 -d\left(\frac{UW}{r}\right) &= d\left(\frac{U^2 \tan \gamma}{r}\right) \\
 &= \frac{2U}{r} \tan \gamma dU - \frac{U^2}{r^2} \tan \gamma dh + \frac{U^2}{r} \sec^2 \gamma d\gamma \\
 d\frac{U^2}{r} &= \frac{2U}{r} dU - \frac{U^2}{r^2} dh \\
 dq &= q \left[2 \frac{dU}{U} + 2 \tan \gamma d\gamma - \beta dh \right] \\
 d(\cos \gamma + \frac{L}{D} \sin \gamma) &= (-\sin \gamma + \frac{L}{D} \cos \gamma) d\gamma = \frac{R}{D} \cos(\gamma - \Gamma) d\gamma \\
 d(\sin \gamma - \frac{L}{D} \cos \gamma) &= (\cos \gamma + \frac{L}{D} \sin \gamma) d\gamma = \frac{R}{D} \sin(\gamma - \Gamma) d\gamma
 \end{aligned}$$

$$dg = -\frac{2GM}{r^3} dr = -2g \frac{dr}{r} = -\frac{2g}{r} dh$$

$$dh = -dW = \tan \gamma dU + U \sec^2 \gamma dy$$

where the angle Γ is the ideal power-off constant speed glide angle, $\tan \Gamma = -D/L$, and R is the resultant aerodynamic force, $R = \sqrt{L^2 + D^2}$.

The linearized equations of perturbed motion then become:

$$\left. \begin{aligned} \left\{ \dot{U} + \left[\frac{2U}{r} \tan \gamma + \frac{2R}{mU} \sin(\gamma - \Gamma) \right] dU \right\} - \left[\frac{U^2}{r^2} \tan \gamma + \beta \frac{R}{m} \sin(\gamma - \Gamma) \right] dh + \left\{ \frac{R}{m} \left[2 \sin(\gamma - \Gamma) \tan \gamma + \cos(\gamma - \Gamma) \right] + \frac{U^2}{r} \sec^2 \gamma \right\} dy = 0 \\ \left[\frac{2U}{r} + \frac{2R}{mU} \cos(\gamma - \Gamma) \right] dU - \left\{ dh + \left[\frac{U^2}{r^2} - \frac{2g}{r} + \beta \frac{R}{m} \cos(\gamma - \Gamma) \right] dh \right\} + \frac{R}{m} \left[2 \cos(\gamma - \Gamma) \tan \gamma - \sin(\gamma - \Gamma) \right] dy - U \sec^2 \gamma dy = 0 \\ - \tan \gamma dU + dh - U \sec^2 \gamma dy = 0 \end{aligned} \right\} (102)$$

Eqs. (102) may be interpreted to represent small perturbed motions either about flight operating points, or from initial flight conditions. They are precise in the differential form shown. Because of the nature of total differentials, the coefficients enclosed in square brackets are, at worst, functions of time only, so the equations are linear. Unfortunately, unless restrictions are applied to keep the coefficients constant, solution will be just about as difficult as for the original unperturbed set. In general, then, Eqs. (102) must be either

- Linear, but with time varying coefficients
- Linear, with constant coefficients, but restricted as to the time span over which the solution is valid

For the equations to take on a constant-coefficient form requires either: the practical existence of a condition of equilibrium, where the operating point conditions are described by constant values of the dependent variables U and W ; or the assumption that the coefficients are evaluated at some starting point ($t = 0$). In either case the equations will be good approximations to the motion

only as long as the perturbed motions remain small relative to the total values of the dependent variables.

Defining a steady-state value of W other than zero implies, unfortunately, that there is a steady-state value of \dot{h} , since $W = -\dot{h}$. The perturbed altitude, $d\dot{h}$, will then have a component, $-W_0 t$, which varies with time, and the linearized equations will be time varying. This fundamental problem is not new. It was encountered in aeronautical stability and control many years ago (Ref. 29-32) for diving and climbing stability calculations in which density variations were considered. In those instances a steady-state operating point corresponding to $\gamma = 0$, $U = \text{constant}$ resulted in tractable and meaningful equations of motion. In the present case density gradient is still, together with gravitational gradient effects [see the coefficients of $d\dot{h}$ in Eqs. (102)], a basic source of difficulty. Now, however, the glide case for $\gamma \neq 0$ is not characterized for very long periods of time by nearly constant values of U (see Figure 23). Nevertheless, the only pertinent operating point (or initial point) conditions yielding solvable equations are, as before, those for $\gamma = 0$, $U = \text{constant}$. The results so obtained are still of considerable physical significance, and can be used to describe the particle motions by a series of "frozen" system solutions. After setting the operating point flight path angle, γ , to zero and expressing L , D in terms of basic aerodynamic coefficients, Eqs. (102) become:

$$\left. \begin{aligned} d\dot{U} + \left[\frac{2q}{U} \left(\frac{C_D S}{m} \right) \right] dU - q\beta \left(\frac{C_D S}{m} \right) d\dot{h} + \left[q \left(\frac{C_L S}{m} \right) + \frac{U^2}{r} \right] dy &= 0 \\ 2 \left[\frac{U}{r} + \frac{q}{U} \left(\frac{C_L S}{m} \right) \right] dU - \left\{ d\ddot{h} + \left[\frac{U^2}{r^2} - \frac{2g}{r} + q\beta \left(\frac{C_L S}{m} \right) \right] d\dot{h} \right\} - q \left(\frac{C_D S}{m} \right) dy &= 0 \\ d\dot{h} - U dy &= 0 \end{aligned} \right\} \quad (103)$$

Eliminating the perturbed flight path angle gives,

$$\left. \begin{aligned} \left\{ d\dot{U} + \left[\frac{2q}{U} \left(\frac{C_D S}{m} \right) \right] dU \right\} + \left\{ \left[\frac{q}{U} \left(\frac{C_L S}{m} \right) + \frac{U}{r} \right] d\dot{h} - q\beta \left(\frac{C_D S}{m} \right) d\dot{h} \right\} &= 0 \\ \left\{ 2 \left[\frac{U}{r} + \frac{q}{U} \left(\frac{C_L S}{m} \right) \right] dU \right\} - \left\{ d\ddot{h} + \frac{q}{U} \left(\frac{C_D S}{m} \right) d\dot{h} + \left[\frac{U^2}{r^2} - \frac{2g}{r} + q\beta \left(\frac{C_L S}{m} \right) \right] d\dot{h} \right\} &= 0 \end{aligned} \right\} \quad (104)$$

If the operating point altitude and speed are assumed to be constant, the coefficients computed with operating point values (denoted by a zero subscript) will also be constant. Identifying the differentials with small perturbations, i.e., $du = u$, $dh = h$, etc., and Laplace transforming with zero initial conditions, yields

$$\left. \begin{aligned} \left(s + \frac{2D_0}{mU_0} \right) u + \left[\left(\frac{L_0}{mU_0} s + \frac{U_0}{r_0} \right) s - \frac{\beta D_0}{m} \right] h &= 0 \\ 2 \left(\frac{U_0}{r_0} + \frac{L_0}{mU_0} \right) u - \left[s^2 + \frac{D_0}{mU_0} s + \left(\frac{U_0^2}{r_0^2} - \frac{2g_0}{r_0} + \frac{\beta L_0}{m} \right) \right] h &= 0 \end{aligned} \right\} \quad (105)$$

Although Eqs. (105) can easily be studied as written, it is more pertinent, in view of the preceding chapters, to specialize them into extra-atmospheric and atmospheric cases. Outside the atmosphere ($L_0 = D_0 = 0$) Eqs. (105) reduce to the elementary form

$$\left. \begin{aligned} su + \frac{U_0}{r_0} sh &= 0 \\ \frac{2U_0}{r_0} u - \left[s^2 + \left(\frac{U_0^2}{r_0^2} - \frac{2g_0}{r_0} \right) \right] h &= 0 \end{aligned} \right\} \quad (106)$$

These correspond to small perturbations about essentially circular orbits. The characteristic equation is

$$\Delta(s) = s \left[s^2 + \left(\frac{U_0^2}{r_0^2} - \frac{2g_0}{r_0} \right) \right] \quad (107)$$

The last result, involving the mean orbital frequency ω_0 , follows directly from Eqs. (48) and (49). Thus, the period of the low frequency particle motions of the vehicle approaches the orbital period as the vehicle leaves the atmosphere.

B. LINEARIZED EQUATIONS FOR ATMOSPHERIC FLIGHT

For flight within the atmosphere the major region of interest corresponds to the condition

$$\left| \frac{dr}{r} \right| \ll \left| \frac{du}{u} \right|$$

For such situations the UW/r term may be neglected, as shown in the preceding chapter. Also,

$$d\left(\frac{U^2}{r}\right) = \frac{2U}{r} du \left(1 - \frac{1}{2} \frac{dr/r}{du/U}\right) \approx \frac{2U}{r} du$$

The use of these assumptions, in evaluating the total differentials connected with Eq. (101), reduces Eqs. (104) to

$$\left\{ d\dot{U} + \left[\frac{2q}{U} \left(\frac{C_{DS}}{m} \right) \right] du \right\} + \left\{ \frac{q}{U} \left(\frac{C_{LS}}{m} \right) dh - q\beta \left(\frac{C_{DS}}{m} \right) dh \right\} = 0 \quad (108)$$

$$\left\{ 2 \left[\frac{U}{r} + \frac{q}{U} \left(\frac{C_{LS}}{m} \right) \right] du \right\} - \left\{ dh + \frac{q}{U} \left(\frac{C_{DS}}{m} \right) dh - \left[\frac{2g}{r} - q\beta \left(\frac{C_{LS}}{m} \right) \right] dh \right\} = 0 \quad (109)$$

The relative magnitudes of the terms in the coefficient of dh in Eq. (109) are, making use of Eq. (82) for L/mg ,

$$\frac{\frac{2g}{r}}{q\beta \left(\frac{C_{LS}}{m} \right)} = \frac{2}{\beta r} \left(\frac{mg}{L} \right) = \frac{2}{\beta r (1 - \bar{u}^2)}$$

Since βr is approximately 900, the ratio is small with respect to 1 (about 5%) for values of $\bar{u} < 0.98$. Then Eq. (109) becomes

$$\left\{ 2 \left[\frac{U}{r} + \frac{q}{U} \left(\frac{C_{LS}}{m} \right) \right] du \right\} - \left\{ dh + \frac{q}{U} \left(\frac{C_{DS}}{m} \right) dh + q\beta \left(\frac{C_{LS}}{m} \right) dh \right\} = 0$$

and the specialization of Eqs. (105) for the atmospheric flight situation is given by,

$$\left. \begin{aligned} \left(s + \frac{2D_0}{mU_0} \right) u + \left(\frac{L_0}{mU_0} s - \frac{\beta D_0}{m} \right) h &= 0 \\ 2 \left(\frac{U_0}{r_0} + \frac{L_0}{mU_0} \right) u - \left(s^2 + \frac{D_0}{mU_0} s + \frac{\beta L_0}{m} \right) h &= 0 \end{aligned} \right\} \quad (110)$$

The characteristic equation for the set is, neglecting 2 relative to βr_o ,

$$\Delta(s) = s^3 + \frac{3D_o}{mU_o} s^2 + 2 \left(\frac{L_o}{mU_o} \right)^2 \left[1 + \left(\frac{D}{L} \right)^2 + \frac{\beta U_o^2 m}{2L_o} \right] s - \frac{2\beta U_o}{r_o} \left(\frac{D_o}{m} \right) = 0 \quad (111)$$

Before examining this result, a similar development, assuming, however, the existence of a constant thrust, $T_o = D_o$, which permits the operating point to be in complete equilibrium, will be undertaken. Accordingly, the sets of equations, Eqs. (101) and (107), (neglecting the defining equation for γ) are modified by the addition of the following indicated thrust terms:

$$\dot{U} - \frac{UW}{r} = \dots + \frac{T_o}{m} \cos \gamma \quad (101)'$$

$$\dot{W} + \frac{U^2}{r} = \dots - \frac{T_o}{m} \sin \gamma$$

$$\begin{aligned} \dot{U} + \dots + \frac{T_o}{m} \sin \gamma d\gamma &= 0 \\ \frac{2U\dot{U}}{r} + \dots + \frac{T_o}{m} \cos \gamma d\gamma &= 0 \end{aligned} \quad (102)'$$

$$\begin{aligned} \dot{U} + \dots + 0 &= 0 \\ \frac{2U\dot{U}}{r} + \dots + \frac{T_o}{m} d\gamma &= 0 \end{aligned} \quad (103)'$$

$$\dot{U} + \dots + 0 = 0 \quad (104, 108)'$$

$$\frac{2U\dot{U}}{r} + \dots + \frac{T_o}{mU} dh = 0 \quad (104, 109)'$$

$$\begin{aligned} su + \dots + 0 &= 0 \\ \frac{2U_o u}{r_o} + \dots + \frac{T_o}{mU_o} sh &= 0 \end{aligned} \quad (105, 106, 110)'$$

Recognizing that $D_o/mU_o = T_o/mU_o$, the complete revised set of Eqs. (110) becomes

$$\begin{aligned} \left(s + \frac{2D_o}{mU_o} \right) u + \left(\frac{L_o}{mU_o} s - \frac{\beta D_o}{m} \right) h &= 0 \\ 2 \left(\frac{U_o}{r_o} + \frac{L_o}{mU_o} \right) u - \left(s^2 + \frac{\beta L_o}{m} \right) h &= 0 \end{aligned} \quad (112)$$

and the characteristic equation, again neglecting 2 relative to βr_o , is

$$\Delta(s) = s^3 + \frac{2D_o}{mU_o} s^2 + 2 \left(\frac{L_o}{mU_o} \right)^2 \left[1 + \frac{\beta U_o^2 m}{2L_o} \right] s - \frac{2\beta U_o}{r_o} \left(\frac{D_o}{m} \right) = 0 \quad (113)$$

The classical two degrees of freedom subsonic phugoid oscillation has a characteristic equation (e.g., Ref. 3),

$$s^2 + \frac{2D_o}{mU_o} s + \frac{2g}{U_o^2} \left(\frac{L_o}{m} \right) = 0 \quad (114)$$

derived for conditions where $T_o = D_o$, lift and weight are equal, i.e., $L_o/m = g$, and density gradient is neglected, i.e., $\beta = 0$. With these same restrictions, Eq. (113) reduces to Eq. (114), indicating that the first three terms of Eqs. (113) and (111) correspond to a mode akin to the familiar phugoid.

The correspondence noted in the above digression can be further clarified by approximately factoring the cubic equations, (111) and (113), in literal terms, i.e.,

$$s^3 + As^2 + Bs + C \doteq \left(s + \frac{C}{B} \right) \left[s^2 + s \left(A - \frac{C}{B} \right) + B \right] \quad (115)$$

which is valid when

$$\left| \frac{AC}{B^2} \right| \ll 1 \quad \text{and} \quad \left| \frac{C^2}{B^3} \right| \ll 1$$

For both equations, the B coefficient is dominated, for \bar{U}_o greater than about 0.15, by the term

$$\frac{\beta U_o^2}{2g} \frac{W}{L_o} = \frac{\beta r_o}{2} \frac{\bar{U}_o^2}{1 - \bar{U}_o^2} \gg 1$$

$$\text{so that} \quad B \doteq \frac{\beta L_o}{m} = g\beta \frac{L_o}{W} = g\beta(1 - \bar{U}_o^2) \quad (116)$$

and, neglecting the 3:2 differential between the A coefficients in Eqs. (111) and (113),

$$\left| \frac{AC}{B^2} \right| \doteq \frac{\left(\frac{2D_o}{mU_o} \right) \left(\frac{2\beta U_o}{r_o} \frac{D_o}{m} \right)}{\left(\frac{\beta L_o}{m} \right)^2} = \frac{4}{\beta r_o} \left(\frac{D_o}{L_o} \right)^2 \ll 1$$

and

$$\left| \frac{C^2}{B^3} \right| = \frac{\left(\frac{2\beta U_o D_o}{r_o m} \right)^2}{\left(\frac{\beta L_o}{m} \right)^3} = \frac{4}{\beta r_o} \left(\frac{D_o}{L_o} \right)^2 \frac{\bar{u}_o^2}{1 - \bar{u}_o^2} \ll 1$$

With the conditions of validity thus shown to be satisfied, the characteristic equations have the approximate factors

$$\Delta(s) = \left(s + \frac{1}{T_p} \right) \left(s^2 + 2\zeta_p \omega_p s + \omega_p^2 \right)$$

where $\frac{1}{T_p} = -\frac{2U_o}{(L/D)r_o} = -\frac{2\sqrt{g/r_o}}{L/D} \bar{u}_o$

$$\omega_p^2 = \beta \frac{L_o}{m} = g\beta(1 - \bar{u}_o^2)$$

$$2\zeta_p \omega_p = \frac{2D_o}{mU_o(1 - \bar{u}_o^2)} = \frac{2g}{U_o(L/D)} = \frac{2\sqrt{g/r_o}}{\bar{u}_o(L/D)} \quad \text{for } T_o = D_o$$

$$= \frac{3g}{U_o(L/D)} \left(1 - \frac{\bar{u}_o^2}{3} \right) = \frac{3\sqrt{g/r_o}}{\bar{u}_o(L/D)} \left(1 - \frac{\bar{u}_o^2}{3} \right) \quad \text{for } T_o = 0 \quad (117)$$

$$\zeta_p = \frac{1}{\sqrt{\beta r_o} \left(\frac{L}{D} \right) \bar{u}_o \sqrt{1 - \bar{u}_o^2}} \quad \text{for } T_o = D_o$$

$$= \frac{\frac{3}{2} \left(1 - \frac{\bar{u}_o^2}{3} \right)}{\sqrt{\beta r_o} \left(\frac{L}{D} \right) \bar{u}_o \sqrt{1 - \bar{u}_o^2}} \quad \text{for } T_o = 0$$

The variation of these parameters for $T_o = 0$ is shown in Figure 25.

The physical forces involved in each of the modes can be studied by constructing time vector diagrams (Ref. 33 and 34) for the typical zero-thrust example given below:

$$\begin{aligned} U_o &= 0.95 & \frac{2D_o}{mU_o} &= 0.127 \times 10^{-3} \\ \frac{L}{D} &= 2.0 & & \\ r_o &= 21.1 \times 10^6 & \frac{L_o}{mU_o} &= 0.1270 \times 10^{-3} \\ \beta &= 23,500^{-1} & U_o &= 24,750 \\ g &= 32.2 & \frac{U_o}{r_o} &= 1.175 \times 10^{-3} \end{aligned}$$

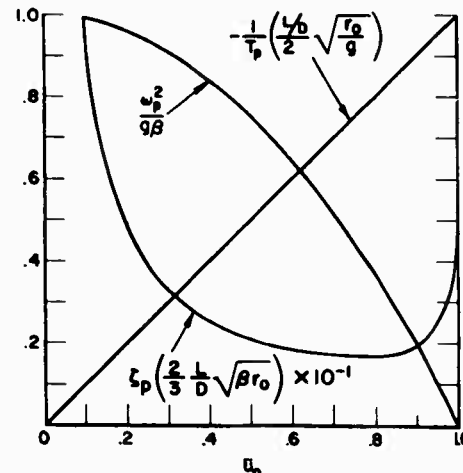


Figure 25. Variation of Characteristic Equation Approximate Factors

Eqs. (110) then become

$$(s + 0.1270 \times 10^{-3})u + (0.1270 \times 10^{-3}s - 0.067 \times 10^{-3})h = 0$$

$$2.604 \times 10^{-3}u - (s^2 + 0.0635 \times 10^{-3}s + 0.1338 \times 10^{-3})h = 0$$

and the exact factors of the characteristic equation are

$$(s - 0.001165)(s^2 + 0.001356s + 0.0001357)$$

$$\text{or, } (s - 0.001165)[s^2 + 2(0.0586)(0.01165)s + (0.01165)^2]$$

The approximate factors, corresponding to Eqs. (117), have the values

$$(s - 0.001175)(s^2 + 0.001363s + 0.0001336)$$

$$\text{or, } (s - 0.001175)[s^2 + 2(0.0590)(0.01156)s + (0.01156)^2]$$

and are seen to be within a few percent of the exact factors.

The time vector diagrams of the lift and drag equations for both the phugoid and aperiodic modes are shown in Figure 26. Of particular interest is the fact that the important drag equation components are the same (i.e., $\frac{\beta D_0}{m}h$ and \dot{u}) for both modes. Therefore a study of the major components of the lift equation should reveal the essential difference in the physical forces active in each mode. The simplified lift equations, based on the vector polygons of Figure 26, are

$$\text{Phugoid mode: } \left(s^2 + \frac{\beta L_0}{m}\right)h = 0$$

$$\text{Aperiodic mode: } 2\left(\frac{U_0}{r_0} + \frac{L_0}{mU_0}\right)u - \frac{\beta L_0}{m}h = 0$$

It appears, therefore, that a downward change in height is accompanied by an upward acceleration giving rise to the phugoid, and by a decrease in forward speed giving rise to the aperiodic divergence. For the phugoid, all the essential dynamics (except for minor damping effects) are contained in the simplified lift equation which directly yields the approximate phugoid frequency

previously derived [Eq. (117)]. For the aperiodic motion, the simplified drag equation must also be used to obtain the complete dynamic picture, the simplified set then being

$$su - \frac{\beta D_0}{m} h = 0$$

$$2 \frac{U_0}{r_0} u - \frac{\beta L_0}{m} h = 0$$

where L_0/mU_0 has been neglected with respect to U_0/r_0 consistent with the conditions chosen for this example. This set yields the time constant, T_p , given in Eqs. (117).

On the basis of the foregoing exploration, the aperiodic mode contains most of the elements of the average motion, as given, for example, by the gliding flight equations of the previous article and pictured in Figure 23. The phugoid oscillation is associated with the "bouncing" commonly encountered in re-entry maneuvers, and is therefore related to the skipping flight situation treated previously. In either mode the major aerodynamic influences act only by virtue of the density gradient effect, β . This explains why the addition of a constant thrust has so small an influence on the characteristic motions. This would not be the case if thrust were assumed to vary with atmospheric density.

The above observations must be restricted to time spans consistent with valid solutions to the constant coefficient equations of motion utilized. For some indication as to how long such times may be, and in line with the preceding discussion, assume that the mean time history of the vehicle-particle is given by the gliding flight solution. Then the average dynamic pressure, q , will be, from Eq. (89),

$$q = \frac{mg}{C_L S} (1 - \bar{u}^2)$$

Taking the time derivative,

$$\frac{dq}{dt} = \frac{mg}{C_L S} \left(-2\bar{u} \frac{d\bar{u}}{dt} \right)$$

and utilizing Eq. (85) for $d\bar{u}/dt$,

$$\frac{dq/dt}{q} = 2 \frac{\sqrt{g/r}}{L/D} \bar{u}$$

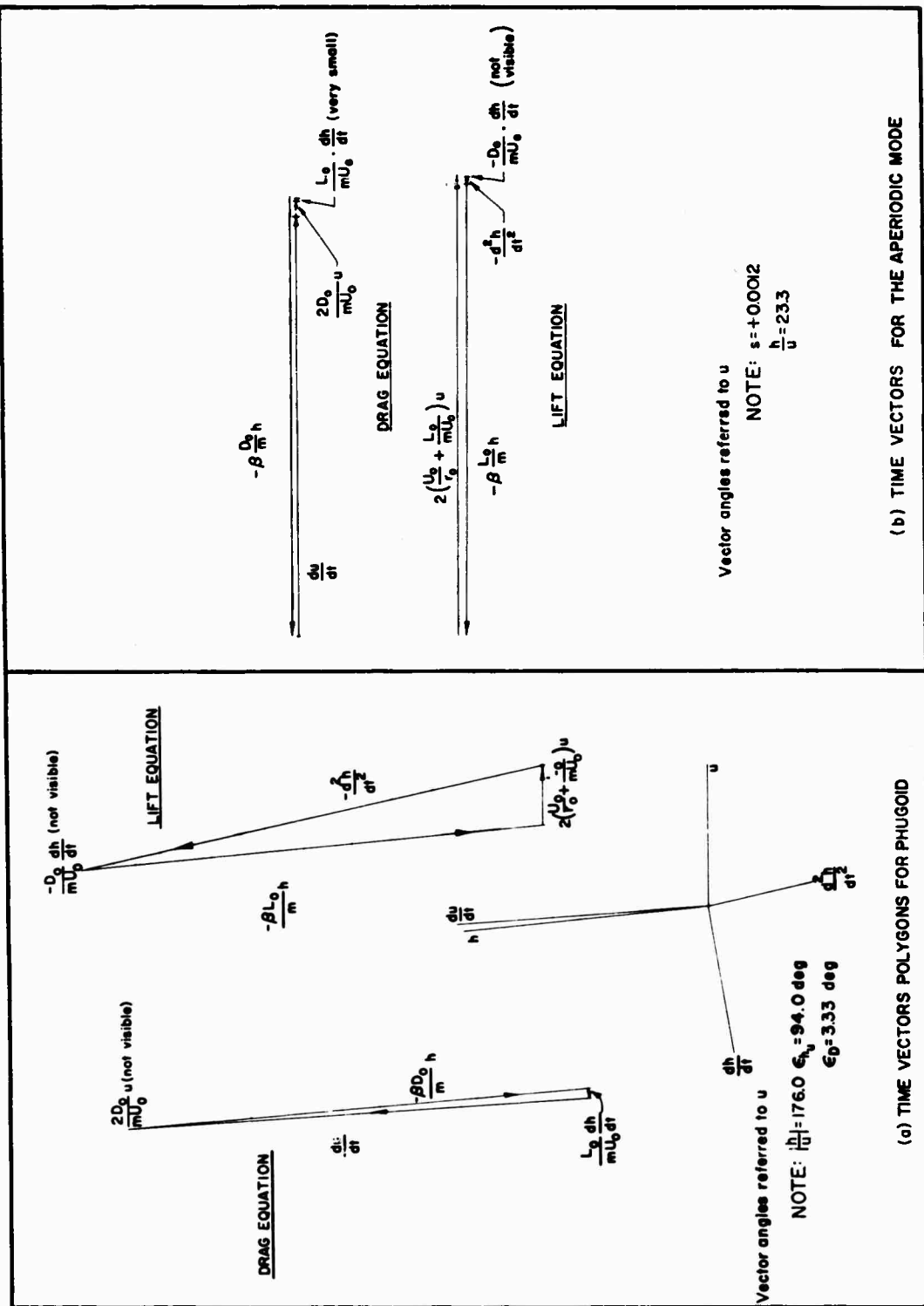


Figure 26. Time Vector Diagrams

Since, from Eq. (117), the approximate value of ω_p^2 is proportional to q ,

$$\frac{d\omega_p}{\omega_p} = \frac{1}{2} \frac{dq}{q} = \frac{\sqrt{g/r}}{L/D} \frac{du}{dt}$$

The time span for which the constant coefficient or "frozen" solution for ω_p will hold within 10% is then

$$\Delta t = 0.10 \sqrt{\frac{r_0}{g}} \frac{L}{D} \frac{1}{\bar{u}_0} \approx \frac{80(L/D)}{\bar{u}_0}$$

Expressed as a fraction of the phugoid period, $P_p = 2\pi/\omega_p$,

$$\frac{\Delta t}{P_p} = \frac{0.10 \sqrt{\beta r_0}}{2\pi} \frac{L}{D} \frac{\sqrt{1 - \bar{u}_0^2}}{\bar{u}_0} = 0.48 \frac{L}{D} \frac{\sqrt{1 - \bar{u}_0^2}}{\bar{u}_0}$$

These relationships, plotted in Figure 27, indicate that the phugoid frequency

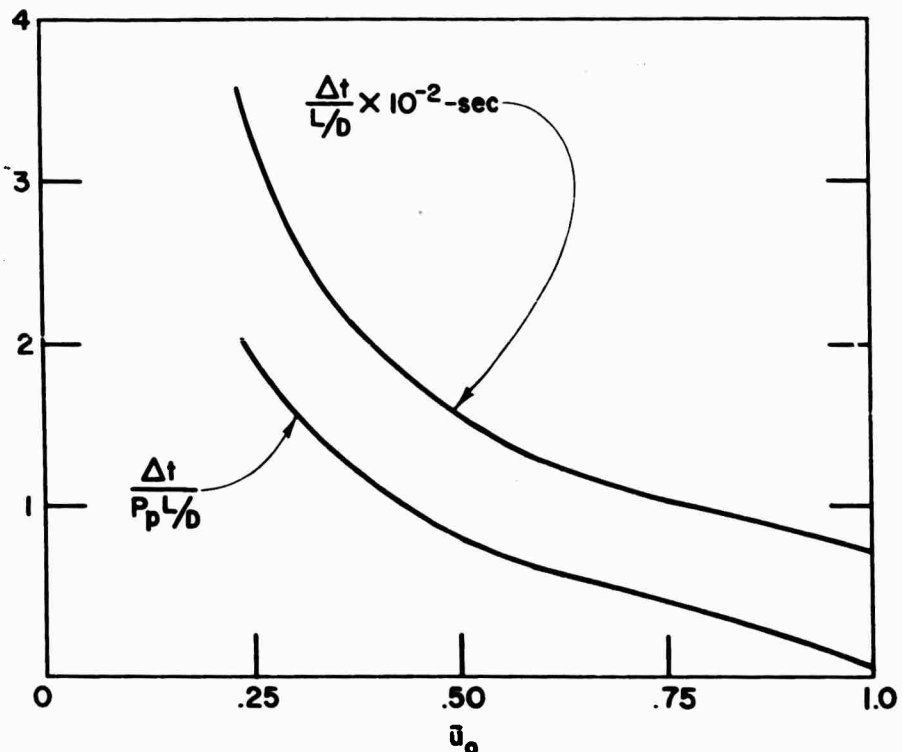


Figure 27. Time Span, Δt , for "Valid" Constant Coefficient Solutions

will remain within 10% of its "frozen" value for times, proportional to L/D , which range from about one-tenth the phugoid period at $\bar{u}_0 = 0.98$ (and $L/D = 1$) to values greater than the period for \bar{u}_0 less than about 0.45. While a solution good for only one-tenth the period of the resulting motion might be considered unreasonably poor, the fact that the actual time involved is of the order of 100 seconds is a highly mitigating circumstance. For example, most flight control systems will invariably have response times at least an order of magnitude faster, and analysis of such systems will not be affected by a 100-second time limit. Also, because of the very slow time variations involved, the "frozen" solutions can be used, with appropriate initial conditions, as point-by-point approximations to the real time-varying situation. Reference 28 presents comparisons of the approximate value of ω_p of Eq. (117) (differently derived) with values of the skipping frequency obtained from complete time-varying numerical computations. In this comparison the approximate value of ω_p is calculated as if the operating point were being continuously varied, i.e., \bar{u} replaces \bar{u}_0 in Eqs. (117). The agreement is excellent, the approximate values being lower than those determined numerically by less than about 5%.

REFERENCES

1. Jones, B. Melvill, "Dynamics of the Airplane," Aerodynamic Theory, Div. N, Vol. V, W. F. Durand, Editor, Durand Reprinting Committee, 1943.
2. Duncan, W. J., The Principles of the Control and Stability of Aircraft, Cambridge University Press, 1952.
3. Dynamics of the Airframe, Northrop Aircraft, Inc., BuAer Report AE-61-4-II, September 1952.
4. Ashkenas, I. L., and D. T. McRuer, Approximate Airframe Transfer Functions and Application to Single Sensor Control Systems, WADC TR 58-82, June 1958.
5. Etkin, B., Dynamics of Flight, Stability and Control, John Wiley and Sons, Inc., New York, 1959.
6. Sommerfeld, A., Mechanics, Academic Press, New York, 1952.
7. Rosser, J. B., R. R. Newton, and G. L. Gross, Mathematical Theory of Rocket Flight, McGraw-Hill Book Co., Inc., New York, 1947.
8. Roberson, R. E., "Attitude Control of Satellites and Space Vehicles," Advances in Space Science, Vol. 2, F. I. Ordway, III, Editor, Academic Press, New York, 1960.
9. Ehricke, Krafft A., "Environment and Celestial Mechanics," Space Flight, Vol. I, D. Van Nostrand Co., Inc., Princeton, 1960.
10. Webster, Arthur Gordon, The Dynamics of Particles and of Rigid, Elastic, and Fluid Bodies, 2nd Ed., Dover Publications, Inc., New York, 1959.
11. Roberson, R. E., and D. Tatistcheff, "The Potential Energy of a Small Rigid Body in the Gravitational Field of an Oblate Spheroid," J. Franklin Institute, Vol. 262, pp. 209-214, September 1956.
12. Roberson, Robert E., "Orbital Behavior of Earth Satellites," Parts I and II, J. Franklin Institute, Vol. 264, No. 3, pp. 181-202, September 1957, and Vol. 264, No. 4, pp. 269-285, October 1957.
13. Dearman, C. C., Jr., Secular Perturbations Due to the Sun and Moon of the Orbit of an Artificial Earth Satellite, Army Ballistic Missile Agency Report No. DSP-TR-5-59, 23 November 1959.
14. Upton, E., A. Bailie, and P. Musen, Lunar and Solar Perturbations on Satellite Orbits, American Rocket Society Preprint 920-59, 1959.
15. Moulton, Forest Ray, An Introduction to Celestial Mechanics, 2nd Rev. Ed., The Macmillian Co., New York, 1958.

16. Blitzer, Leon, Morris Weisfeld, and Albert D. Wheelon, "Perturbations of a Satellite's Orbit Due to the Earth's Oblateness," J. Applied Physics, Vol. 27, No. 10, pp. 1141-1149, October 1956.
17. Roberson, Robert E., "Effect of Air Drag on Elliptic Satellite Orbits," Jet Propulsion, Vol. 28, No. 2, pp. 90-96, February 1958.
18. King-Hele, D. G., and R. H. Merson, "Satellite Orbits in Theory and Practice," J. British Interplanetary Society, Vol. 16, No. 8, pp. 446-471, July-August 1958.
19. Nielsen, Jack N., Frederick K. Goodwin, and William A. Mersman, Three-Dimensional Orbits of Earth Satellites, Including Effects of Earth Oblateness and Atmospheric Rotation, NASA Memo 12-4-58A, December 1958.
20. Cook, G. E., Aerodynamic Drag of Near Earth Satellites, Royal Aircraft Establishment Technical Note No. G.W. 531, September 1959.
21. Jaramillo, Trinidad J., The Combined Non-Linear Effects of Earth Oblateness and Atmospheric Drag on a Near-Earth Satellite, WADC TR 59-513, October 1959.
22. King-Hele, D. G., G. E. Cook, and D. M. C. Walker, The Contraction of Satellite Orbits under the Influence of Air Drag. Part 1. With Spherically Symmetrical Atmosphere, Royal Aircraft Establishment Technical Note No. G.W. 533, November 1959.
23. Chapman, Dean R., An Approximate Analytical Method for Studying Entry Into Planetary Atmospheres, NASA TR R-11, 1959.
24. Allen, H. Julian, "Hypersonic Flight and the Re-Entry Problem (The Twenty-First Wright Brothers Lecture)," J. Aeronautical Sciences, Vol. 25, No. 4, pp. 217-229, April 1958.
25. Gazley, C., Jr., Deceleration and Heating of a Body Entering a Planetary Atmosphere from Space, The RAND Corporation Paper P-955, February 18, 1957.
26. Eggers, Alfred J., Jr., H. Julian Allen, and Stanford E. Neice, A Comparative Analysis of the Performance of Long-Range Hypervelocity Vehicles, NACA Report 1382, 1958.
27. Robinson, Alfred C., and Algimantas J. Besonis, On the Problems of Re-Entry Into the Earth's Atmosphere, WADC TR 58-408, August 1958.
28. Campbell, George S., "Long Period Oscillations During Atmospheric Entry," ARS Jour., Vol. 29, No. 7, pp. 525-527, July 1959.
29. Duncan, W. J., and W. J. Scull, Free Motion of a Stable Glider in an Atmosphere of Variable Density, Aeronautical Research Council R. and M. 2081, March 1941.

30. Scheubel, F. N., "The Effect of Density Gradient on the Longitudinal Motion of an Aircraft, Luftfahrtforschung, Vol. XIX, No. 4, May 1942, RTP Translation No. 1739.
31. Olenski, Z., T. Ciastula, and N. W. Gooden, A Method of Determining Performance in Various Types of Flight in a Vertical Plane from the Given Performance in One Type, Royal Aircraft Establishment Report Aero 2054, July 1945.
32. Neumark, S., "Longitudinal Stability, Speed and Height," Aircraft Engineering, November 1950. (First issued as RAE Report Aero 2265, May 1948.)
33. Breuhaus, W. O., Resume of the Time Vector Method as a Means for Analyzing Aircraft Stability, WADC TR 52-299, November 1952.
34. Doetsch, K. H., The Time Vector Method for Stability Investigations, Aeronautical Research Council R. and M. 2945, August 1953.
35. Roberson, R. E., "Attitude Control of a Satellite Vehicle -- an Outline of the Problems," Proceedings of the VIIIth International Astronautical Congress, Springer-Verlag, 1958.
36. Abzug, Malcolm J., "Perturbations of an Attitude-Controlled Satellite," Preliminary Draft of a Ph.D. Dissertation, University of California, Los Angeles.

APPENDIX

SUMMARY OF AXIS SYSTEMS FOR AEROSPACE VEHICLE STABILITY AND CONTROL

This appendix summarizes the major types of axis systems required for an adequate analytical description of aerospace vehicles. It contains a series of axis system definitions and illustrations, a summary table of these reference systems and associated nomenclature, and a chart which summarizes the most common transformations between systems.

The systems presented are intended to be adequate only for aerospace stability and control situations where the principal gravitational effects upon the vehicle rigid body dynamics are due to the earth's field.* Inertial space is accordingly defined as a geocentric equatorial system referred to the First Point of Aries. In this situation, the effects of other bodies are considered as forcing functions. For regions where it is essential that forces due to the sun and/or moon be considered as dependent on vehicle attitude (i.e., producing terms which would appear in the homogeneous equations of motion), additional systems are required. For the sun and moon these would be, respectively, a heliocentric ecliptic system and a selenocentric equatorial system. If these systems were added to those shown, the definition of inertial space would be shifted to the heliocentric ecliptic system.

The ground rules used in defining the systems and nomenclature shown are:

1. The systems defined must be sufficient for use in describing aerospace vehicle dynamic situations in which approximate dynamics of the vehicle plus some controller are of major interest. For some purposes, such as early boost or late re-entry phases, the axes involved in conventional aerodynamic stability and control (as used here, XYZ , $X_p Y_p Z_p$, $X_n Y_n Z_n$, and XYZ) plus a geocentric equatorial inertial system and, perhaps, attitude sensor reference axes, would be sufficient. In other phases, however, the geocentric radius is not necessarily an adequate vertical reference (Ref. 35).

*In a more general sense, the systems are suitable for situations where a solitary principal gravitating mass is present.

This point is emphasized in Figure A-1, which illustrates some vertical reference possibilities. Directional references are similarly

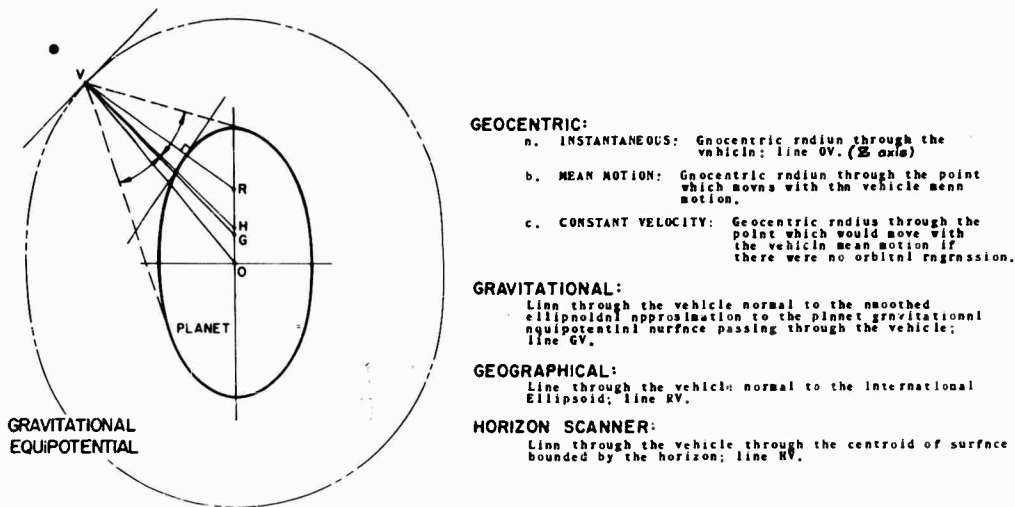


Figure A-1. Vertical Reference Possibilities

nonunique. Accordingly, several additional systems are required to provide for alternate attitude references and/or departure of the vehicle from a Keplerian trajectory.

2. The notation advanced should, insofar as possible, be compatible with both astronautical and aeronautical usage.
3. Both the systems chosen and the notation used should reduce to those used in aeronautical stability and control as one limit. As can be detected by a detailed examination of the figures, this criterion makes necessary an awkward-appearing choice in the definition of the geocentric equatorial inertial system, i.e., the $-Z$ axis is directed toward the First Point of Aries. This condition derives from the decision that the vehicle body axis system should correspond to that conventionally used on aerodynamic vehicles, viz., X "forward," Y out the right wing, and Z "down." Starting with this

latter system, and a west to east orbit, and working backward makes the result noted inevitable. The reason, of course, for choosing the body axis system as a starting point is to preserve unchanged the extensive notation and physical appreciation already built up for aerodynamic vehicles.

4. When possible, the rotational sequences involved in going from one system to another should be similar. Thus, the various axes in the vehicle are derived by similar rotations from the body-fixed reference axes.
5. The number of symbols used should be minimized, consistent with clarity. Thus, the unit vectors \underline{i} \underline{j} \underline{k} , with appropriate subscripts, are used for all vehicle-centered systems which do not contain some externally based vertical reference possibility as an axis. Similarly, the Euler angles relating all vehicle-centered systems are taken as Ψ , Θ , and Φ , with appropriate subscripts. This selection preserves well understood physical notions of yaw, pitch, and roll motions of one system relative to another.
6. The symbols used should be easily reproducible. This criterion has been met as long as one has handy a typewriter, standard Leroy gothic alphabet, and someone capable of writing X, Y, and Z in script.

Of all these requirements and desires, the third is unquestionably the most important because aerospace vehicles are also aircraft. The axis systems selected to satisfy the third point, however, need not be confined to those defined here. M. Abzug, also recognizing the logic of compatibility, has thoroughly examined most of the possibilities (Ref. 36). He notes that some awkward features, such as the direction of the $\underline{-z}$ axis toward \mathbf{T} , negative rotation, etc. are inevitable. Some degree of arbitrariness also exists, such as easterly or westerly headings, etc. Therefore the axes chosen here are not all uniquely defined by the requirements and desires (except for the body-centered systems). However, the end results presented here are reasonable and should provide at least a basis for constructive criticism.

The various systems, transformations, and summary tables follow. Figure A-2 shows the basic steps in the development sequence from inertial space to the fundamental body-centered set, **XYZ**, via the trajectory defining quantities $\Delta\Omega$, ι , w , and v . This entire sequence can be specialized to a minimum of two systems, as shown in Figure A-3, if oblateness is ignored or negligible. An alternate route from inertial space to **XYZ** is illustrated in Figure A-4. This sequence introduces latitude, longitude, and northerly heading angle in lieu of the trajectory elements.

The systems noted above are the only ones actually used in this report. When rigid body dynamics are considered, however, further systems are needed. The fundamental, body-fixed, set **XYZ** is shown in Figure A-5. Its relationship with the body-centered **XYZ** system is shown in Figure A-6. The rotational sequences between **XYZ** and **XYZ** are summarized in Table A-I. Similar sequences can be used to relate principal axes, $X_p Y_p Z_p$, moving element axes $X_n Y_n Z_n$, auxiliary attitude axes, xyz , etc. as required with either **XYZ** or **XYZ**.

Finally, Table A-II recapitulates the various sets and relationships and indicates a tentative nomenclature for unit vectors and resolution angles.

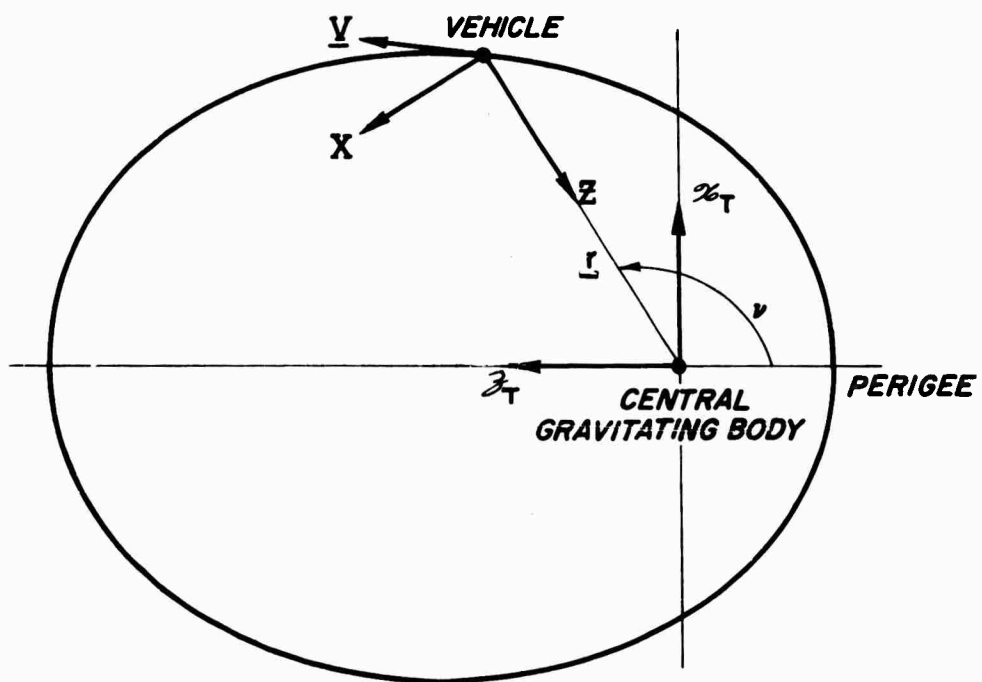
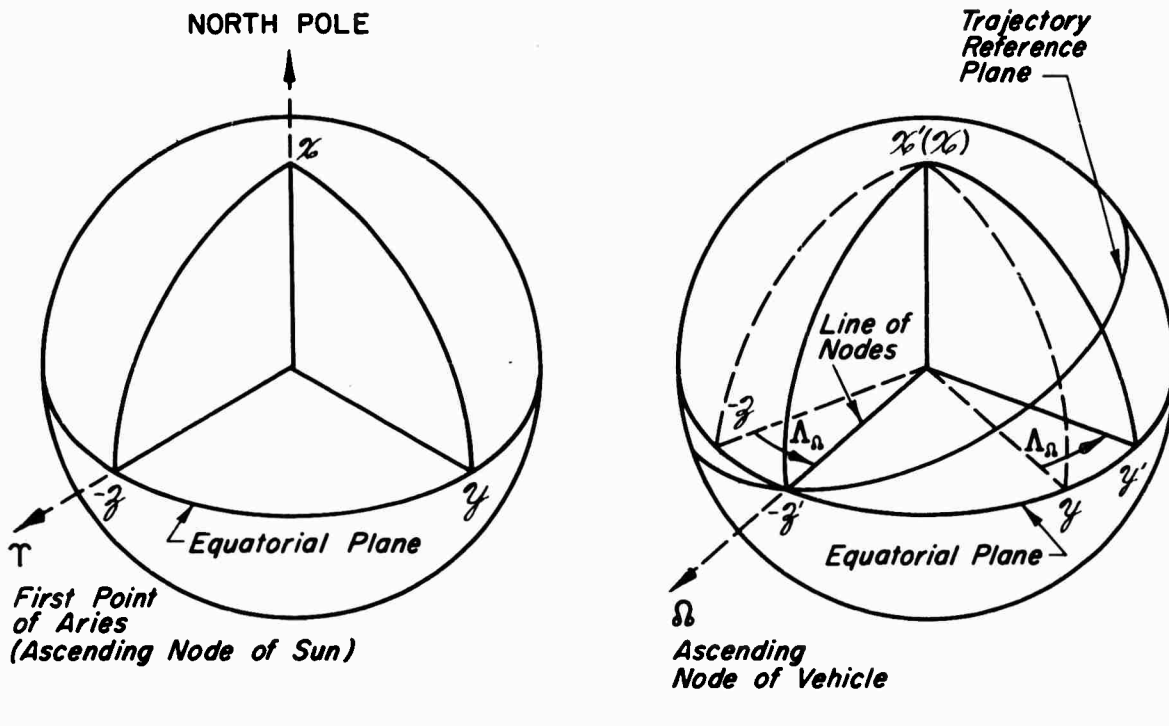


Figure A-3. Simplified Situation for Homogeneous Spherical Central Body

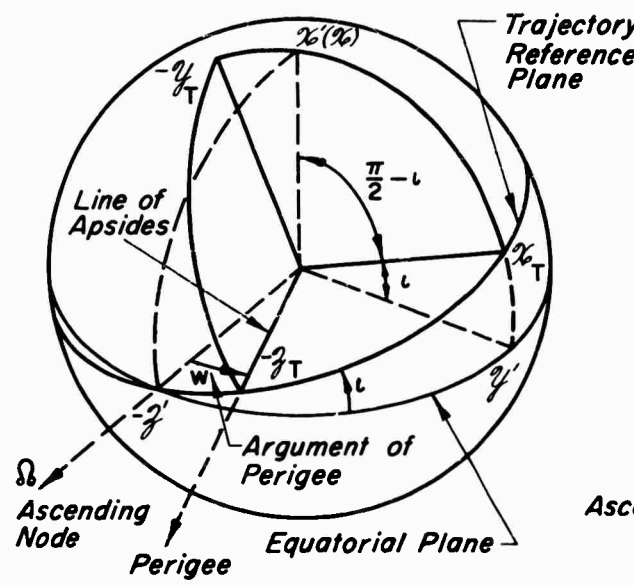


**ARIES DIRECTED
GEOCENTRIC AXES (xyz)**

**ASCENDING-NODE-DIRECTED
GEOCENTRIC AXES ($x'y'z'$)**

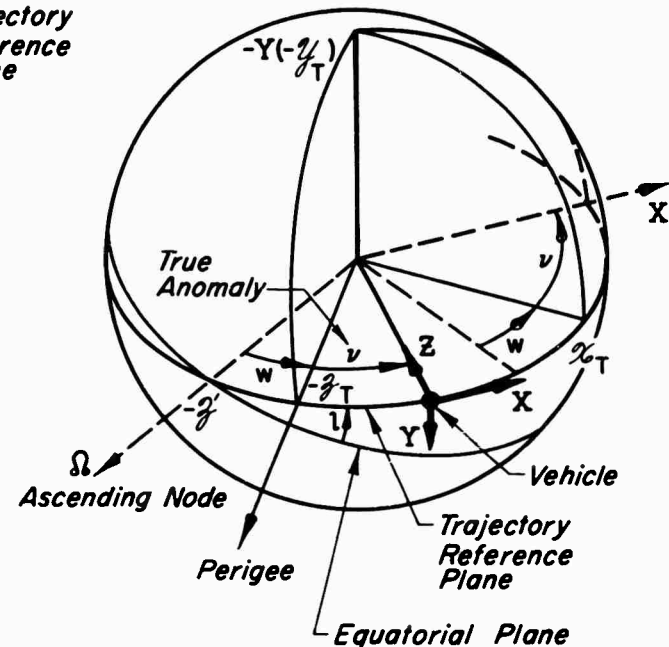
Derived from xyz by rotation about x through Λ_a , the longitude of the vehicle trajectory ascending node.

Figure A-2. Basic Axis System Development
(Homogeneous Spherical Earth)



TRAJECTORY REFERENCE
PLANE GEOCENTRIC AXES ($x'_T y'_T z'_T$)

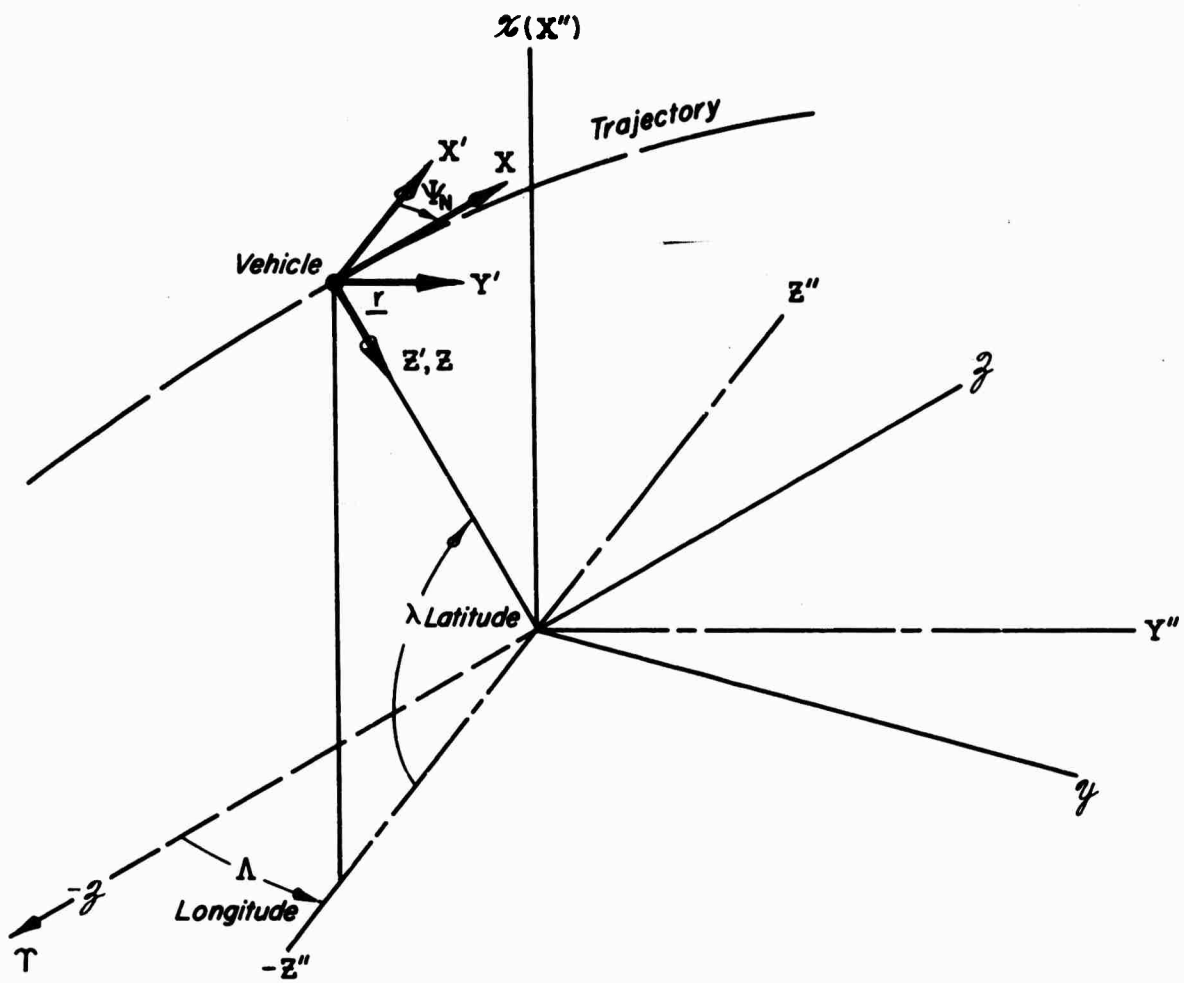
Derived from $x'_T y'_T z'_T$ by rotation about z'_T through $\pi/2 - i$, the co-inclination; and then about y_T through w , the argument of perigee.



VEHICLE-CENTERED
GEOCENTRICALLY-DIRECTED
AXES (xyz)

Derived from $x'_T y'_T z'_T$ by rotation about y_T through ν , the true anomaly; and then translation along $-z$ to the vehicle center-of-mass.

Figure A-2. (Continued)



PHYSICAL SITUATION

$x'y'z$ Aries-Directed Geocentric System

$x'y'z'$ Northerly- and Geocentrically-Directed Vehicle-Centered System

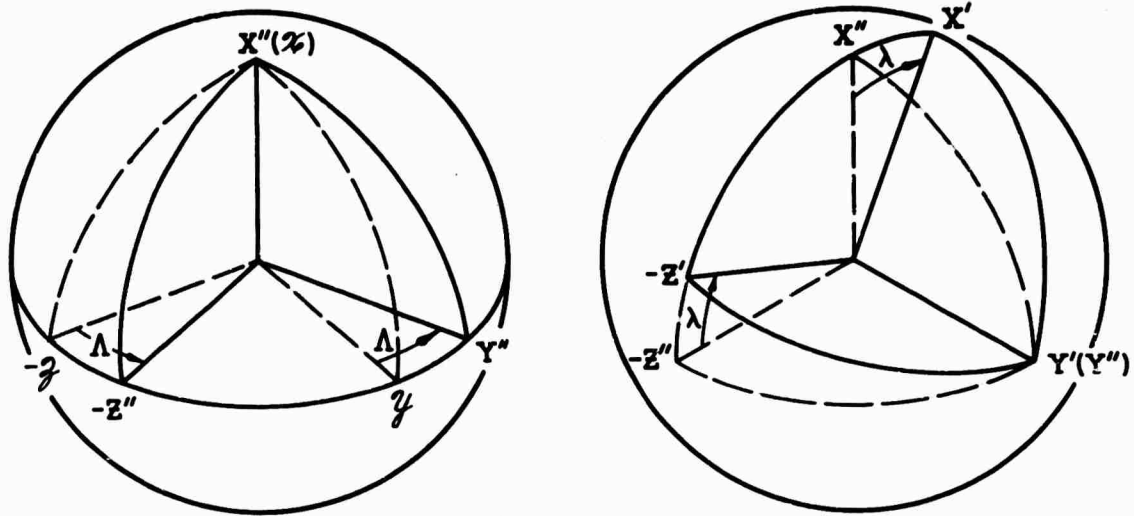
x' In Direction of Increasing Latitude

y' In Direction of Increasing Longitude

z' Directed Down Geocentric Radius

xyz Vehicle-Centered Geocentrically-Directed System

Figure A-4. Supplementary Relationships Between Vehicle-Centered Geocentrically Directed and Aries-Directed Geocentric Systems

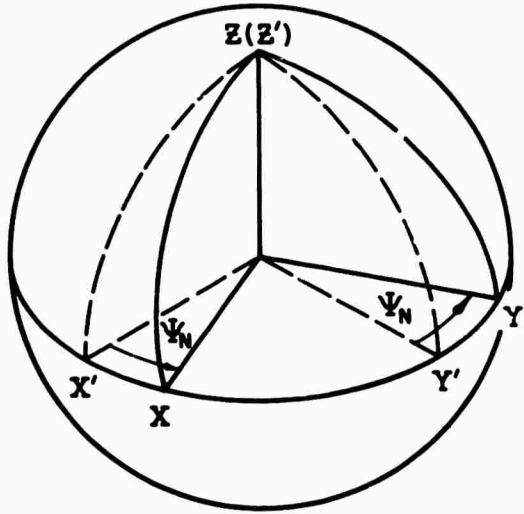


INTERMEDIATE SYSTEM ($X''Y''Z''$)

Derived from rotation of $X''Y''Z''$ about X'' through the longitude, Λ , measured from the $-Z''$ axis.

NORTHERLY- AND GEOCENTRICALLY-DIRECTED VEHICLE-CENTERED SYSTEM ($X'Y'Z'$)

Derived from $X''Y''Z''$ by rotation about Y'' through the latitude angle λ ; and then translation along $-Z'$ to the vehicle center-of-mass.



VEHICLE-CENTERED GEOCENTRICALLY-DIRECTED SYSTEM ($X Y Z$)

Derived from $X'Y'Z'$ by rotation about Z' through the northerly based heading angle Ψ_N .

Figure A-4. (Continued)

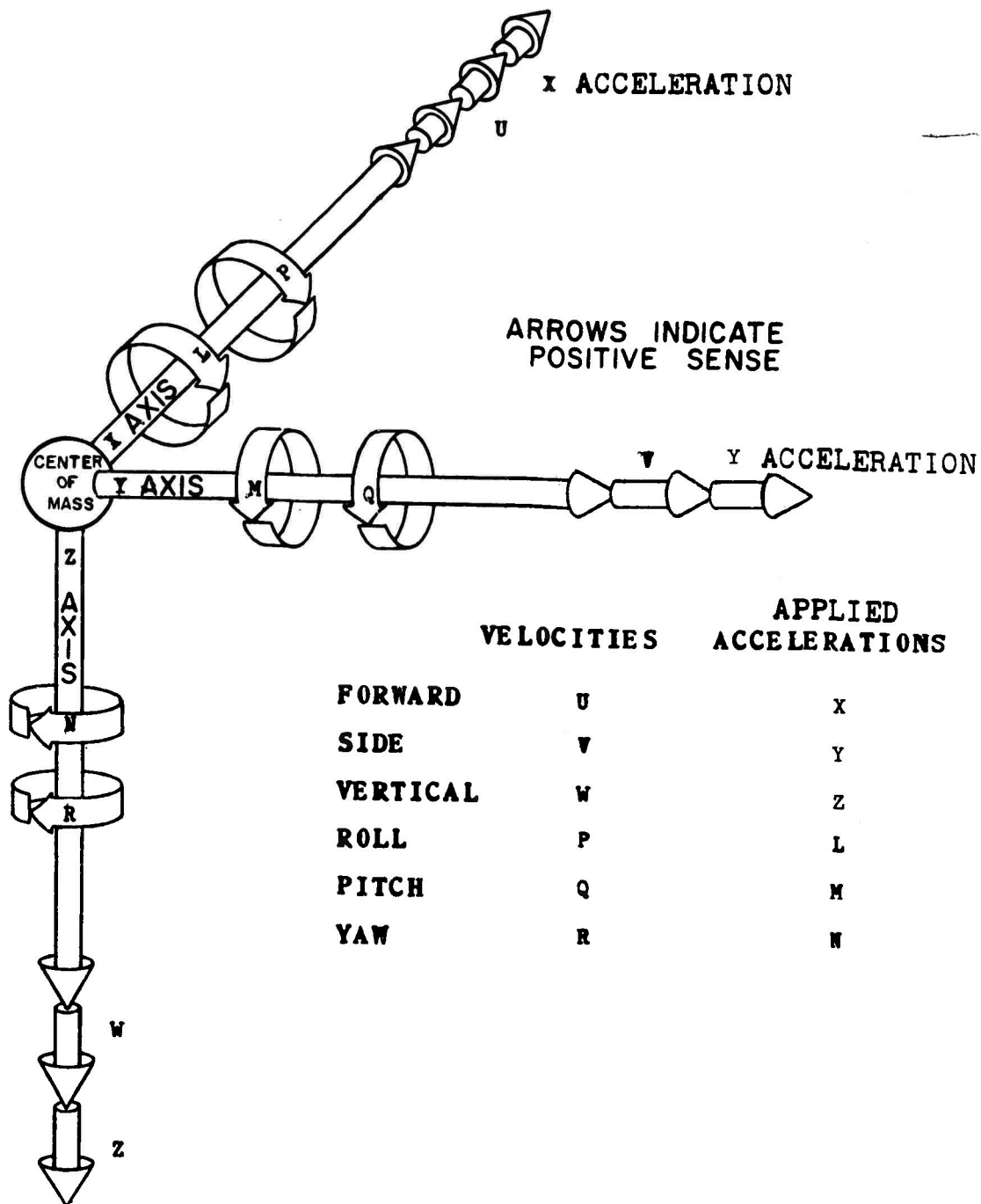


Figure A-5. Vehicle-Fixed Axis System and Notation

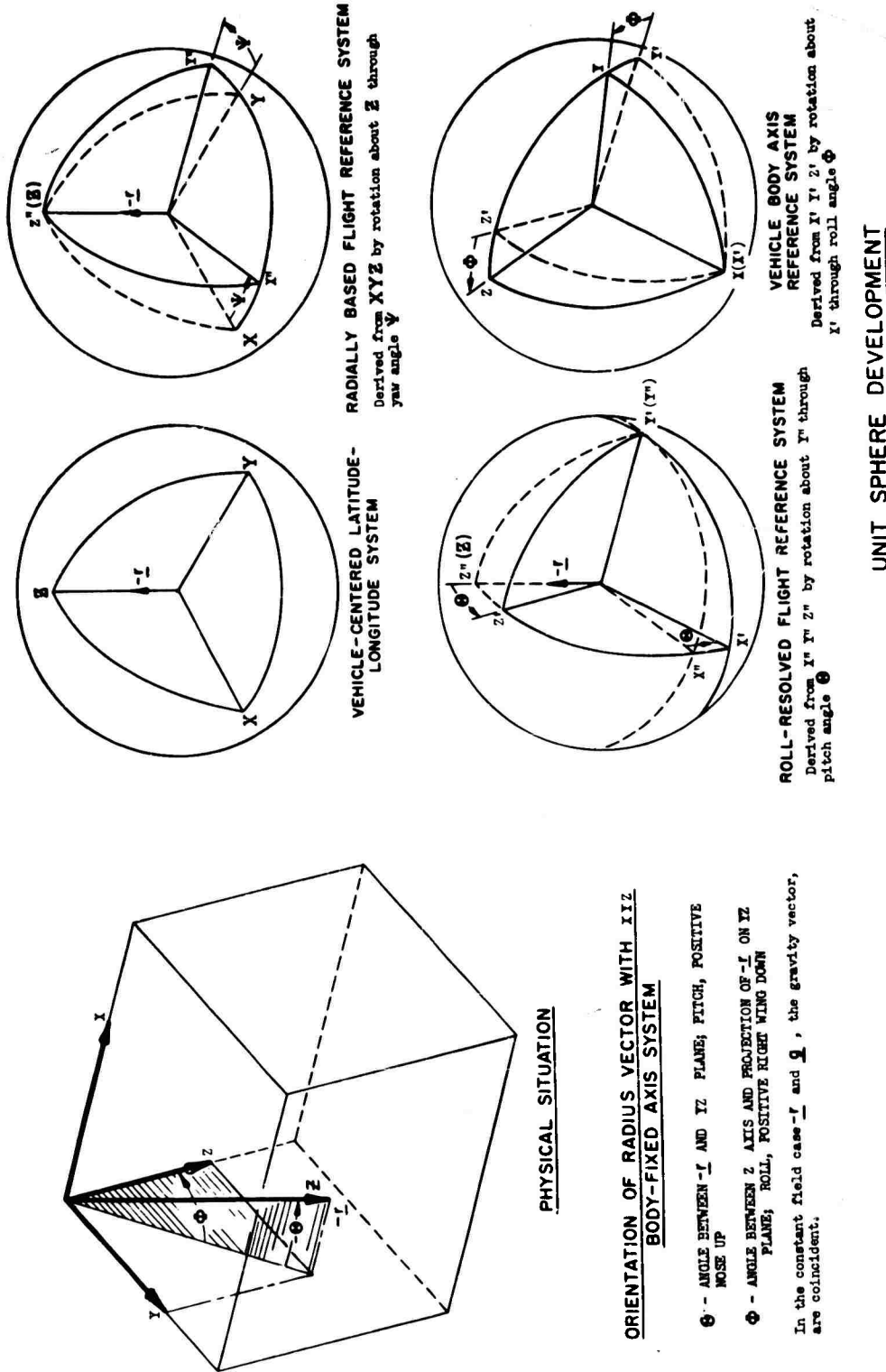


Figure A-6. Relationship Between Vehicle-Centered Geocentrically-Directed and Vehicle-Fixed Axis Systems

TABLE A-1
RELATIONSHIPS BETWEEN AXES ORIENTED TO EACH OTHER VIA Ψ , Θ , AND Φ

DIRECTION COSINES

COMPLETE ARRAY:	m	n
$\frac{1}{2} \begin{bmatrix} \cos \Psi \cos \Theta \cos \Phi & \cos \Psi \cos \Theta \sin \Phi & -\sin \Psi \cos \Phi \\ \cos \Psi \sin \Theta \cos \Phi & \cos \Psi \sin \Theta \sin \Phi & \sin \Psi \cos \Phi \\ \cos \Psi \sin \Theta \sin \Phi & -\sin \Psi \sin \Phi & \cos \Psi \end{bmatrix}$	m	n
$\frac{1}{2} \begin{bmatrix} \cos \Psi \sin \Theta \cos \Phi & \cos \Psi \sin \Theta \sin \Phi & \sin \Psi \cos \Phi \\ \cos \Psi \sin \Theta \sin \Phi & -\sin \Psi \sin \Phi & \cos \Psi \sin \Phi \\ \cos \Psi \sin \Theta \cos \Phi & \sin \Psi \sin \Phi & \cos \Psi \end{bmatrix}$	m	n
$\frac{1}{2} \begin{bmatrix} \cos \Psi \sin \Theta \cos \Phi & \cos \Psi \sin \Theta \sin \Phi & \sin \Psi \cos \Phi \\ \cos \Psi \sin \Theta \sin \Phi & -\sin \Psi \sin \Phi & \cos \Psi \sin \Phi \\ \cos \Psi \sin \Theta \cos \Phi & \sin \Psi \sin \Phi & \cos \Psi \end{bmatrix}$	m	n

As an array, this may be read either left to right or down. As matrices, these correspond to:

$$[E] = \begin{bmatrix} \frac{1}{2} & \frac{1}{2} & 0 \\ \frac{1}{2} & \frac{1}{2} & 0 \\ 0 & 0 & \frac{1}{2} \end{bmatrix} \quad \begin{array}{l} \text{(The array being read)} \\ \text{left to right} \end{array}$$

$$[E] = \begin{bmatrix} \frac{1}{2} & 0 & 0 \\ 0 & \frac{1}{2} & 0 \\ 0 & 0 & \frac{1}{2} \end{bmatrix} \quad \begin{array}{l} \text{(The array being read)} \\ \text{down} \end{array}$$

FACTORED FORM:

$$[E] = \begin{bmatrix} 1 & 0 & 0 \\ 0 & \cos \Phi & \sin \Phi \\ 0 & -\sin \Phi & \cos \Phi \end{bmatrix} \begin{bmatrix} \cos \Theta & 0 & -\sin \Theta \\ 0 & 1 & 0 \\ \sin \Theta & 0 & \cos \Theta \end{bmatrix} \begin{bmatrix} \cos \Psi & \sin \Psi & 0 \\ -\sin \Psi & \cos \Psi & 0 \\ 0 & 0 & 1 \end{bmatrix} \cdot [\Phi][\Theta][\Psi] \cdot [E'] \cdot [\Psi^{-1}][\Theta^{-1}][\Phi^{-1}]$$

LINARIZED FORM:

$$(\Psi = \Psi_0 + \psi, \Theta = \Theta_0 + \theta, \Phi = \Phi_0 + \phi) \quad \text{Magnitudes of the perturbed quantities } \psi, \theta, \text{ and } \phi \text{ are such that their sines are equal to unity and their products are negligible.}$$

$$\begin{bmatrix} \begin{bmatrix} \cos \Psi_0 \cos \Theta_0 \\ \cos \Psi_0 \sin \Theta_0 \\ -\theta(\cos \Psi_0 \sin \Theta_0) \end{bmatrix} & \begin{bmatrix} \sin \Psi_0 \cos \Theta_0 \\ \sin \Psi_0 \sin \Theta_0 \\ -\theta(\sin \Psi_0 \sin \Theta_0) \end{bmatrix} & \begin{bmatrix} -\sin \Theta_0 \\ \theta(\cos \Theta_0) \\ 0 \end{bmatrix} \\ \begin{bmatrix} \cos \Psi_0 \sin \Theta_0 - \sin \Psi_0 \cos \Theta_0 \\ -\psi(\cos \Psi_0 \sin \Theta_0 + \cos \Psi_0 \cos \Theta_0) \\ \theta(\cos \Psi_0 \cos \Theta_0, \sin \Theta_0) \end{bmatrix} & \begin{bmatrix} \sin \Psi_0 \sin \Theta_0 \sin \Phi_0 \\ \sin \Psi_0 \sin \Theta_0 \cos \Phi_0 \\ \phi(\sin \Psi_0 \sin \Theta_0 \cos \Phi_0) \end{bmatrix} & \begin{bmatrix} -\theta(\sin \Psi_0 \sin \Theta_0 \cos \Phi_0) \\ \phi(\sin \Psi_0 \cos \Theta_0 \sin \Theta_0) \\ \phi(\sin \Psi_0 \sin \Theta_0 \cos \Theta_0) \end{bmatrix} \\ \begin{bmatrix} \cos \Psi_0 \sin \Theta_0 \cos \Phi_0 - \sin \Psi_0 \cos \Phi_0 \\ -\psi(\cos \Psi_0 \sin \Theta_0 \sin \Phi_0 + \cos \Psi_0 \cos \Phi_0) \\ \theta(\cos \Psi_0 \cos \Theta_0, \sin \Phi_0) \end{bmatrix} & \begin{bmatrix} \sin \Psi_0 \sin \Theta_0 \cos \Phi_0 \\ \sin \Psi_0 \sin \Theta_0 \sin \Phi_0 \\ \phi(\sin \Psi_0 \sin \Theta_0 \sin \Phi_0) \end{bmatrix} & \begin{bmatrix} -\theta(\sin \Psi_0 \sin \Theta_0 \cos \Phi_0) \\ \phi(\sin \Psi_0 \cos \Theta_0 \sin \Phi_0) \\ \phi(\sin \Psi_0 \sin \Theta_0 \sin \Phi_0) \end{bmatrix} \\ \begin{bmatrix} \cos \Psi_0 \sin \Theta_0 \cos \Phi_0 + \sin \Psi_0 \sin \Phi_0 \\ \psi(-\sin \Psi_0 \sin \Theta_0 \cos \Phi_0 + \cos \Psi_0 \sin \Phi_0) \\ \theta(\cos \Psi_0 \cos \Theta_0, \cos \Phi_0) \end{bmatrix} & \begin{bmatrix} \sin \Psi_0 \sin \Theta_0 \cos \Phi_0 - \cos \Psi_0 \sin \Phi_0 \\ \sin \Psi_0 \sin \Theta_0 \sin \Phi_0 \\ \phi(-\sin \Psi_0 \sin \Theta_0 \cos \Phi_0) \end{bmatrix} & \begin{bmatrix} -\theta(\sin \Psi_0 \cos \Theta_0 \cos \Phi_0) \\ \phi(\sin \Psi_0 \cos \Theta_0 \cos \Phi_0) \\ -\phi(\sin \Psi_0 \sin \Theta_0 \sin \Phi_0) \end{bmatrix} \end{bmatrix} - [E] \cdot [E'] + [e]$$

Where: $[E_0]$ is the matrix made up of the operating point quantities alone (underlined), $[e]$ is obtained by subtracting $[E_0]$ from $[e]$, and $[e']$ is the matrix made up of the perturbation quantities alone.

For the special case where $\Psi_0 = \Theta_0 = \Phi_0 = 0$,

$$[E] = \begin{bmatrix} 1 & \psi & -\theta \\ -\psi & 1 & \phi \\ \theta & -\phi & 1 \end{bmatrix}$$

Similarly, $[E'] = [E_0] + [e']$, where $[e'] = [e] - [E_0]$, but is obtained by subtracting $[E_0]$ term by term from $[E^{-1}]$.

TABLE
SUMMARY OF MAJOR AXES

NAME	DEFINING AXES	UNIT VECTORS	DEFINITION
Aries-Directed Geocentric System	$x'y'z'$	$\underline{l} \underline{m} \underline{n}$	x directed along north polar axis; z' (Sun's ascending node as seen from the Earth)
Ascending-Node-Directed Geocentric Axes	$x'y'z'$	$\underline{l}' \underline{m}' \underline{n}'$	$x'y'z'$ rotated about x through Λ_Ω , for inertial space when regression of apogee
Trajectory Reference Plane Geocentric Axes	$x'y'z'$	$\underline{l} \underline{m} \underline{n}$	$x'y'z'$ rotated about z' through the argument of perigee, w . Approximate and variation of the line of apsides
Vehicle-Centered Geocentrically-Directed System	$X Y Z$	$\underline{l} \underline{m} \underline{n}$	$X_T Y_T Z_T$ rotated about Y_T through the center of-mass (or other reference point) in stability and control problems
Northerly- and Geocentrically-Directed Vehicle-Centered System	$X'Y'Z'$	$\underline{l}' \underline{m}' \underline{n}'$	$x'y'z'$ rotated about x through the vehicle's yaw angle, $X''Y''Z''$ rotated about Y'' through the vehicle's pitch angle, $X'Y'Z'$ rotated about X' through the vehicle's roll angle. Occasionally used as inertial space in vehicle dynamics.
Vehicle-Fixed Reference Axes	$X Y Z$	$\underline{i} \underline{j} \underline{k}$	$X Y Z$ rotated about Z through yaw angle, $X''Y''Z''$ rotated about Y through pitch angle, $X'Y'Z'$ rotated about X through roll angle.
Vehicle Principal Axes	$X_p Y_p Z_p$	$\underline{i}_p \underline{j}_p \underline{k}_p$	$X Y Z$ rotated about Z through an angle, $X''Y''Z''_p$ rotated about Y_p through an angle, $X'_p Y'_p Z'_p$ rotated about X'_p through an angle. Can also derive from $X Y Z$ by rotation.
Attitude Reference Axes	$x y z$	$\underline{l} \underline{m} \underline{n}$	$X Y Z$ rotated about Z through an angle, $x_1 y_1 z_1$ rotated about y_1 through an angle, $x_2 y_2 z_2$ rotated about x_2 through an angle. $x y z$ ordinarily reduces to $X Y Z$ when the vehicle is in a fixed attitude.
Moving Element Axes (Subscript "n" identifies n^{th} moving element)	$X_n Y_n Z_n$	$\underline{i}_n \underline{j}_n \underline{k}_n$	$X Y Z$ rotated about Z through an angle, $X''Y''Z''_n$ rotated about Y_n through an angle, $X'_n Y'_n Z'_n$ rotated about X'_n through an angle.

TABLE A-II
SUMMARY OF MAJOR AXIS OR REFERENCE SYSTEMS

RS	DESCRIPTION AND/OR DERIVATION	ASSOCIATED PH
	\mathbf{x} directed along north polar axis; \mathbf{z} directed to \mathbf{T} , the First Point of Aries (Sun's ascending node as seen from the earth)	Basic inertial reference vehicles
	\mathbf{XYZ} rotated about \mathbf{x} through Λ_B , the longitude of the vehicle ascending node. Approximation for inertial space when regression of the line of nodes is negligible	Rotation of line of nodes
	$\mathbf{X'Y'Z'}$ rotated about \mathbf{z}' through the trajectory inclination, $\pi/2 - i$; then about \mathbf{y}_T through the argument of perigee, ω . Approximation for inertial space when regression of the line of nodes and variation of the line of apsides are negligible	Rotation of line of apsides
	$\mathbf{x}_T \mathbf{y}_T \mathbf{z}_T$ rotated about \mathbf{y}_T through the true anomaly, v ; origin is then translated to the center-of-mass (or other reference point) in the vehicle. Used as inertial space for most aerodynamic stability and control problems	Center of mass movement
	\mathbf{XYZ} rotated about \mathbf{x} through the vehicle longitude, Λ ; (intermediate system $\mathbf{X''Y''Z''}$) then rotated about $\mathbf{Y''}$ through the vehicle latitude, λ ; origin is then translated to the center-of-mass (or other reference point) in the vehicle. Related to \mathbf{XYZ} via the northerly heading angle Ψ_N . Occasionally used as inertial space in aerodynamic vehicle automatic control	Implies heading reference torques due to earth's longitude variations in
	\mathbf{XYZ} rotated about \mathbf{z} through yaw angle Ψ to form intermediate system $\mathbf{X''Y''Z''}$ $\mathbf{X''Y''Z''}$ rotated about $\mathbf{y''}$ through pitch angle Θ to form intermediate system $\mathbf{X'Y'Z'}$ $\mathbf{X'Y'Z'}$ rotated about $\mathbf{x'}$ through roll angle Φ to form \mathbf{XYZ}	Rigid body motions
	\mathbf{XYZ} rotated about \mathbf{z} through an angle Ψ_p to form intermediate system $\mathbf{X''Y''Z''}_p$ $\mathbf{X''Y''Z''}_p$ rotated about $\mathbf{y''}_p$ through an angle Θ_p to form intermediate system $\mathbf{X'_pY'_pZ'_p}$ $\mathbf{X'_pY'_pZ'_p}$ rotated about $\mathbf{x'_p}$ through an angle Φ_p to form $\mathbf{X_pY_pZ_p}$ Can also derive from \mathbf{XYZ} by rotation through similar sequence	
	\mathbf{XYZ} rotated about \mathbf{z} through an angle Ψ_a to form the intermediate system $\mathbf{x_1y_1z_1}$ $\mathbf{x_1y_1z_1}$ rotated about $\mathbf{y_1}$ through an angle Θ_a to form the intermediate system $\mathbf{x_2y_2z_2}$ $\mathbf{x_2y_2z_2}$ rotated about $\mathbf{x_2}$ through an angle Φ_a to form \mathbf{xyz} \mathbf{xyz} ordinarily reduces to \mathbf{XYZ} when oblateness and attitude sensor alignment effects are removed	Supplementary system in for: attitude reference \mathbf{XYZ} . More than one required, e.g., \mathbf{xyz} could mean motion, and another define attitude sensor
	\mathbf{XYZ} rotated about \mathbf{z} through an angle Ψ_n to form the intermediate system $\mathbf{X''Y''Z''}_n$ $\mathbf{X''Y''Z''}_n$ rotated about $\mathbf{y''}_n$ through an angle Θ_n to form the intermediate system $\mathbf{X'_nY'_nZ'_n}$ $\mathbf{X'_nY'_nZ'_n}$ rotated about $\mathbf{x'_n}$ through an angle Φ_n to form $\mathbf{X_nY_nZ_n}$	Supplementary axes required, moving parts within the

TABLE A-II

F MAJOR AXIS OR REFERENCE SYSTEMS

DESCRIPTION AND/OR DERIVATION	ASSOCIATED PHYSICAL EFFECTS
ar axis; β directed to \mathbf{T} , the First Point of Aries seen from the earth)	Basic inertial reference frame for aerospace vehicles
rough Λ_n , the longitude of the vehicle ascending node. Approximation gression of the line of nodes is negligible	Rotation of line of nodes
β' through the trajectory inclination, $\pi/2 - i$; then about \mathbf{y}_T through ν . Approximation for inertial space when regression of the line of nodes of apsides are negligible	Rotation of line of apsides
\mathbf{y}_T through the true anomaly, ν ; origin is then translated to the center- of-mass point) in the vehicle. Used as inertial space for most aerodynamic problems	Center of mass movement in trajectory plane
rough the vehicle longitude, Λ ; (intermediate system $\mathbf{X}''\mathbf{Y}''\mathbf{Z}''$) then the vehicle latitude, λ ; origin is then translated to the center-of-mass in the vehicle. Related to \mathbf{XYZ} via the northerly heading angle Ψ_N . tial space in aerodynamic vehicle automatic control	Implies heading reference (north); gravity torques due to earth's oblateness; latitude- longitude variations in gravitational field
ough yaw angle Ψ to form intermediate system $\mathbf{X}''\mathbf{Y}''\mathbf{Z}''$ rough pitch angle Θ to form intermediate system $\mathbf{X}'\mathbf{Y}'\mathbf{Z}'$ rough roll angle Φ to form \mathbf{XYZ}	Rigid body motions
ugh an angle Ψ_p to form intermediate system $\mathbf{x}_p''\mathbf{y}_p''\mathbf{z}_p''$ rough an angle Θ_p to form intermediate system $\mathbf{x}_p'\mathbf{y}_p'\mathbf{z}_p'$ rough an angle Φ_p to form $\mathbf{x}_p\mathbf{y}_p\mathbf{z}_p$ by rotation through similar sequence	
rough an angle Ψ_a to form the intermediate system $\mathbf{x}_1\mathbf{y}_1\mathbf{z}_1$ through an angle Θ_a to form the intermediate system $\mathbf{x}_2\mathbf{y}_2\mathbf{z}_2$ through an angle Φ_a to form \mathbf{xyz} o \mathbf{XYZ} when oblateness and attitude sensor alignment effects are removed	Supplementary system introduced to account for: attitude reference axes different from \mathbf{XYZ} . More than one such set is often re- quired, e.g., \mathbf{xyz} could move with the vehicle mean motion, and another set, $\mathbf{x}'\mathbf{y}'\mathbf{z}'$ would define attitude sensor axes
ugh an angle Ψ_n to form the intermediate system $\mathbf{x}_n''\mathbf{y}_n''\mathbf{z}_n''$ through an angle Θ_n to form the intermediate system $\mathbf{x}_n'\mathbf{y}_n'\mathbf{z}_n'$ through an angle Φ_n to form $\mathbf{x}_n\mathbf{y}_n\mathbf{z}_n$	Supplementary axes required to account for moving parts within the vehicle

UNCLASSIFIED

Aeronautical Systems Division, Wright-Patterson Air Force Base, Ohio. Rpt No. ASD-TR-61-068. OPERATING POINTS, PARTICLE DYNAMICS, & COORDINATE SYSTEMS FOR AEROSPACE VEHICLE STABILITY AND CONTROL. Final Rpt, Mar 62, 109p. incl illus & tables, 36 Refs.

Unclassified Report

Conventional aeronautical stability and control usage is extended into the aerospace flight regime with particular reference to the definition of operating points and coordinate systems. Implied and studied in this extension are the basic particle-dynamic equations of motion, the magnitudes of possible external forces, and the flight

UNCLASSIFIED

1. Dynamics
2. Coordinate systems
3. Orbital flight paths

I. Project 8219, Task 821904
II. Contract AF33(616)-5961

III. Systems Technology, Inc, Inglewood, Calif.

IV. D.T. McRuer & Irving Ashkenas

V. In ASTIA collection
VI. Avail fr OTS

UNCLASSIFIED

(over)

Aeronautical Systems Division, Wright-Patterson Air Force Base, Ohio. Rpt No. ASD-TR-61-668. OPERATING POINTS, PARTICLE DYNAMICS, & COORDINATE SYSTEMS FOR AEROSPACE VEHICLE STABILITY AND CONTROL. Final Rpt, Mar 62, 109p. incl illus & tables, 36 Refs.

Unclassified Report

Conventional aeronautical stability and control usage is extended into the aerospace flight regime with particular reference to the definition of operating points and coordinate systems. Implied and studied in this extension are the basic particle-dynamic equations of motion, the magnitudes of possible external forces, and the flight

1. Dynamics
2. Coordinate systems
3. Orbital flight paths

I. Project 8219, Task 821904
II. Contract AF33(616)-5961

III. Systems Technology, Inc, Inglewood, Calif.

IV. D.T. McRuer & Irving Ashkenas

V. In ASTIA collection
VI. Avail fr OTS

UNCLASSIFIED

(over)

regimes of fundamental interest. Simplified solutions of the particle-dynamic equations of motion are obtained, and certain low-frequency modes common to both particle and rigid-body motion are explored.

regimes of fundamental interest. Simplified solutions of the particle-dynamic equations of motion are obtained, and certain low-frequency modes common to both particle and rigid-body motion are explored.

UNCLASSIFIED

Aeronautical Systems Division, Wright-Patterson Air Force Base, Ohio. Rpt No. ASD-TR-61-668. OPERATING POINTS, PARTICLE DYNAMICS, & COORDINATE SYSTEMS FOR AEROSPACE VEHICLE STABILITY AND CONTROL. Final Rpt. Mar 62, 109p. incl illus & tables, 36 Refs. Unclassified Report

Conventional aeronautical stability and control usage is extended into the aerospace flight regime with particular reference to the definition of operating points and coordinate systems. Implied and studied in this extension are the basic particle-dynamic equations of motion, the magnitudes of possible external forces, and the flight

Aeronautical Systems Division, Wright-Patterson Air Force Base, Ohio. Rpt No. A -TR-61-668. OPERATING POINTS, PARTICLE DYNAMICS, & COORDINATE SYSTEMS FOR AEROSPACE VEHICLE STABILITY AND CONTROL. Final Rpt. Mar 62, 109p. incl illus & tables, 36 Refs. Unclassified Report

Conventional aeronautical stability and control usage is extended into the aerospace flight regime with particular reference to the definition of operating points and coordinate systems. Implied and studied in this extension are the basic particle-dynamic equations of motion, the magnitudes of possible external forces, and the flight

UNCLASSIFIED

regimes of fundamental interest. Simplified solutions of the particle-dynamic equations of motion are obtained, and certain low-frequency modes common to both particle and rigid-body motion are explored.

UNCLASSIFIED

regimes of fundamental interest. Simplified solutions of the particle-dynamic equations of motion are obtained, and certain low-frequency modes common to both particle and rigid-body motion are explored.

(over)

(over)